2016

The Utilization of Morphological and Genetic Diagnostic Techniques for the Description of Trematode Species Collected from Waterbirds from Lake Winnibigoshish, Minnesota, USA

Tyler Joseph Achatz
Minnesota State University Mankato

The utilization of morphological and genetic diagnostic techniques for the description of trematode species collected from waterbirds from Lake Winnibigoshish, Minnesota, USA

By

Tyler J. Achatz

A Thesis Submitted in Partial Fulfillment of the

Requirements for the Degree of

Masters of Science

In

Biology

Minnesota State University, Mankato

Mankato, Minnesota

April 2016

04/07/16

The utilization of morphological and genetic diagnostic techniques for the description of trematode species collected from waterbirds from Lake Winnibigoshish, Minnesota, USA.

Tyler J. Achatz

This thesis has been examined and approved by the following members of the student's committee.

_____
Advisor Dr. Robert Sorensen

_____
Committee Member Dr. Timothy Secott

_____
Committee Member Dr. David Sharlin

Abstract

The utilization of morphological and genetic diagnostic techniques for the description of trematode species collected from waterbirds from Lake Winnibigoshish, Minnesota, USA.

Name: Tyler J. Achatz
Degree: Masters of Science
Instituiton: Minnesota State University, Mankato
Mankato, Minnesota 2016

Historically, morphological techniques for species identification were the leading diagnostic methodology, however, the increased usage of genetic techniques has led to a decrease in reports of morphometrics. The decrease in morphological reports increases the chance of missing diagnostic morphometrics. The three studies described herein used morphological and genetic diagnostic methods to identify trematodes from five families in order to improve genetic and morphological information for trematode species identification.

The first study identified ten species of trematodes from intestines of waterbirds previously collected from Lake Winnibigoshish, Minnesota. Nine of the species were sequenced for 28S ribosomal DNA (rDNA). Two species were also examined using ITS rDNA sequences. One species was sequenced for a portion of CO1 mitochondrial DNA as well. Morphology for all nine species was reported along with one additional species identified through morphology alone.

The second study identified morphological and genetic variation of 28S rDNA of *Neopsilotrema lisitsynae* from North American waterfowl along with an analysis ofultrastructure using scanning electron microscopy. This was the first report of *N. lisitsynae* in North America, along with identification in four new hosts. Morphometrics of North American worms were found to vary highly in comparison to the original description from Ukraine-collected worms. Additionally, three features of *Neopsilotrema* were shown inaccurate in some cases: tegumental spines may be absent, egg number may be greater than 5, and the ovary may be located in a dextral, sinistral or medial position relative to the body. One variable nucleotide site was identified as well.

The final study identified a new species *Neopsilotrema itascae* from lesser scaup using identical methods as the *N. lisitsynae* study. *Psilotrema mediopora* was also reclassified based upon morphology into *Neopsilotrema.*All three studies reported expansions of currently described morphometrics and diagnostic genetic sequences which may be used for future work involving species diagnosis.

Acknowledgements

First and foremost, I thank Dr. Robert Sorensen for his guidance, support, and patience. His door was always open whenever I needed help in any regard. He continually supported my work and my desire to help others learn. His passion for parasitology was always contagious to the undergraduates who helped work on the project. Without his guidance and assistance, this thesis would not have been possible.

I extend thanks to Dr. Timothy Secott and Dr. David Sharlin for their help throughout the project. I greatly appreciate their assistance with both technical and logical problems. I also thank Dr. Bentley for his assistance with scanning electron microscopy. I also thank Dr. Vasyl Tkach of the University of North Dakota for his assistance obtaining literature.

Additionally, thank you Holly Bloom and Scott Malotka for your support and help completing the project along with all of the undergraduates who helped throughout. I thank Dana Bennett for her immense amount of help with every aspect of the project. The scale of what was accomplished would not have been possible without her assistance.

I also thank Minnesota State University, Mankato for the opportunity along with funding from both the Biology and Psychology departments. In addition, I thank the Minnesota Department of Natural resources for granting permits for waterbird collection.

Lastly, I thank my family for all of their support throughout my time at Minnesota State, University. To my father Gordon, I thank you for continually supporting my desire to learn and pursue Biology along with your guidance and love. To my late mother Nancy, I thank you for more than I could ever write.

Table of Contents

List of Tables

List of Figures

Chapter 1: Genetic and morphological description of select trematodes from waterbirds harvested at Lake Winnibigoshish, Minnesota, USA.

Abstract

Trematodes of the Families Echinostomatidae (*Echinoparyphium recurvatum*, *Echinoparyphium speotyto*, *Echinoparyphium sp.*), Leyogonimidae (*Leyogonimus polyoon*), Microphallidae (*Maritrema obstipum*), Paramphistomatidae (*Zygocotyle lunata*), and Psilostomidae (*Sphaeridiotrema pseudoglobulus*, Psilostomidae spp**.**) were collected from hunter-shot birds during fall 2012 and spring 2013 from Lake Winnibigoshish, Minnesota, USA. All species, except *M. obstipum*, were genetically described using 28S ribosomal (r) DNA sequences, while *E. speotyto* and *Echinoparyphium sp.* were described using ITS sequences as well. *Z. lunata* was examined at a cytochrome c oxidase (CO1) mitochondrial (mt) DNA locus to infer phylogenetic relationships with its closest related taxa that have been sequenced previously. This study used 28S rDNA to validate species identification and confirm morphological ranges of *E. recurvatum*, describes *E. speotyto* in *Anas platyrhynchos* for the first time, along with the first genetic description of the species, and reports a novel 39-spined *Echinoparyphium* species. Furthermore, this study reports the sequence of a 28S rDNA amplicon sequence associated with *L. polyoon* for the first time, in addition to providing a morphometric survey for several morphotypes of *L. polyoon* recovered from *Fulica americana*. Measurements associated with *M. obstipum* were compared to the morphometrics from conspecifics described in other North American and Asian studies to

better describe variation with the species. *Z. lunata* did not vary much in morphology amongst hosts examined; however; some variation was detected relative to prior collections. Sequences of 28S rDNA for *Z. lunata* showed a shared genotype with *Zibethicus wardius.* Sequence data for the CO1 locus in *Z. lunata* is provided to offer a potentially diagnostic sequence at a locus more variable than 28S *S. pseudoglobulus* was found to have a wider range of morphology, which overlapped *Sphaeridotrema globulus* values, including egg size, which is a key diagnostic trait separating these species. Three species from Family Psilostomidae were distinguished using 28S rDNA sequences.

Introduction

Digenean trematodes are a cosmopolitan group of approximately 24000 species of parasites that infect vertebrate hosts (Poulin & Morand 2004). These worms possess a complex life cycle with a vertebrate definitive host and, typically, a molluscan—very often snail—first intermediate host (Roberts & Janovy 2005). Life cycles of trematodes have been shown to be highly specific in intermediate host usage and broader in definitive host usage (McCarthy 1990; Basch 1976; Willey 1941).

Historically, species identification of trematodes primarily utilized adult and the larval cercariae stages. Cryptic morphology, the occurrence when different species appear morphologically similar, has been problematic for many taxa of trematodes for various reasons (McLaughlin et al. 1993; Sorensen et al. 1997; Kudlai et al. *in press*). Adult stages are typically only identifiable through postmortem examination or following anthelminthic treatment of the host. Likewise, trematodes often lack strong specificity for

definitive host species, as such, it is very likely to find the same trematode in different hosts at different locations, which provides confusion for diagnostic studies. Species identification of the larval stages typically require the completion of the life cycle by exposing uninfected individuals to infective stages of the parasite and later collecting the adult stage during necropsy of the experimental host. This overall process can be costly and in some cases impractical, as when specific definitive host requirements are unknown for unidentified larval stages (McCarthy 1990; Sorensen et al. 1997; Moszcynska et al. 2009). Diagnostic studies of trematodes can also be hampered by the fact that morphology of individuals varies based on a large number of factors including, the host species, techniques used for collecting, storing, and handling the worms, and the worm's age or maturity stage (Gracyzk 1991). This age-effect is most pronounced among specimens collected from naturally infected hosts due to the inability to know the infection history of the hosts. Nonetheless, accurate identification of parasites from naturally infected hosts is especially relevant to wildlife management, pathogen diagnosis, and general ecological studies of trematodes and their hosts (Cole & Franson 2006).

One instance of difficult species diagnosis is seen in the differentiation between *Sphaeridiotrema pseudoglobulus* McLaughlin, Scott, & Huffman, 1993 and *Sphaeridiotrema globulus* Rudolphi, 1814. Both species share somewhat similar morphologies, with the exception of egg size and number; eggs are typically larger in *S. pseudoglobulus*, but more numerous in *S. globulus*. While these species are generally similar to one another, S. *pseudoglobulus* has been associated with bird die-off events

and *S. globulus* has been argued to be normal biota in avian hosts (Szidat 1937; Gagnon 1990; McLaughlin et al. 1993)

The advent of molecular techniques (i.e. diagnostic sequencing) has elucidated the ability to detect genetically distinct taxa, including those present within cryptic groups. An abundance of studies examining the internal transcribed spacers (ITS) and 28S regions of ribosomal DNA (rDNA) have resulted in a large library of diagnostic digenean sequences. Both genes are beneficial for diagnostic purposes due to their conserved nature, high copy number and their reasonable size for cost-effective sequencing. The conserved nature of 28S rDNA has historically been useful for distinguishing differences among more inclusive taxonomic levels, like families and genera (Barker et al. 1993; Tkach et al. 1999; Atopkin 2011); however, recent phylogenetic analyses have been carried out using the 28S locus for several groups of trematodes that demonstrated novel relationships including the presence of crypticism and species synonymy (Atopkin 2011; Tkach et al. 2016). The ITS locus has been similarly used to differentiate between inclusive taxa and species (Sorensen et al. 1998; Nolan & Cribb, 2005). For instance, species within Family Echinostomatidae have undergone several revisions due to detection of ITS sequence variation amongst cryptic species (Morgan & Blair 1995; Minchella et al. 1997; Sorensen et al. 1998; Detwiler et al. 2010; Tkach et al. 2016).

Increase in use of mitochondrial (mt) DNA has shown cytochrome c oxidase (CO1) sequences capable of species identification (Hebert et al. 2003; Ward et al. 2005; Saunders 2008; Moszczynska et al 2009). Several regions of CO1 have been used for

comparison, most of which been restricted to a conserved region known as the barcode region (Bowles et al. 1995; Morgan & Blair 1998; Morgan et al. 2005; Mosczysnka et al. 2009; Saijuntha et al. 2011). Vilas et al. (2005) argued the mtDNA is more effective than ITS for cryptic species diagnosis due to the higher mutation rate in mtDNA; nonetheless, all three of these loci are used routinely and in concert and they are often useful for diagnostic purposes.

Unfortunately, as the genetic diagnosis of trematodes has increased in use, morphological features of these species are reported less frequently. An awareness of morphologically diagnostic traits among cryptic species cannot be unveiled unless morphometric values associated with samples used in genetic studies are collected or reported. This practice is only made worse when genetic data is used to make claims related to the taxonomic status of organism, without providing a morphological basis for the validity of such a claim.

This study examined a variety of trematodes found in apparently healthy waterbirds that were harvested in fall 2012 and spring 2013 from Lake Winnibigoshish, Minnesota to identify the parasite community residing in their gastrointestinal tracts. The identification of the trematodes included describing the morphometric characteristics for them and providing genetic sequences that could offer diagnostic value for future studies. The primary impetus for undertaking this study at this time was the occurrence of trematode-related mortality events at Lake Winnibigoshish that were responsible for the death of thousands of waterbirds, predominately lesser scaup and American coot. While previous

studies have examined deceased waterfowl for epidemiological purposes at Lake Winnibigoshish, no study has examined the trematode biota of healthy waterbirds at this lake. The timing of this study also follows the identification of the exotic aquatic snail, *Bithynia tentaculata,* at Lake Winnibigoshish, which is noteworthy because this snail is known to serve as the first-intermediate host for the parasites linked to the waterbird mortality events (Roy & Herwig 2010; Hermann & Sorensen 2011). Expansion of the range of *B. tentaculata* comes with the potential for the introduction or establishment of other novel trematodes in areas it has recently colonized, which further merits the potential value of trematode diversity studies at this site to gather baseline data about the members of the trematode community in waterbirds in north-central Minnesota.

Materials and Methods

Parasite collection and preparation

Intestines of waterbirds from Lake Winnibigoshish in Minnesota, USA, were collected from waterfowl hunters in fall 2012 and spring 2013 (Table 1.1; Fig. 1.1). Upon collection, intestines were frozen and transported to Minnesota State University, Mankato until a time when parasites could be collected through dissection of the intestinal tissue. Small intestine tissue was segmented into 15cm linear sections, while cecae and large intestines were not subdivided into smaller segments prior to examination. Parasites were removed from the intestinal contents with the aid of a binocular dissecting microscope. Collected worms were stored in 10% buffered formalin or frozen for morphological or molecular analysis, respectively.

Trematode taxa described in this study were selected at convenience based upon availability for further analysis. In other words, the taxa that were selected were those that possessed sufficient individuals to provide the necessary tissue for morphological and genetic studies. Individual worms were prepared for light microscopy by staining them with Semichon's acetocarmine before they were dehydrated in ascending concentrations of ethanol. Upon dehydration, worms were cleared using xylene and mounted in Kleermount® (Carolina) or Canada balsam. Specimens were observed using an Olympus CH2 microscope and digital images were captured with a trinocular-mounted Moticam 10MP camera. Characteristics of the worms were measured using Moticam Images Plus 2.0 ML software (Motic). Statistical analysis of measurement data was carried out using a Kruskal-Wallis, nonparametric, one-way analysis of variance using SigmaPlot software (Systat).

Abbreviations used for body measurements are as follows: body length–BL; body width–BW; body depth–BD; forebody length–FORE; oral sucker length–OSL; oral sucker width–OSW; pharynx length–PHL; pharynx width–PHW; ventral sucker length–VSL; ventral sucker depth–VSD; cirrus-sac length–CSL; cirrus-sac width–CSW; anterior seminal vesicle length–SVL1; anterior seminal vesicle width–SVW1; posterior seminal vesicle length–SVL2; posterior seminal vesicle width–SVW2; anterior testis length–ATL; anterior testis width–ATW; anterior testis depth–ATD; anterior testis length–ATL; anterior testis width–ATW; anterior testis depth–ATD; posterior testis length–PTL; posterior testis width–PTW; posterior testis depth–PTD; distance between the posterior extremity of posterior testis to posterior margin of body–TEND; ovary length–OVL;

ovary width–OVW; ovary diameter–OVD; uterus length–UTL; egg number–E; egg-length–EL; and egg-width–EW. Abbreviations for OSpL–oral spine length; OSpW–oral spine width; ASpL–aboral spine length; ASpW–aboral spine width; DSpL–dorsal spine length; DSpW–dorsal spine width; CSpL–corner spine length; CSpW–corner spine width. Proportions based on Kostadinova (2005a) were generated for: maximum body width to body length–BW%; maximum depth to body length–BD%; forebody length to body length—FO%; length of post-testicular field to body length–T%; and oral sucker to ventral sucker–OS:VS. All measurements given in text, tables and figures are in micrometers.

Molecular analysis

DNA of individual worms was extracted using a ZR Genomic DNA™-Tissue MiniPrep kit (Zymo Research) and eluted in 35 µL of water. A portion of the 28S, ITS, and CO1 loci were amplified with the primer pairs described in Table 1.2, which also lists their associated nucleotide sequences, annealing temperatures, and sources. PCR amplifications were done using 0.25 µL of each primer (10µm), 7.5 µL of GoTaq® green master mix (Promega), 50 ng of template DNA and raised to a volume of 15 µL with ddH_2O. Run conditions for PCR were 94 ^oC for 2 minutes followed by 35 cycles of 30 seconds at 94 ^oC, 30 seconds at 50 ^oC, and 1 minute at 72 ^oC. After 35 cycles the temperature was set to 72 ^oC for 10 minutes. Amplicons were run on a 1% agarose gel, gel excised, and purified using ZR Gel DNA Recovery Kit (Zymo Research). Recovered amplicons were cycle sequenced using a modified protocol from Whalen (2011): BigDye™ terminators using 1 µL of BigDye™, 1 µL of 5x BigDye™ reaction buffer, 2 µL of either forward or reverse primer associated with the amplicon and 24 ng of PCR

product, with the following run conditions: an initial 5 minutes at 95 ^{o}C followed by 99 cycles of 30 seconds at 95 ^{o}C, 20 seconds at the annealing temperature of the primer, and 4 minutes at 60 ^{o}C. Sequencing products were run on an ABI Prism 377 DNA sequencer after clean up using either a ZR Sequencing Clean-up kit (Zymo Research) or ethanol precipitation. Electropherograms for sequences were refined using BaseFinder (Giddings et al. 1998) to increase certainty in nucleotide identification.

Alignment and Phylogenetic analysis

When possible, contiguous sequences were assembled and aligned using Mega7 (Kumar & Hedges 2016). Alignments were performed using ClustalW with the parameters of 15 for a gap opening penalty and 6.66 for a gap extension penalty for all pairwise and multiple alignments. Three alignments were generated with sequences obtained within the study and from GenBank (Tables 1.3-1.5) (Benson et al. 2012). The first alignment used 28S rDNA sequences (1001 nucleotides [nt]). The second alignment used ITS sequences obtained from *Echinoparyphium spp.* in comparison to other members of *Echinoparyphium* (504 nt). The third alignment used the 194 nucleotide CO1 sequences (JB locus) obtained for *Zygocotyle lunata* to identify its placement within Superfamily Paramphistomoidea. Species outside of those contained within this study that were used to generate the phylogenies were selected based upon two criteria. The first criterion was to select members of the same genus from within GenBank, with the most important criteria being that the entire locus in question was sequenced. In the cases where members of the same genus were not available, nearest relatives, which may have been members of the same Family or Superfamily, were used.

Maximum likelihood (ML) and maximum parsimony (MP) analyses were performed using Mega7 with 500 bootstraps for each analysis. ML phylogenies utilized different optimized models of substitution based upon model selection analysis within Mega7. The 28S rDNA alignment used a general time reversible model with gamma distributed among-site rate variation (GTR+G) (Lanave et al. 1984; Tavara 1986; et al. 1990). The ITS phylogenies utilized the Hasegawa-Kishino-Yano (HKY) (Hasegawa et al. 1985). The CO1 alignment used the Hasegawa-Kishino-Yano model, with gamma distributed among-site rate variation (HKY+G). ML phylogenies for COI utilized consensus trees due to limited genetic divergence amongst species examined. For all alignments, MP phylogenies utilized a subtree-pruning-regrafting (SPR) search method. Uncorrected p-distances, which quantify the proportion of nucleotide sites that are different between any two sequences being compared, was used as a raw measurement of genetic similarity between any two pairs of genetic samples. Calculation of uncorrected p-distance values was performed using Mega7.

Results

In this study, 10 distinct trematode species were identified from 5 different Families that provided an opportunity to expand and clarify their morphological description and, in most cases, associate diagnostic nucleotide sequence data with that species. Each of these species is discussed individually with comments describing their noteworthy details. The species are organized according their Family.

Notes on Family Echinostomatidae Looss, 1899:

The number of collar spines is one of the key diagnostic traits for species diagnosis within Family Echinostomatidae. When collar spines are lost, a scar remains indicating prior spine presence (Kanev et al. 1998). If scar tissue of a spine was detected, it was added to the collar spine count. Measurement of spine locations and the corresponding size of these spines is also considered diagnostic. In many cases, exact location of dorsal spines (i.e. oral vs aboral) could not be made due to the use of individuals that were mounted on slides in a lateral position rather than a dorso-ventral position. When dorsal spines could not be differentiated along the oral-aboral axis, they were denoted as dorsal, omitting the oral-aboral reference (Kanev et al. 2009).

Echinoparyphium recurvatum Linstow, 1873

Family Echinostomatidae Looss, 1899

Host: *Anas platyrhynchos*

Location in host: Anterior to late-middle small intestine

Genotype: 28S (Fig. 1.2)

Description: *Echinoparyphium recurvatum* Linstow, 1873 individuals were identified as members of *Echinoparyphium* due to small, elongate body form with a long to extremely long forebody, up to 47% of body length (Fig. 1.3a). Additionally, spines were long, sharply pointed in a double row.

Echinoparyphium recurvatum was diagnosed due to presence of 45 cephalic collar spines including 5 corner spines per lappet. Corner spines were larger than other collar spines (Table 1.6). The tegument was armed with spines visible up until the equatorial portion of body. Maximum body width was found at the level of the ventral sucker. The oral sucker

was oval, terminal, extending anterior to the cephalic collar, and opening towards the ventral surface of the worm. Pharynx was muscular, located at the level of or below the cephalic collar. Ventral sucker was large, strongly muscular (Table 1.7). Bifurcation of the cecal fork was visible immediately anterior of ventral sucker. Ceca were thin-walled with terminal ends often obscured by vitellaria.

Two tandem, elongate-oval testes were present. Cirrus sac did not extend beyond the level of the ventral sucker (Fig. 1.4). A seminal receptacle could be located some distance anterior of the anterior testis. The subspherical ovary was anterior to seminal receptacle. Few, large eggs were seen in gravid adults (Table 1.8). Vitellaria extended from near the posterior extremity of the body in a confluent field to midway between ventral sucker and ovary. Post-testicular field was short only representing 21% of body.

The morphology of 45-spined *Echinoparyphium* species have been disputed (Huffman & Fried 2012). As such the *Echinoparyphium recurvatum* diagnosis was confirmed using 28S rDNA sequences. Unfortunately, two additional *Echinoparyphium* species were identical across the entire amplicon. Both of the additional species, *Echinoparyphium rubrum* (Tkach et al. 2012) and *Echinoparyphium cinctum* (Tkach et al. 2001), were described as having 43 collar spines, in comparison to this study's worms, which have 45 collar spines. *E. rubrum* can further be differentiated against *E. recurvatum* due to *E. rubrum* possessing of 4 corner spines, in comparison to *E. recurvatum*, which has 5 corner spines. Also, the posterior testis in *E. rubrum* is noted to be smaller than the anterior testis. In contrast, *E. recurvatum*, in this study, had a much larger posterior testis

than the anterior testis. Differentiation from *E. cinctum* can be justified due to the elongated cirrus sac in *E. cinctum* that extends beyond the posterior margin of the ventral sucker in contrast to the *E. recurvatum* in this study, in which the cirrus is smaller and does not extend beyond the posterior margin of the ventral sucker. On this basis, stating that the worms in this study are *Echinoparyphium recurvatum* Linstow, 1873, rather than *Echinoparyphium rubrum* or *Echinoparyphium cinctum* is appropriate.

No intraspecific variation was seen in 28S rDNA sequences of the two contiguous sequences identified.

Echinoparyphium speotyto Buscher, 1978

Family Echinostomatidae Looss, 1899

Host: *A. platyrhynchos (Anseriformes: Anatidae*)

Location in host: Anterior small intestine

Genotype: 28S (Fig.1.2); ITS (Fig. 1.4)

Description: Collected *Echinoparyphium speotyto* Buscher, 1978 were small, elongate-oval with an extremely long forebody that composed up to 39% of the body length. The aforementioned traits, short post-testicular field, 25% of body length in this case (Fig 1.3b), and many of the traits described below demonstrate that these worms most closely aligned with the genus *Echinoparyphium.* Morphometrics were compared to Buscher's (1978) original description of *E. speotyto* collected from the burrowing owl (*Speotyto cunicularia*) from Oklahoma. General comparability of specimens from the two samples support the *E. speotyto* species diagnosis for the worms described here (Table 1.9).

E. speotyto has been described as widest at the level of the ventral sucker by Buscher (1978), however, all individuals in this study were partially rotated laterally preventing accurate measurement. The body was found to taper posterior to the testes. The cephalic collar held 41 spines with 5 corner spines on each lappet. Tegument appeared armed with small spines visible until the level of the ventral sucker. Oral sucker projected anterior of the cephalic collar, opening ventrally. Pharynx was below cephalic collar and muscular. Ventral sucker was large, strongly muscular, in the second quarter of body (Table 1.10). The cecal fork bifurcated immediately anterior to ventral sucker. Cecae appeared thin-walled, reaching near the posterior margin of body, which was typically obscured by vitellaria.

Testes were tandem, elongate-oval, and slightly irregular. Occasionally, vitelline fields obscured the testes. Vitelline fields were composed of large vitelline clusters with small vitelline cells, which were confluent posterior to the testes and extended to slightly posterior to midway between ovary and ventral sucker. Elongate-oval cirrus sac did not extend below the level of the ventral sucker. Prominent pars prostatica present anterior to the seminal vesicle (Fig. 1.5).

Ovary appeared subspherical, located anterior of anterior testis, slightly post-equatorial. Mehlis gland was distinct. Few, large eggs were present. Excretory pore identified in a terminal location on the posterior extreme of the body.

Only one sequence was obtained for the 28S and ITS rDNA loci. The closest GenBank matches for the obtained 28S rDNA sequence differed by one nucleotide (Hicks et al. no date due to direct submission (Tkach et al. 2016). However, neither echinostomatids of the similar sequences from GenBank were identified to the species level, nor were morphometrics or associated morphology reported for the GenBank samples.

Sequences obtained for a portion of the ITS region were identical to *E. recurvatum* and an unidentified *Echinoparyphium* from muskrats (Detwiler et al. 2010). However, *E. speotyto* collected here differ from both species based upon collar spine number; *E. speotyto* contains 41 spines while *E. recurvatum* contains 45 spines and the unidentified *Echinoparyphium* possessed 43. The divergence in spines, along with sizable morphological difference from *E. recurvatum,* is supportive of the *E. speotyto* species diagnosis.

Echinoparyphium sp.

Family Echinostomatidae Looss, 1899

Host: *A. platyrhynchos (Anseriformes: Anatidae*)

Location in host: Middle of small intestine

Genotype: 28S (Fig. 1.2); ITS (Fig. 1.4)

Description: *Echinoparyphium* sp. closely matched the morphological description of *Echinoparyphium* due to the presence of a long forebody composing approximately a quarter of the body length, a small, elongate-oval body with a relatively short post-testicular field composing less than 25% of overall body length (Fig. 1.3c). Additionally, the traits described below most accurately describe *Echinoparyphium*.

The number of spines was unusual with 39 cephalic collar spines present with 4 corner spines on each lappet. Spines were arranged in double row; however, most were broken and unable to be used for accurate measurement. No currently accepted species of *Echinoparyphium* has been described with 39 spines. That being said, *Echinoparyphium indicum* Rai, 1962 was originally described as an *Echinoparyphium* species with 38 spines, which has been argued to actually be 39 (Buscher 1978). The species itself is no longer recognized as a member of *Echinoparyphium*; however, due to the lack of other currently accepted *Echinoparyphium* species with 39 spines, *E. indicum* is compared to the *Echinoparyphium* sp. described here (Tables 1.11-1.12).

Morphological comparison to *E. indicum* showed dramatic divergence as *E. indicum* tended to have larger body form (BL> 5000) with smaller structures (i.e. much smaller spines and oral sucker). Whereas, *Echinoparyphium* sp. was much smaller in body size (BL< 3000) while structures tended to be equitable to larger. Further, *E. indicum* has ovoid testes, whereas the species in this study has elongate-oval testes. In addition, the vitellaria of worms from in this study extends to near the middle point between the ovary and ventral sucker, contrary to *E. indicum* in which vitellaria stop near the anterior margin of the anterior testis.

Echinoparyphium sp. described here show the widest portion of the body was at the ventral sucker. The oral sucker was located terminally, extending anterior, opening towards the ventral surface. Pharynx was muscular close to the cephalic collar. The ventral sucker was large, strongly muscular with a smooth interior margin. Tegument was

armed with small spines extending to the level of ventral sucker. Esophagus noted as long, with cecal fork immediately anterior to genital pore. Cecae simple, reaching to posterior of worm often obscured by vitellaria. Vitelline follicles were large and non-compact, almost confluent with posterior testis.

Testes tandem, elongate-oval, in third quarter of body. Testis shape was smooth to slightly irregular. Elongate-oval cirrus sac extended almost to posterior margin of ventral sucker with a simple, internal seminal vesicle. Pars prostica was small, not clearly defined.

Mehlis gland was located anterior to testes, conspicuous and large with a uterine seminal receptacle located dorsally. The subspherical to subglobular ovary was found anterior to the seminal receptacle, post-equatorial, subspherical in shape. Few, large eggs were found within the uterus. Genital pore was found some distance anterior to the ventral sucker.

For the two contiguous 28S rDNA sequences obtained, there were no matches to currently reported sequences on GenBank. One sequence was obtained for both collection seasons from *A. platyrhynchos.* No genetic divergence was detected between *Echinoparyphium* sp. from the two collection seasons. A portion of an ITS sequence was obtained from a fall worm; no currently reported sequences on GenBank are identical.

Leyogonimus polyoon Braun, 1902

Family Leyogonimidae Linstow, 1887

Hosts: *Fulica americana*

Location in host: Anterior to middle small intestine

Genotype: 28S (Fig. 1.6)

Description: Body shape of *L. polyoon* Braun, 1902 in the present study was highly polymorphic, as described by Lotz & Font (2008), varying between pyriform to elongate-oval (Fig. 1.7). When viewed laterally, post-equatorial distention could be seen in gravid individuals. Tegumental scale-like spines were present across the entire body (Fig. 1.8). All specimens had a lobular ovary at the level of the ventral sucker, vitelline fields confined to the anterior margin of the body near the level of the ovary, descending posterior in many discrete bands. Large cecae, which overlapped the testis, and a lateral facing cirrus were in the third quarter of the body. For most specimens, the large number of eggs obscured most structures posterior to or including the ventral sucker. The number of eggs was not counted beyond 100, however, the total value is estimated to be over 1000. While egg number was not counted from *L. polyoon* described by Sey (1968), the line drawing in that paper showed fewer eggs than seen in the present study (Table 1.13). No intraspecific variation was detected in 28S rDNA sequences across 20 individuals.

Maritrema obstipum van Cleave & Mueller, 1932

Family Microphallidae Ward, 1901

Hosts: *Aythya collaris*

Location in host: Posterior small intestine

Description: The genus *Maritrema* was diagnosed due to the J-shaped cirrus, post-cecal uterus, presence of a ventral sucker and lateral horse-shoe shaped vitellarian rings surrounding the gonads and excretory system (Fig. 1.9); *M. obstipum* van Cleave &

Mueller, 1932 was diagnosed due to dextral position of the ovary, highly divergence cecae, equitable sucker ratio, and the ventral sucker was noted as spinous, however, concentric, sub-tegumental rings could not be seen.

M. obstipum Van Cleave & Mueller, 1932 were compared to the description given by Etges (1953) and Chung et al. (2011) (Table 1.14). Individuals from the present study were much smaller than Chung et al. (2011) in regards to body size (BL= 277 vs 451) and other morphometrics (e.g. OSL, VSL, ect.). While the specimens from Etges (1953) were more comparable in body form and morphometrics, however, as with Chung et al. (2011), some structures, such as the oral and ventral suckers were smaller in the present study when compared to Etges (1953). Egg size was comparable between all compared studies.

Seuqences of 28S rDNA could not be obtained due to the limited number of individuals collected, as all specimens were used for morphological analysis

Sphaeridiotrema pseudoglobulus McLaughlin, Scott, & Huffman, 1993

Family Psilostomidae Loos, 1900

Hosts: *A. platyrhynchos, Aythya affinis*

Location in host: Anterior small intestine

Genotype: Not reported due to lack of novel nucleotide sequence

Description: Similar to the description by McLaughlin et al. (1993), *Sphaeridiotrema pseudoglobulus* McLaughlin, Scott, & Huffman, 1993 was identified due to its mushroom-like body form; the forebody extended from the subspherical to subglobular

hindbody (Fig. 1.13). A large portion of the hindbody was occupied with the large, powerful ventral sucker. In addition, the posterior end of hindbody held two testes which were often obscured by vitellaria; the testes were found to be either tandem within the vitellaria, one testis posterior to the vitellaria causing a protrusion in the tegument, or with the posterior testis displaced to a position, opposite, and lateral to the anterior testis.

Sequences of a region of 28S rDNA matched prior studies on *S. pseudoglobulus* by Bergmame et al. (2011) and Tkach et al. (2016), supporting species diagnosis for the worms collected from *A. platyrhynchos* and *A. affinis* (data not shown). However, *A. platyrhynchos* only contained immature adults, which were not used for morphological analysis. Morphometric comparison between the *S. pseudoglobulus* in the present study and McLaughlin et al. (1993) and *Sphaeridiotrema globulus* Rudolphi, 1814 (Price 1934) is given in Table 1.15.

Undefined Psilostomidae Species A

Family Psilostomidae Loos, 1900

Hosts: *A. sponsa*

Location in host: Posterior small intestine

Genotype: 28S (Fig. 1.11)

Description: The morphology of Psilostomidae species A did not match any currently described genera or species. Morphological analysis was limited due to the small number of fixed specimens. The body was minute to small, elongate-oval with a short post-testicular field (Fig. 1.12a; Tables 1.16-1.17). The oral sucker was larger than pharynx. The sucker ratio indicated a much larger ventral sucker than oral sucker. Ventral sucker

was large, powerful in the first third of the body. Unusually, no cirrus could be identified, which is a characteristic trait of Family Psilostomidae (Kostadinova 2005b). Gravid adults held 10 eggs (est. 7% body length). Vitellaria was composed of well-defined clusters, contiguous posterior to posterior testis, extending to the posterior margin of the ventral sucker.

Sequences of 28S rDNA placed the species within Family Psilostomidae in a clade with another unidentified Psilostomidae species (KT956954) from a prior study (Tkach et al. 2016). In comparison to Tkach et al.'s (2016) Psilostomidae sp., unknown species A only diverged by 1 nucleotide. Contiguous 28S rDNA sequences obtained from the 2 specimens studied here did not vary from one another.

Undefined Psilostomidae Species B

Family Psilostomidae Loos, 1900

Hosts: *A. sponsa*

Location in host: Anterior small intestine

Genotype: 28S (Fig. 1.11)

Description: Psilostomidae species B did not have a morphological match under currently described genera or species. Species B was found to have a minute to small, elongate-oval body with transversely oval testes, which filled most of the body width (Fig. 1.12b). The post-testicular field was found to be longer, consisting up to almost 40% of the body length. The oral sucker was found to be larger than the pharynx, while being smaller than the ventral sucker. The ventral sucker was highly muscular, in the first quarter of the body. Ovary was subspherical, immediately posterior to the ventral sucker (Tables 1.16-

1.17). Eggs were few, less than 10 composing approximately 8% of the body length. The cirrus was bipartite with the genital pore medial, below the level of the cecal fork. Vitellaria are in small, well-defined, lateral clusters that do not combine, extending to the anterior margin of the ventral sucker.

There was no divergence between the two contiguous 28S rDNA sequences obtained. Sequences for the amplicon of 28S rDNA were identical to an unidentified Psilostomidae species (KT956955) that has not been currently described (Tkach et al. 2016).

Undefined Psilostomidae Species C

Family Psilostomidae Loos, 1900

Hosts: *Bucephala albeola*

Location in host: Posterior small intestine to large intestine

Genotype: 28S (Fig. 1.11)

Description: Psilostomidae species C also did not have any morphological match. The body was minute, elongate-oval with vitelline fields extending laterally, up to the level of the pharynx (Fig. 1.12c). Vitellaria appeared in large, dense clusters in two distinct fields, which remain distinct. The post-testicular field composed up to slightly over a quarter of the body length (Table 1.17). Oral sucker was larger than pharynx, while ventral sucker was much larger than the oral sucker. Ventral sucker was located in the first third of the body. Testes are transversely pyriform, filling the majority of the body width. Cirrus sac does not extend beyond the posterior margin of the ventral sucker. The cirrus contained a bipartite seminal vesicle with the anterior seminal vesicle smaller to equitable to the posterior seminal vesicle. Both vesicles appeared sacculate (Table 1.16). Genital pore

appeared to open in medial part of body, near level of pharynx. Relationship to the cecal fork could not be identified on any individuals examined.

Two contiguous 28S rDNA sequences were obtained and no divergence was detected. The 28S rDNA sequences matched another undescribed Psilostomidae species (KT956953) from a recent study (Tkach et al. 2016). However, as with species B, no formal morphological description has been reported for the species.

Zygocotyle lunata Diesing, 1836

Family Zygocotylidae Ward 1917

Hosts: *A. platyrhynchos, A. collaris, Aix sponsa, Aythya americana*

Location in host: Posterior small intestine, large intestine, and ceca

Genotype: 28S (Fig. 1.13); CO1 (Fig. 1.14)

Description: Adult *Z. lunata* Diesing, 1836 were compared between collected hosts (Table 1.18) showing minimal variation. Comparison to prior descriptions showed sizable variation between studies (i.e. BL= 9110 *vs* 4839 in *C. melancorphya vs A. collaris*, respectively); however, variation may be due to the different definitive hosts, sample collection sites, duration of infection, and limited sample size (Table 1.19).

Collected *Z. lunata* were elongate-oval with a small to medium body length (i.e. 1-10mm) with two oral diverticula posterior to the oral sucker. The cecal fork was immediately posterior to esophageal bulb with simple cecae reaching near anterior margin of the ventral sucker. Ventral sucker had a ventro-terminal location with well-defined margins extending anterior to near the ovary with two muscular papillae on

posterior margin, much larger than the oral sucker. Ovary was median, closely associated with the seminal receptacle and Mehlis gland. Egg number varied highly between individuals, reaching upwards of 114 in an individual. Testes were apparently lobed, tandem with posterior testis equitable to or larger than anterior testis. Vitelline fields extended from posterior margin of the oral sucker to anterior-lateral margins of the ventral sucker, lateral to ceca (Fig. 1.15).

Sequences of 28S rDNA was taken from a total of 6 *Z. lunata* from *A. platyrhynchos* collected in the fall (3), *A. platyrhynchos* collected in the spring (1) and *A. collaris* (2). No differences in 28S rDNA sequences were detected between worms from the different hosts. Sequences of CO1 were taken from *Z. lunata* from *A. platyrhynchos* from both seasons, with no divergence detected them, which is supportive of identification of the worms studied here as members of *Z. lunata*.

Discussion

The results of this study increase our understanding of morphometric characteristics of the 10 trematode species evaluated. In most cases, diagnostic nucleotide sequence data was used to confirm the identity of these species and to document some extent of intra- and inter-specific variability among these species at these loci. Discussion points related to morphometric, genetic, or phylogenetic attributes of each of these species, are discussed below for each species.

Echinoparyphium recurvatum Linstow, 1873

The crypticism of members within *Echinoparyphium* is a recurring conflict when performing diagnostic studies within this genus. Previous studies have shown that a more comprehensive morphometric and genetic analysis of the genus *Echinoparyphium* is needed due to multiple, divergent, unidentified *Echinoparyphium* individuals. *Echinoparyphium recurvatum* was suggested to be classified as a paraphyletic genus. Several well-known echinostomatid species (e.g., *Echinostoma revolutum, and Echinoparyphium recurvatum)* have been repeatedly misdiagnosed in the past both in the terms of synonymizing and splitting species, which continue to hamper current studies. (McCarthy 1990; Kanev et al. 1998; Sorensen et al. 1998; Saijuntha et al. 2011).

Many recent studies of *E. recurvatum* only report genetic sequences, while historically *E. recurvatum* has been identified through morphology with the inclusion of many morphotypes (Lee et al. 1990; Kanev et al. 2008; Saijuntha et al. 2011; Tkach et al. 2016). This has further led to what is suspected to be a complex of species under the name *E. recurvatum*.

The morphotypes of *E. recurvatum* found in this study were smaller in many regards; although, similar to Korean isolates found by Lee et al (1990) and Sohn (1998). Additionally, some features (e.g., CSL, CSW, and ATW) were found below reported ranges. The overlap of measurements among Lee et al. (1990), Sohn (1998), Kanev et al. (2008), Sereno-Uribe et al. (2015) and the present study, in addition to the presence of 45 spines with 5 corner spines in all data sets supports the *E. recurvatum* Linstow, 1873

diagnosis, in addition to providing further evidence of the wide morphometric range associated with the species.

The two contiguous 28S rDNA sequences of *E. recurvatum* were genetically identical to the published sequence retrieved from a recent systematic study on the family Echinostomatidae (Tkach et al. 2016) within the 1001nt 28S rDNA alignment. Interestingly, the matching sequence (Tkach et al. 2016) came from *E. recurvatum* collected in *Radix ovata* snails from Slovakia. Unfortunately, no adult morphology was reported in that study preventing morphological comparison. Additionally, *E. rubrum* (Tkach et al. 2012) and *E. cinctum* (Tkach et al. 2001), both of which possess 43 collar spines worms were found identical to *E. recurvatum* even though the three species are highly divergent in morphology.

Unfortunately, the genetic similarity between *E. recurvatum* from this study, *E. cinctum* and *E. rubrum* hinders the utilization of the 28S rDNA amplicon as a species-specific diagnostic sequence in the absence of morphological considerations. Rather, 28S rDNA can only be used to identify the complex of species, which can then be further diagnosed through morphological characteristics.

Echinoparyphium speotyto Buscher, 1978

Echinoparyphium speotyto individuals were found in the anterior small intestine of a mallard collected in spring 2013; *E. speotyto* was original described as inhabiting the anterior small intestine of the burrowing owl, *Speotyto cunicalaria*. This is the first report of *E. speotyto* within *A. platyrhynchos*.

No genetic sequence associated with *E. speotyto* has been reported previously. As such, species diagnosis relied upon morphological characteristics. The well-developed pars prostica along with presence of 41 spines with 5 corner spines supports this identification due to the similarity of morphometrics from Buscher (1978).

Based upon the ML and MP phylogenies for 28S rDNA (Figs. 1.16-17), *Hypoderaeum conoideum* (Tkach et al. 2016), an Echinostomatidae sp. (Hicks et al. no date due to direct submission) and *Echinoparyphium* sp. (Tkach et al. 2016) were found to be genetically closest to *E. speotyto*. *Hypoderaeum* has been described as having an intimate genetic relationship with *Echinoparyphium*, as such its relative relationship to *E. speotyto* is unsurprising. *H. conoideum* diverges morphologically in the presence of a very short forebody, small needle-like spines, and a spine count of over 45 (Azizi et al. 2015). Further, genetic divergence in 28S rDNA from *H. conoideum* was found at 0.8% [7nt] (uncorrected p-distance), supportive of distinct species. In comparison, both *Echinoparyphium* sp. and Echinostomatidae sp. were found to only vary by 0.1% [1nt] from *E. speotyto*, potentially indicating distinct species, but further data is necessary to substantiate such a claim.

E. speotyto was found identical to *E. recurvatum* (Kostadinova et al. 2003) and *Echinoparyphium* sp. (Detwiler et al. 2010) in the ITS sequences obtained and with only one nucleotide (0.2% uncorrected p-distance) varying from a third *Echinoparyphium* sp. (Detwiler et al. 2010) in the 504nt ITS alignment (Figs. 1.18-19.). Unfortunately, the short sequences available from the worms collected at Lake Winnibigoshish, MN, limited

the utility of this locus for diagnostic purposes because the nucleotide data gathered was from a highly conserved region of this locus. As such, additional genetic or morphological data is required to be confident that *E. speotyto* is the best diagnosis for these *Echinoparyphium* isolates. This is the first genetic description of *E. speotyto* with its morphology described.

Echinoparyphium sp.

Echinoparyphium sp. was harvested from mallards collected in fall 2012 and spring 2013, showing no seasonal divergence in 28S rDNA sequences. Morphological features could not be compared due to the only spring individual being utilized for genetic analysis. Gross morphology was compared between seasons prior to DNA extraction showing no major divergence (Data not shown).

As noted previously, no currently accepted member of *Echinparyphium* has 39 collar spines, however, *E. indicum*, a previously recognized species, has 38 to 39 collar spines. The variation in compared body size between *E. indicum* Rai, 1962 (Mehra 1980) and the *Echinoparyphium* species presented here could be due to host, population, or environmental factors; however, it is unlikely the other measurements and proportions, such as oral and dorsal spine sizes, would vary so highly within a species. This evidence supports the unidentified *Echinoparyphium* species presented as being distinct from *E. indicum*.

Echinoparyphium sp. is genetically most closely related to *Echinoparyphium aconiatum* (Tkach et al. 2016), with 0.8% [7nt] divergence in the 28S rDNA sequences (Figs. 1.16-

1.17.) and is most closely related to *Echinoparyphium mordwilkoi (*Staneviciute et al. 2015) at the ITS region with 1.98% [10nt] divergence (Figs. 1.18-19.). Both *E. aconiatum* and *E. mordwilkoi* are currently described to have 45 spines in contrast to the 39 spines in the present study (Grabda-Kazubska & Kiseliene 1991). Huffman & Fried (2012) have stated the spine count of *E. mordwilkoi* has not been accurately determined to date so certainty about any claims of morphological similarity or difference relative to *E. mordwilkoi* are tentative.

Due to both the genetic and morphological divergence, the identified *Echinoparyphium* sp. seems best to be a distinct species. Yet, until additional studies using more divergent loci or the life cycle of this species can better resolve specific placement, it should remain unidentified as *Echinoparyphium* sp.

Leyogonimus polyoon Braun, 1902

L. polyoon Linstow, 1887 has been associated with bird die-offs in North America, primarily effecting American coot (Cole & Friend 1999). Interestingly, this species was only found in this study as an adult within the American coot (*F. americana*) and, when present, was at high intensities (data not shown).

Limited morphological measures have been given provided for *L. polyoon* Linstow, 1887 since its initial description by Linstow. Cole & Franson (2006) described it as 700 to 1000µm long; however, morphometrics with specific structures were not published. Similarly, Sey (1968) reported *L. polyoon* in *Gallinula chloropus* from Europe, but also

did not provide morphologically details for those samples. This creates some difficulty with accurate species diagnosis, especially because the specimens examined in this study appeared to be highly polymorphic in terms of body form. In appearance, the body appeared globuluar, elongate oval, or pyriform with an almost spherical or distended three-dimensional shape. The change in body form seemed to occur in relation to sexual maturity; the more gravid adults were more spherical containing innumerable eggs, while less gravid or immature adults appeared elongate-oval. This change may be a direct result of the uterus swelling with eggs, displacing other structures.

When the density of eggs was low or the rotation of the body was ideal, the lateral cirrus sac was an ideal diagnostic trait. Other diagnostic traits such as the lobular ovary, testes located in the third quarter with overlapping ceca were occasionally present; however, these features were only obvious in a small group of the worms studied here. In all individuals, vitelline fields that are located in the second quarter of the body in lateral thick clusters were conserved. Unfortunately, most of the observable traits are shared with *Metoliophilus* Macy & Bell, 1968; the difference being a shared genital opening in *Leyogonimus* compared to separate male and female pores in *Metoliophilus* (Lotz & Font 2008).

For living *L. polyoon,* it has been noted egg shedding can be induced to better visualize internal structures (M. Sterner 2015 *pers. comm*. March). However, the only reliable methods for identification of deceased, highly gravid adults appear to be the presence of associated pathogenesis, shared genital pore, or genetic analysis.

Maximum Parsimony and Likelihood analysis using 28S rDNA placed *L. polyoon* with morphologically similar taxa (Fig. 1.16-17). Comparison of 28S rDNA sequences to the closest related taxa available, (*Allassogonoporus* Oliver, 1938, *Collyricloides* Vaucher, 1969, *Collyricium* Kossack, 1911, and *Cortrema* Tang, 1951), supported taxonomic placement within Order Plagiorchiida (Fig. 1.8). Genetic divergence (uncorrected p-distance) from the closest genera, *Allassogonoporus* (4.1% [37nt]), *Collyricloides* (4.4% [40nt]), *Cortrema* (4.7% [43nt]), and *Collyricium* (5.2% [47nt]) supports placement of *L. polyoon*'s as distinct genus within a distinct family.

Maritrema obstipum van Cleave & Mueller, 1932

Metacercariae of *M. obstipum* have been identified in the midwestern United States previously, however, this is the first report of adults present in wild waterfowl in the area (Muzall & Prachaeil, 2007). Original description of *M. obstipum* did not note a spinous plate, rather only a spinous ventral sucker. Deblock (1973) described a subgenus of *Maritrema, Maritrema* (*Atriospinosum*), with *M. obstipum* as the type species. *M.* (*A.*) *obstipum. Martirema* (*Atriospinosum*) was described to have a modified genital pore with a spinous plate and sub-tegumental rings. Chung et al. (2011) did not report the presence of genital pore modifications. In the current study, there were apparent spines on the entire ventral surface of the ventral sucker along with a dense subset closer to the genital pore opening. However, the spines were not dense enough or associated with a distinct structure beyond the normal ventral sucker musculature.

Measurements of *M. obistipum* from this study were smaller than prior descriptions from the United States and Korea, however, Etges (1953) described the species as highly

polymorphic in his description. Several body forms were described by Etges (1953) dependent on excretory system features and development processes that could account for the variability seen. Interestingly, adjusted proportions showed the current sample of *M. obstipum* to be similar to Etges's study, while values from Chung et al. (2011) diverged greatly. The differences in gross morphology may be due to the polymorphic nature of these traits in this species; however, it is unusual that values would diverge to such an extent. The lack of genetic data from the present study and previous studies of *M. obstipum* prevents further analysis or a more specific diagnosis.

Sphaeridiotrema pseudoglobulus McLaughlin, Scott, & Huffman, 1993

In comparison to McLaughlin et al. (1993), body length and width of worms collected for this study were found to be smaller and closer in size to *Sphaeridiotrema globulus* Rudolphi, 1814 (Price 1934). Interestingly, the size of many structures (i.e. suckers, gonads) was strongly reduced in the specimens measured here. Ratios of structure sizes (i.e. ovary length to width) also appear to vary highly from prior studies (Table 1.15).

Egg size, which is one of the crucial diagnostic traits separating *S. globulus* and *S. pseudoglobulus,* was found to drop below those currently described for *S. pseudoglobulus* into the range of *S. globulus* for the worms in this study. This increased range of egg length furthers the difficulty of morphological identification between these 2 species, indicating the need for use of alternative methods of diagnosis such as nucleotide differences. Further, calculated proportions of body features (e.g. BW%) do not appear diagnostic for species identification of these two species due to highly convergent proportional measures.

Undefined Psilostomidae species A.

The morphology of species A was most comparable to *Psilostomum*. However, species A diverges from the current description of *Psilostomum* in the larger ventral to oral sucker proportion and the apparent lack of a cirrus. The apparent lack of cirrus may be due to the quality of specimens measured here; however, additional individuals were examined, but not measured and they also lacked a cirrus. Further, 28S rDNA diverged by 5.8% [53nt] from *Psilostomum* across the 1001 nt compared along with distinct distant placement in both ML and MP analyses (Figs. 1.16-1.17). Genetic divergence in combination with morphology is supportive of these worms being considered resident of a distinct, undescribed genus.

Undefined Psilostomidae species B and C.

The morphology of Species B and C was similar to members of *Neopsilotrema* Kudlai, Pulis, Kostadinova, & Tkach, 2016 (*in press*). Species B shared sizable overlap with *Neopsilotrema lisitsynae* Kudlai, Pulis, Kostadinova, & Tkach, 2016 (*in press*), but differed in having a much shorter post-testicular field. Species C was similar to other *Neopsilotrema* species in regards to placement and appearance of the vitelline fields, a smaller body size, and other morphometric values (Kudlai et al. *in press*).

Species B and C diverged from one another at 1% [9nt] in 28S rDNA, supportive of distinct species. Sequences of 28S rDNA placed species B and C closest to *Neopsilotrema* with 1.9% [17nt] and 1.4% [13nt] divergence respectively. This divergence is close to the described intrageneric variation for members of *Plagiorchis* Lühe, 1899 (0.3-1.8%), but well beyond other taxa, such as *Echinostoma* Rudolphi, 1809

(0.25-0.41%) (Georgiva et al. 2014; Zikmundová et al. 2014); however, both species were placed into a distinct sister group relative to *Neopsilotrema* in both ML and MP analyses (Figs. 1.16-1.17). Based upon similar morphology and 28S rDNA divergence, species B and C may be placed into *Neopsilotrema* tentatively, until further distinction can be made, however, this is expected to be an exceedingly temporary placement.

Zygocotyle lunata Diesing, 1836

Z. lunata is one of two currently accepted species within family Zygocotylidae Ward, 1917. Morphological features of *Z. lunata* varied similarly to previous studies (Sutton & Lunaschi, 1987; Ostrowski de Núñez et al 2011). Many studies have examined morphology and life cycle aspects of *Z. lunata,* while minimal genetic analysis has been performed (Fried et al. 2009; van Steenkiste et al 2014).

Z. lunata individuals examined across hosts and seasons, were identical at both loci examined. Although, a different region of CO1 of *Z. lunata* has been sequenced in a prior study, it was not used for comparison here due to the lack of an overlapping regions (van Steenkiste et al. 2014). The 28S rDNA sequences obtained here for *Z. lunata* were identical to *Wardius zibethicus* (JQ670847) Barker & East, 1915, the other member of Family Zygocotylidae. The genetic similarity is surprising as both species are distinct in host use patterns (avian *vs* mammal) and body structures (muscular papillae present *vs* absence). The CO1 sequences of *W. zibethicus* have not been obtained; as such, genetic comparisons could not be made. The close genetic relationship at the 28S rDNA locus indicates its lack of utility for species diagnosis. Low 28S rDNA sequence divergence was seen between *Gastrothylax* (1.8% [16nt]) and *Paramphistomum* (1.9% [17nt]), other

members of Superfamily Paramphistomoidea, Fischoeder, 1901. This amount of divergence is equitable to interspecific variation reported in Family Haploporidae Nicoll, 1914 (0.9-2.1%) by Blasco-Costa et al. (2009). Generic placement was as expected in both maximum parsimony and likelihood analysis (Fig. 1. 16-17) with *Zygocotyle* being within a clade containing other members of its Superfamily.

Nucleotide sequences at CO1 for *Z. lunata* could not be compared to those of *Wardius* due to a lack of available sequence data on GenBank. Genetic divergence detected between other members of Superfamily Paramphistomoidea in the 194 nt CO1 alignment ranged from 5.4% [11nt] to 9.8% [20nt] (*Paramphistomum* and *Gastrothylax*) and was somewhat lower than intergeneric divergence reported by Saijuntha et al. (2011) amongst *Echinostoma* sp. (8-16%). The CO1 sequence data reported herein was compared to members of Superfamily Echinostomatoidea indicating 14.4% to 15.3% (data not shown). Maximum parsimony and likelihood analysis placed *Z. lunata* with members of *Paramphistomum*. However, *Paramphistomum* species were not placed within one clade, rather the two species not associated with *Zygocotyle* were places as individual clades (Fig. 1.20-21).

The observation of the lack of divergence between *Zygocotyle* and *Wardius*, along with the close genetic relationship to sister taxa at both 28S and CO1 loci supports previous study of another member of Superfamily Paramphistomoidea. Ghatani et al. (2014) that found 28S rDNA to be conserved amongst members of Family Gastrothylacidae preventing diagnostic utility, while CO1 sequences were found to differentiate between

species. In combination, the utilization of CO1 for species diagnosis appears most reliable for members of Superfamily Paramphistomoidea.

The examples and arguments given for the 10 species from the 5 Families described here demonstrate that no single diagnostic technique can have universal utility. Morphological descriptions that include morphometric measures and ratios along with genetic information are necessary and should continue to be the goal of all diagnostic studies. Future studies should expand the list of available diagnostic sequences to include more divergent loci and, when possible perform life cycle studies to demonstrate morphological characteristics of all life cycle stages for the utmost clarity of species identity.

References

Atopkin, D. M. (2011). Genetic characterization of the *Psilotrema* (Digenea: Psilostomatidae) genus by partial 28S ribosomal DNA sequences. *Parasitology International*, 60 (4), 541–543.

Azizi, H., Farahnak, A., Mobedi, I., & Molaei Rad, M. (2015). Experimental Life Cycle of *Hypoderaeum conoideum* (Block, 1872) Diez, 1909(Trematoda: Echinostomatidae) Parasite from the North of Iran. *Iran Journal of Parasitology*, 10(1), 102–109.

Barker, S. C., Blair, D., Garrett, A. R., & Cribb, T. H. (1993). Utility of the D1 domain of nuclear 28S rRNA for phylogenetic inference in the Digenea. *Systematic Parasitology*, 26, 181–188.

Basch, P. F. (1976). Intermediate host specificity in *Schistosoma mansoni*. Experimental *Parasitology*, 39, 150–169.

Benson, D. A., Cavanaugh, M., Clark, K., Karsch–Mizrachi, I., Lipman, D. J., et al. (2012). GenBank. *Nucleic Acids Research*, 41(D1).

Bergmame, L., Huffman, J., Cole, R., Dayanandan, S., Tkach, V. V., & McLaughlin, J. D. (2011). *Sphaeridiotrema globulus* and *Sphaeridiotrema pseudoglobulus* (Digenea): Species differentiation based on mtDNA (barcode) and partial LSU–rDNA sequences. *Journal of Parasitology*, 97(6), 1132–1136.

Blasco-Costa, I., Balbuena, J. A., Kostadinova, A., & Olson, P. D. (2009). Interrelationships of the Haploporinae (Digenea: Haploporidae): A molecular test of the taxonomic framework based on morphology. *Parasitology International,* 58(3), 263–269.

Bowles, J., Blair, D., & McManus, D. P. (1995). A molecular phylogeny of the genus *Echinococcus*. *Parasitology*, 110(3), 317–328.

Buscher, H. (1978). *Echinoparyphium speotyto* sp. n. (Trematoda: Echinostomatidae) from the burrowing owl in Oklahoma, with a discussion of the genus *Echinoparyphium*. *Journal of Parasitology*, 64, 52–58.

Chung, O., Sohn, W., Chai J., Seo, M., & Lee, H. (2011). Discovery of *Maritrema obstipum* (Digenea: Microphallidae) from migratory birds in Korea. *Korean Journal of Parasitology*, 49(4), 457–460.

Cole, R. A. & Friend, M. (1999). Miscellaneous parasitic diseases. In M. Friend & J. C. Franson (Eds.), *Field Manual of Wildlife Diseases: General Field Procedures and Diseases of Birds* (249–258). Washington, D.C.: USGS.

Cole, R. A., & Franson, J. C. (2006). Recurring waterbird mortalities of unusual etiologies. In: G. C. Boere, C. A. Galbraith, & D. A. Stroud (Eds.), *Waterbirds around the world* (pp. 439–440). Edinburgh: The Stationery Office.

Detwiler, J. T., Bos, D. H., & Minchella, D. J. (2010). Revealing the secret lives of cryptic species: Examining the phylogenetic relationships of echinostome parasites in North America. *Molecular Phylogenetics and Evolution, 55*(2), 611–620.

Detwiler, J. T., Zajac, A. M., Minchella, D. J., & Belden, L. K. (2012). Revealing cryptic parasite diversity in a definitive host: Echinostomes in muskrats. *Journal of Parasitology, 98*(6), 1148–1155.

Deblock, S. (1973). Contribution à l'étude des Microphallidae Travassos, 1920 (Trematoda). XXVII. A propos d'espèces décrites au Japon par S. Yamaguti: A. Invalidation du genre *Maritreminoides* Rankin. Creation de genres satellites du genre *Maritrema*: *Quasimaritrema*, Maritremopsis et Quasintaritremopsis. *Ann. Parasitol. Hum. Comp.*, 48, 543–557 (In French).

Digiani, M. C. (1997). El cisne de cuello negro *Cygnus melancorypha*: nuevo hospedador de *Zygocotyle lunata* (Diesing) (Trematoda: Paramphistomatidae). Neotropica 43, 84 (In Spanish).

Etges, F. J. (1953). Studies on the life histories of *Maritrema obstipum* (Van Cleave and Mueller,1932) and *Levinseniella amnicolae* n. sp. (Trematoda: Microphallidae). *Journal of Parasitology*, 39, 643–662.

Fried, B., Huffman, J., Keeler, S. & Peoples, R. C. (2009). The biology of the caecal trematode *Zygocotyle lunata*. *Advances in Parasitology*, 69, 1–40.

Gagnon, C. (1990). Pathological consequences of infection by *Cyathocotyle bushiensis* (Khan, 1962) and *Sphaeridiotrema globulus* (Rudolphi, 1814) in two species of dabbling ducks. M.S. Thesis. McGill University, Montreal, Quebec, Canada.

Galaktionov, K. V., Blasco-Costa, I., & Olson, P. D. (2012). Life cycles, molecular phylogeny and historical biogeography of the 'pygmaeus' microphallids (Digenea: Microphallidae): Widespread parasites of marine and coastal birds in the Holarctic. *Parasitology*, 139(10), 1346–1360.

Georgieva, S., Faltýnková, A., Brown, R., Blasco-Costa, I., Soldánová, M., et al. (2014). *Echinostoma 'revolutum'* (Digenea: Echinostomatidae) species complex revisited: Species delimitation based on novel molecular and morphological data gathered in Europe. *Parasites Vectors Parasites & Vectors*, 7(1). doi: 10.1186/s13071–014-0520-8

Ghatani, S., Shylla, J., Roy, B., & Tandon, V. (2014). Multilocus sequence evaluation for differentiating species of the trematode Family Gastrothylacidae, with a note on the utility of mitochondrial CO1 motifs in species identification. *Gene*, 548, 277–284.

Giddings, M. C., Severin, J., Westphall, M., Wu, J., & Smith, L. M. (1998). A software system for data analysis in automated DNA sequencing. *Genome Research*, 8(6), 644–665.

Grabda-Kazubska B. & Kiseliene V. (1991). The life cycle of *Echinoparyphium mordwilkoi* Skrjabin, 1914 (Trematoda: Echinostomatidae). *Acta Parasitologica Polonica*, 36,167–173.

Graczyk T., (1991). Variability of metacercariae of *Diplostomum spathaceum* (Rudolphi, 1819) (Trematoda, Diplostomidae). *Acta Parasitol*., 36, 135–139.

Hasegawa, M., Kishino, H., & Yano, T. (1985). Dating of the human-ape splitting by a molecular clock of mitochondrial DNA. *Journal of Molecular Evolution*, 22(2), 160–174.

Heneberg, P., & Literák, I. (2013). Molecular phylogenetic characterization of *Collyriclum faba* with reference to its three host-specific ecotypes. *Parasitology International*, *62*(3), 262–267.

Herbert, P. D., Cywinska, A., Ball, S. L., & deWaard, J. R. (2003). Biological identifications through DNA barcodes. *Proceedings of the Royal Society. B, Biological Sciences*, 270(1512), 313–321.

Herrmann, K. K., & Sorensen, R. E. (2011). Differences in natural infections of two mortality-related trematodes in lesser scaup and American coot. *The Journal of Parasitology*, 97(4), 555–558.

Huffman, J. & Fried, B. (2012). The Biology of *Echinoparyphium* (Trematoda, Echinostomatidae). *Acta Parasitologica*, 57(3), 199–210.

Kanarek, G., Zalesny, G., Sitko, J., & Tkach, V. V. (2014). Phylogenetic relationships and systematic position of the families Cortrematidae and Phaneropsolidae (Platyhelminthes: Digenea). *Folia Parasitologica*, 61(6), 523–528.

Kanarek, G., Zaleśny, G., Czujkowska, A., Sitko, J., & Harris, P. D. (2015). On the systematic position of *Collyricloides massanae* Vaucher, 1969 (Platyhelminthes: Digenea) with notes on distribution of this trematode species. *Parasitology Research Parasitol Res*, 114(4), 1495–1501.

Kanev, I., Sorensen, R., Sterner, M., Cole, R., & Fried, B. (1998). The identification and characteristics of *Echinoaryphium rubrum* (Cor, 1914) comb. new (Trematode, Echinostomatidae) based on experimental evidence of the life cycle. *Acta Parasitologica*, 43(4), 181–188.

Kanev, I., Fried, B., & Valentin, R. (2008). Identification problems with species in the *Echinoparyphium recurvatum* complex from physid snails in the USA. *Parasitology Research*, 103, 963–965.

Kanev, I., Fried, B., & Radev, V. (2009). Collar spine models in the genus Echinostoma (Trematoda: Echinostomatidae). *Parasitology Research Parasitol Res, 105*(4), 921–927.

Kostadinova, A., Herniou, E. A., Barrett, J., & Littlewood, D. T. J. (2003). Phylogenetic relationships of *Echinostoma* Rudolphi, 1809 (Digenea: Echinostomatidae) and related genera re-assessed via DNA and morphological analyses. *Systematic Parasitology*, (54), 159–176.

Kostadinova, A. (2005a). Family Echinostomatidae Looss, 1899. In: A. Jones, R. A. Bray, D. I. Gibson (Eds.), *Keys to the Trematoda Vol. 2* (pp. 9–64). Wallingford - London: CABI Publishing and The Natural History Museum.

Kostadinova, A. (2005b). Family Psilostomidae Looss, 1900.In: A. Jones, R. A. Bray, D. I. Gibson (Eds.), *Keys to the Trematoda Vol. 2* (pp. 99–118). Wallingford - London: CABI Publishing and The Natural History Museum.

Kudlai, O., Cutmore, S. C., & Cribb, T. H. (2015a). Morphological and molecular data for three species of the Microphallidae (Trematoda: Digenea) in Australia, including the first descriptions of the cercariae of *Maritrema brevisacciferum*

Shimazu et Pearson, 1991 and *Microphallus minutus* Johnston, 1948. *Folia Parasitologica*, 62, doi: 10.14411/fp.2015.053

Kudlai, O., Stunzenas, V., & Tkach, V. V. (2015b). The taxonomic identity and phylogenetic relationships of Cercaria pugnax and C. helvetica XII (Digenea: Lecithoendriidae) based on morphological and molecular data. *Folia Parasitologica*, *62*, doi: 10.14411/fp.2015.003

Kudlai, O., Pulis, E. E., Kostadinova, A., & Tkach, V.V. (*in press*). *Neopsilotrema* n. g. (Digenea: Psilostomidae) and three new species from ducks (Anseriformes: Anatidae) in North America and Europe. *Systemtatic Parasitology.*

Kumar, S., & Hedges, S. B. (2016). Advances in time estimation methods for molecular data. *Molecular Biology and Evolution*, 33(4), 863–869.

Lanave, C., Preparata, G., Saccone, C., & Serio, G. (1984). A new method for calculating evolutionary substitution rates. *Journal of Molecular Evolution*, 20(1), 86–93.

Lee, S. H., Sohn, W. M., & Chai, J. Y. (1990). *Echinostoma revolutum* and *Echinoparyphium recurvatum* recovered from house rats in Yangyang-gun, Kangwon-do. *Korean Journal of Parasitology*, 28(4), 235–240.

Lotz, J. M., & Font, W. F. (2008). Family Leyogonimidae Dollfus, 1951. In: R.A. Bray, D.I. Gibson, and A. Jones (Eds.), *Keys to the Trematoda Vol. 3* (pp. 537–540). London: CAB International and Natural History Museum.

McLaughlin, J. D., Scott, M. E. & Huffman, J. E. (1993). *Sphaeridiotrema globulus* (Rudolphi, 1814): evidence for two species known under a single name and a description of *Sphaeridiotrema pseudoglobulus* n. sp. *Canadian Journal of Zoology*, 71, 700–707.

McCarthy, A. M. (1990). Speciation of echinostomes: evidence for the existence of two sympatric sibling species in the complex *Echinoparyphium recurvatum*. *Journal of Parasitology*, 90, 35–42.

Mehra, H. R. (1980). *The fauna of India and adjacent countries. Platyhelminthes Vol. 1 Trematoda*. Calcutta: Eka Press.

Minchella, D. J., Sorensen, R. E., Curtis, J., & Bieberich, A. A. (1997). Molecular biology of trematodes: advances and applications. In B. Fried & T. K. Graczyk (Eds.), *Advances in Trematode Biology* (pp. 405–446). Boca Raton: CRC Press.

Morgan, J. A. & Blair, D. (1995). Nuclear rDNA ITS sequence variation in the trematode genus *Echinostoma*: an aid to establishing relationships within the 37-collar-spine group. *Parasitology*, 111 (5), 609–615.

Morgan, J. A. T., & Blair, D. (1998). Relative merits of nuclear ribosomal internal transcribed spacers and mitochondrial CO1 and ND1 genes for distinguishing among *Echinostoma* species (Trematoda). *Parasitology*, 116(03), 289–297.

Morgan, J. A., Dejong, R. J., Adeoye, G. O., Ansa, E. D., Barbosa, C. S., et al. (2005). Origin and diversification of the human parasite *Schistosoma mansoni*. *Molecular Ecology*, *14*(12), 3889–3902.

Moszczynska, A., Locke, S. A., McLaughlin, J. D., Marcogliese, D. J., & Crease T. J. (2009). Development of primers for the mitochondrial cytochrome c oxidase I gene in digenetic trematodes (Platyhelminthes) illustrates the challenge of barcoding parasitic helminths. *Molecular Ecology Resources*, 9, 75–82.

Muzzall, P. M., & Pracheil, B. M. (2007). Parasites of Tadpole Madtom, *Noturus gyrinus* (Mitchill, 1817) (Ictaluridae), from Silver Creek, Michigan, U.S.A., with a

Checklist of the North American Parasites of Tadpole Madtom. *Comparative Parasitology,* 74(1), 154–159.

Nolan, M. J. & Cribb, T. H. (2005). The use and implications of ribosomal DNA sequencing for the discrimination of digenean species. *Advances in Parasitology,* 60, 101–163.

O'Dwyer, K., Blasco-Costa, I., Poulin, R., & Faltýnková, A. (2014). Four marine digenean parasites of *Austrolittorina* spp. (Gastropoda: Littorinidae) in New Zealand: Morphological and molecular data. *Systematic Parasitology Syst Parasitol,* 89(2), 133–152.

Olson, P. D., Cribb, T. H., Tkach, V. V., Bray, R. A., & Littlewood, D. T. J. (2003). Phylogeny and classification of the Digenea (Platyhelminthes : Trematoda). *International Journal of Parasitology,* (33), 733–755.

Ostrowski de Núñez, M. Davies, D., & Spatz, L. (2011). The life cycle of *Zygocotyle lunata* (Trematoda, Paramphistomoidea) in the subtropical region of South America. *Revista Mexicana de Biodiversidad*, 82: 581–588.

Poulin, R. & Morand S. (2004). Parasite Biodiversity. *Parasitology,* 131, 725–726.

Price, E. W. (1934). Losses among wild ducks due to infestation with *Sphaeridiotrema globulus* (Rudolphi) (Trematoda; Psilostomidae). *Proc. Helm. Soc. Wash*., 1(2), 31–34.

Roberts, L. & Janovy, J. (2005). *Foundations of Parasitology (7th ed.).* New York: McGraw-Hill Publishing Company.

Rodríguez, F., Oliver, J., Marín, A., & Medina, J. (1990). The general stochastic model of nucleotide substitution. *Journal of Theoretical Biology*, 142(4), 485–501.

Roy, C., & Herwig, C. (2010). Investigation of trematodes and faucet snails responsible for lesser scaup and american coot die-offs. In G. D. DelGiudice, M. Grund, J. S. Lawrence, & M. S. Lenarz (Eds.), *Summaries of Wildlife Research Findings 2010* (pp. 20–27). St. Paul: Minnesota Department of Natural Resources.

Saunders, G. W. (2008). A DNA barcode examination of the red algal family Dumontiaceae in Canadian waters reveals substantial cryptic species diversity. The foliose *Dilsea-Neodilsea* complex and *Weeksia*. *Botany*, 86, 773–789.

Saijuntha, W. & Tantrawatpan, C. (2011). Genetic characterization of *Echinostoma revolutum* and E*chinoparyphium recurvatum* (Trematoda: Echinostomatidae) in Thailand and phylogenetic relationships with other isolates inferred by ITS1 sequence. *Parasitology Research*, 108, 751–755.

Sereno-Uribe, A. L., Pinacho-Pinacho, C. D., Cordero, V., & Garcia Varela, M. (2015). Morphological and molecular analyses of larval and adult stages of *Echinoparyphium recurvatum* von Linstow 1873 (Digenea: Echinostomatidae) from central Mexico. *Journal of Helminthology*, 89, 458–464.

Sey, O. (1968). Trematodes from birds living along the Tisza. *Tiscia (Szeged)*, 4, 59–68.

Shalaby, I. M. I. & Amerc, S. A. M. (2012). Preliminary Molecular Identification of Two Helminthes (*Moniezia* sp. and *Paramphistomum* sp.) in the Province of Taif, Saudi Arabia. *World Applied Sciences Journal*, 17(8), 986–991.

Sohn, W. M. (1998). Life history of *Echinoparyphium recurvatum* (Trematoda: Echinostomatidae) in Korea. *The Korean Journal of Parasitology, 36*(2), 91–98.

Sorensen, R. E., Kanev, I., Fried, B., & Minchella, D. J. (1997). The occurrence and identification of *Echinostoma revolutum* from North American *Lymnaea elodes* snails. *Journal of Parasitology*, 83, 169–170.

Sorensen, R. & Minchella, D. (1998). Parasite influences on host life history: *Echinostoma revolutum* parasitism of *Lymnaea elodes* snails. *Oecologia*, 115, 188–195.

Stanevičiūtė, G., Stunžėnas, V., & Petkevičiūtė, R. (2015). Phylogenetic relationships of some species of the family Echinostomatidae Odner, 1910 (Trematoda), inferred from nuclear rDNA sequences and karyological analysis. *Comparative Cytogenetics CCG, 9*(2), 257–270.

Sutton, C. A. & Lunaschi, L. I. (1987). On some digeneans found in Argentine wild vertebrates. *Neotropica*, 33, 89–95 (In Spanish).

Szidat, L. (1937). About some new Caryophyllaeiden from East Prussian fishing. *Journal of Parasites*, 9, 771–786 (In Russian).

Tavare, S. (1986). Some probabilistic and statistical problems in the analysis of DNA sequences. *Lectures on Mathematics in the Life Sciences (American Mathematical Society)*, 17, 57– 86.

Tkach, V. V., Grabda-Kazubska, B., Pawlowski, J., & Świderski, Z. (1999). Molecular and morphological evidence for close phylogenetic affinities of the genera *Macrodera, Leptophallus, Metaleptophallus* and *Paralepoderma* (Digenea, Plagiorchiata). *Acta Parasitology*, 44,170–179.

Tkach, V. V., Pawlowski, J., & Mariaux, J. (2000). Phylogenetic analysis of the suborder Plagiorchiata (Platyhelminthes, Digenea) based on partial lsrDNA sequence. *International Journal for Parasitology*, 30(1), 83–93.

Tkach, V. V., Pawlowski, J., Mariaux, J., & Swiderski, Z. (2001) Molecular phylogeny of the suborder Plagiorchiata and its position in the system of Digenea. In D. T. J. Littlewood & R. A. Bray (Eds.), *Interrelationships of platyhelminthes* (pp. 186–193). London: Taylor & Francis Inc.

Tkach, V. V., Littlewood, D. T., Olson, P. D., Kinsella, J. M., & Swiderski, Z. (2003). Molecular phylogenetic analysis of the Microphalloidea Ward, 1901 (Trematoda: Digenea). *Systematic Parasitology Syst Parasitol*, 56(1), 1–15.

Tkach, V. V., Schroeder, J., Greiman, S., & Vaughan, J. (2012). New genetic lineages, host associations and circulation pathways of *Neorickettsia* endosymbionts of digeneans. *Acta Parasitologica*, *57*(3), 285–292.

Tkach, V. V., Kudlai, O., & Kostadinova, A. (2016). Molecular phylogeny and systematics of the Echinostomatoidea Looss, 1899. *International Journal of Parasitology*, 46(3), 171–185.

van Steenkiste, N., Locke, S. A., Castelin, M., Marcogliese, D. J., & Abbott, C. (2015). New primers for DNA barcoding of digeneans and cestodes (Platyhelminthes). *Molecular Ecology Resources*, 15(4), 945–952.

Vilas, R., Criscione, C. D. & Blouin, M. S. (2005). A comparison between mitochondrial DNA and the ribosomal internal transcribed regions in prospecting for cryptic species of platyhelminth parasites. *Parasitology*, 131(6), 839–846.

Ward, R. D., Zemlak, T. S., Innes, B. H., Last, P. R., & Herbert, P. D. (2005). DNA barcoding Australia's fish species. *Philopsophical Transactions of the Royal Society B: Biological Sciences*, 360(1462), 1847–1857.

Willey, C. H. (1941). The life history and bionomics of the trematode, *Zygocotyle lunata* (paramphistomidae). *Zoologica*, 26, 65–88.

Whalen, S. (2011). Analysis of the genetic structure of *Bithynia tentaculata* snail populations in Wisconsin and Minnesota. (Master's thesis). Minnesota State University, Mankato, MN.

White, T. J., Bruns, T., Lee, S., & Taylor, J. W. (1990). Amplification and direct sequencing of fungal ribosomal RNA genes for phylogenetics. In M. S. Innis, D. H. Gelfand, J. J. Sninsky, & T. J. White (Eds.), *PCR Protocols: A Guide to Methods and Applications* (pp. 315–322). New York: Academic Press, Inc.

Yan, H., Wang, X., Lou, Z., Li, L., Blair, D., et al. (2013). The mitochondrial genome of *Paramphistomum cervi* (Digenea), the first representative for the Family Paramphistomidae. *PLoS ONE, 8*(8), doi: 10.1371/journal.pone.0071300

Zheng, X., Chang, Q., Zhang, Y., Tian, S., Lou, Y., et al. (2014). Characterization of the complete nuclear ribosomal DNA sequences of *Paramphistomum cervi*. *The Scientific World Journal*, *2014*, doi: 10.1155/2014/751907

Zikmundová, J., Georgieva, S., Faltýnková, A., Soldánová, M., & Kostadinova, A. (2014). Species diversity of *Plagiorchis* Lühe, 1899 (Digenea: Plagiorchiidae) in lymnaeid snails from freshwater ecosystems in central Europe revealed by molecules and morphology. *Systematic Parasitology, 88*(1), 37–54.

Table 1.1 Number of each waterbird species collected in each season.

Bird species	Common name	Fall	Spring
Aix sponsa	Wood duck	7	3
Anas carolinensis	Green-winged teal	0	1
Anas platyrhynchos	Mallard	10	11
Anas discors	Blue-winged teal	15	2
Anas acuta	Pintail	1	0
Aythya americana	Redhead	1	0
Aythya marila	Greater scaup	1	1
Aythya collaris	Ring-necked duck	13	7
Aythya affinis	Lesser scaup	10	1
Bucephala albeola	Bufflehead	3	2
Bucephala clangula	Common goldeneye	0	4
Fulica americana	American coot	11	1

Table 1.2. Primers used for DNA amplification for species diagnosis. The abbreviation (bp) is the approximate number of base pairs expected in various species. Region refers to whether the primer pair is specific to mitochondrial the cytochrome oxidase (CO1) locus, the internal transcribed region of ribosomal DNA (ITS), or 28S ribosomal DNA. (^{o}C) is the annealing temperature used during the initial PCR and in the subsequent sequencing PCR.

Primer name	Primer sequence (5'-3')	(bp)	Region	(^{o}C)	Reference
JB3-CO1F	TTTTTTGGGCATCCTGAGGTTTAT	250	CO1	54	Morgan & Blair 1998
JB13-CO1R	TCATGAAAACACCTTAATACC			50	
ITS5 [F]	GGAAGTAAAAGTCGTAACAAG	1200	ITS	49	White et al. 1990
ITS4 [R]	TCCTCCGCTTAGTGATATGC			54	
DIG12-28SF	AAGCATATCACTAAGCGG	1200	28S	50	Tkach et al. 1999; Atopkin 2011
1200R-28SR	GCATAGTTCACCATCTTTCGG			54	

Table 1.3. GenBank accession numbers of Superfamily Echinostomatoidea members for 28S and ITS alignments.

Family	Genus species	Accession #	Locus	Reference
Echinostomatidae	*Echinoparyphium aconiatum*	KT956912	28S	Tkach et al. 2016
Echinostomatidae	*Echinoparyphium cinctum*	AF184260	28S	Tkach et al. 2001
Echinostomatidae	*Echinoparyphium recurvatum*	KT956913	28S	Tkach et al. 2016
Echinostomatidae	*Echinoparyphium rubrum*	JX262943	28S	Tkach et al. 2012
Echinostomatidae	*Echinoparyphium sp.*	KT956914	28S	Tkach et al. 2016
Echinostomatidae	*Echinostomatidae sp.*	GU270100	28S	Hicks et al. (Direct submission)
Echinostomatidae	*Echinostoma revolutum*	AY222246	28S	Olsen et al. 2003
Echinostomatidae	*Euparyphium cf. murinum*	KT956917	28S	Tkach et al. 2016
Echinostomatidae	*Hypoderaeum conoideum*	KT956919	28S	Tkach et al. 2016
Echinostomatidae	*Echinoparyphium mordvilkowi*	KJ542640	ITS	Staneviciute et al. 2015
Echinostomatidae	*Echinoparyphium recurvatum*	AY168931	ITS	Kostadinova et al. 2003
Echinostomatidae	*Echinoparyphium sp.*	GQ463135	ITS	Detwiler et al. 2010
Echinostomatidae	*Echinoparyphium sp.*	GQ463136	ITS	Detwiler et al. 2010
Echinostomatidae	*Hypoderaeum conoideum*	AJ564385	ITS	Marcilla et al. unpublished
Psilostomidae	*Neopsilotrema affinis*	KT956953	28S	Tkach et al. 2016
Psilostomidae	*Neopsilotrema lakotae*	*in press*	28S	Kudlai et al. *in press*
Psilostomidae	*Psilochasmus oxyurus*	AF151940	28S	Tkach et al. 2000
Psilostomidae	*Psilostomidae sp.*	KT956954	28S	Tkach et al. 2016
Psilostomidae	*Psilostomum brevicolle*	KT956950	28S	Tkach et al. 2016

Table 1.4. GenBank accession numbers of Superfamily Haploporoidae and Microphalloidea members for 28S, ITS, and CO1 alignments.

Family	Species	Accession #	Locus	Reference
Superfamily Haploporoidae				Blasco-Costa et al. 2009
Haploporidae	*Dicrogaster contracta*	FJ211262	28S	
Superfamily Microphalloidea				
Collyriclidae	*Collyriclum faba*	JQ231122	28S	Heneberg & Literak 2013
Cortrematidae	*Cortrema magnicaudata*	KJ700420	28S	Kanarek et al. 2014
Lecithodendriidae	*Lecithodendrium sp.*	KJ126726	28S	Kudlai et al. 2015
Microphallidae	*Maritrema minutus*	KT355823	28S	Kudlai et al. 2015
Microphallidae	*Microphallus similis*	HM584138	28S	Galaktionov et al. 2012
Pleurogenidae	*Allassogonoporus amphoraeformis*	AF151924	28S	Tkach et al. 2000
Pleurogenidae	*Collyricloides massanae*	KP682451	28S	Kanarek et al. 2015
Pleurogenidae	*Parabascus joannae*	AY220619	28S	Tkach et al. 2003
Prosthogonimidae	*Prosthogonimus cuneatus*	AY220634	28S	Tkach et al. 2003
Prosthogonimidae	*Schistogonimus rarus*	AY116869	28S	Tkach et al. 2003
Microphallidae	*Microphallus sp.*	HM584140	ITS	Galaktionov et al. 2012
Microphallidae	*Microphallus sp.*	KJ868203	CO1	O'Dwyer et al. 2014

Table 1.5. GenBank accession numbers of Superfamily Paramhphistomoidea members for 28S and CO1 alignments.

Family	Genus species	Accession #	Locus	Reference
Gastrothylacidae	*Gastrothylax crumenifer*	JX518971	28S	Ghatani et al. 2014
Paramphistomidae	*Paramphistomum cervi*	KJ459936	28S	Zheng et al. 2014
Zygocotylidae	*Wardius zibethicuz*	JQ670847	28S	Detwiler et al. 2012
Gastrothylacidae	*Carmyerius spatiosus*	JQ806363	CO1	Ghatani et al. 2014
Gastrothylacidae	*Fishoederious cobboldi*	JX518951	CO1	Ghatani et al. 2014
Gastrothylacidae	*Fishoederious elongatus*	JQ806365	CO1	Ghatani et al. 2014
Gastrothylacidae	*Gastrothylax crumenifer*	JX518944	CO1	Ghatani et al. 2014
Gastrothylacidae	*Velasquezotrema tripurensis*	JQ688407	CO1	Ghatani et al. 2014
Paramphistomidae	*Paramphistomum cervi*	KF475773	CO1	Yan et al. 2013
Paramphistomidae	*Paramphistomum epiclitum*	LC113923	CO1	Sanguankiat et al. 2016
Paramphistomidae	*Paramphistomum sp.*	AB688990	CO1	Mehrez and Amer 2011

Table 1.6. Morphometric comparison of *E. recurvatum* cephalic collar and spines from current and prior studies from assorted geographical locations.

	Lee et al. 1990	Sohn 1998	Kanev et al. 2008		Sereno-Uribe et al. 2015	Present study		
Source	Korea	Korea	Europe	USA	Mexico	Minnesota, USA		
Metric	Range	Range ($\bar{x}$)	Range	Range	Range ($\bar{x}$)	$\bar{x}$±SE	Range	n
Collar width	290-340	260-310 (280)	310-660	280-588	-	230±22	181-296	5
OSpL	-	-	42-48	38-50	49-66 (57)	60±3	48-73	9
OSpW	-	-	-	-	-	13±1	10-15	10
ASpL	-	-	55-65	55-66	-	57±3	31-71	11
ASpW	-	-	-	-	-	13±1	5-16	11
DSpL	-	-	-	-	-	59±3	38-73	15
DSpW	-	-	-	-	-	11±0	8-15	15
CSpL	-	53-70	64-76	66-72	-	57±2	48-74	16
CSpW	-	-	-	-	-	14±1	11-20	16

Table 1.7. Morphometric comparison of *E. recurvatum* body form and structures from current and prior studies from assorted geographical locations.

	Lee et al.1990	Sohn 1998	Kanev et al. 2008		Sereno-Uribe et al. 2015	Present study		
Source	Korea	Korea	Europe	USA	Mexico	Minnesota, USA		
Metric	Range	Range ($\bar{x}$)	Range	Range	Range ($\bar{x}$)	$\bar{x}$±SE	Range	n
BL	3500-4700	2010-3090 (2760)	2430-4860	2480-4460	2750-3220 (2940)	3009±80	2558-3366	12
BW	500-650	460-610 (550)	460-650	420-660	400-550 (460)	367±45	323-412	2
BD	-	-	-	-	-	469±43	287-808	10
FORE	645*	-	-	-	-	885±72	599-1562	12
OSL	120-150	92-120 (100)	86-128	72-118	-	113±13	67-171	9
OSW	120-150	92-110 (90)	-	-	78-120 (96)	80±7	73-88	2
OSD	-	-	-	-	-	83±6	57-111	8
PHL	110-130	60-80 (70)	80-140	-	93-110 (100)	68±7	56-79	3
PHW	90-110	30-70 (40)	65-110	-	80-100 (90)*	53±8	42-68	3
VSL	320-400	290-360 (330)	260-380	280-380	90-150 (150)	229±18	100-344	12
VSW	320-390	300-380 (330)	-	-	260-380 (320)	256±29	228-285	2
VSD	-	-	-	-	-	289±24	120-368	10
BW%	17*	-	-	-	-	13±0	13	2
BD%	-	-	-	-	-	16±1	10-28	10
FO%	15*	-	-	-	-	30±2	23-47	12
T%	24*	-	-	-	-	22±1	20-24	7
OS:VS	1:3.2*	-	-	-	-	1:3.1±0.4	1:2.1-4.2	6

*Inferred from associated line drawing

Table 1.8. Metric comparison of *E. recurvatum* gonad and gonad-associated structures from current and prior studies from assorted geographical locations.

	Lee et al. 1990	Sohn 1998	Kanev et al. 2008		Sereno-Uribe et al. 2015	Present study		
Source	Korea	Korea	Europe	USA	Mexico	Minnesota, USA		
Metric	Range	Range ($\bar{x}$)	Range	Range	Range ($\bar{x}$)	$\bar{x}$±SE	Range	n
CSL	300-400	200-330 (260)	-	-	270-430 (350)	223±15	169-286	7
CSW	130-180	80-130 (110)	-	-	190-260 (230)	105±9	75-139	7
ATL	280-420	230-370 (320)	240-380	280-360	240-320 (290)	267±34	87-405	9
ATW	210-280	150-210 (180)	220-360	220-300	200-360 (300)	120±26	43-158	4
ATD	-	-	-	-	90-220 (150)	161±21	122-242	5
PTL	390-480	260-400 (350)	240-380	280-360	-	320±32	115-416	9
PTW	180-290	160-200 (180)	220-360	220-300	280-450 (370)	126±30	40-174	4
PTD	-	-	-	-	110-180 (140)	131±9	107-163	5
TEND	1000*	-	-	-	-	672±22	579-753	8
OVL	223*	80-130 (110)	100-200	120-160	110-140 (120)	108±9	53-130	7
OVW	134*	92-150 (120)	-	-	100-130 (120)	110±10	54-132	7
E	8*	-	up to 20	up to 20	-	9±2	1-17	10
EL	82-97	96-105 (100)	96-136	95-128	70-96 (85)	83±2	72-98	20
EW	54-59	64-71 (60)	60-90	62-94	40-56 (47)	44±2	5-55	19

*Inferred from associated line drawing

Table 1.9. Morphometric comparison of collar and spine characteristics of *E. speotyto* between the present study materials and original description by Buscher (1978).

	Present study			Buscher (1978)
Feature	Range	$\bar{x}$±SE	n	Range ($\bar{x}$)
Collar width	201	201±0	2	210-270 (240)
OSpL	40-50	44±3	4	28-46 (39)
OSpW	9-12	10±1	4	7-11 (9)
ASpL	40-42	41±1	2	40-55 (52)
ASpW	9-10	10±1	2	9-11 (10)
DSpL	38-45	41±1	14	-
DSpW	8-11	9±1	14	-
CSpL	40-50	44±2	7	40-64 (42^{A}, 55^{B})
CSpW	8-12	10±1	7	9-14 (9^{A}, 12^{B})

[A]Latero-oral corner spines
[B]Non-latero-oral corner spines

Table 1.10. Morphometric comparison of *E. speotyto* between the present study materials and original description by Buscher (1978).

Feature	Present study			Buscher (1978)
	Range	$\bar{x}$±SE	n	Range ($\bar{x}$)
BL	1769-2191	2019±91	4	1850-3100 (2470)
FORE	460-502	531±51	3	-
OSL	78-89	84±4	3	83-104 (91)
OSW	59-65	62±2	3	-
VSL	207-255	231±10	4	230-370 (300)
VSW	128-179	156±14	4	200-310 (260)
CSL	101-162	131±13	4	-
CSW	52-95	71±10	4	-
ATL	169-217	198±11	4	170-283 (227)
ATW	122-139	130±5	4	130-206 (167)
PTL	175-257	223±20	4	180-295 (244)
PTW	103-152	128±23	4	140-229 (179)
TEND	377-476	430±20	4	-
OVL	76-113	101±3	4	90-166 (130)
OVW	74-106	93±2	4	100-166 (124)
E	1-9	5±2	3	Up to 25
EL	85-97	92±2	6	80-98 (89)
EW	50-58	55±2	6	47-60 (51)
FO%	23-30	27±2	3	-
T%	12-24	19±1	4	-
OS:VS	1:3.3-4	1:3.8±0.2	3	-

Table 1.11. Morphometric comparison of collar and spine characteristics between *Echinoparyphium* sp. and *Echinoparyphium indicum* Rai, 1962 (Mehra 1980).

Feature	*Echinoparyphium* sp.			*Echinoparyphium indicum*[1]
	Range	$\bar{x}$±SE	n	Range
Collar width	148-246	197	2	-
ASpL	-	47	1	26-33
ASpW	-	15	1	6-8
DSpL	38-45	41±1	6	-
DSpW	11-13	12±1	6	-
CSpL	46-48	47±1	2	39-62
CSpW	17	17±0	2	13-19

Table 1.12. Morphometric comparison between *Echinoparyphium* sp. and *Echinoparyphium indicum* Rai, 1962 (Mehra 1980).

Feature	*Echinoparyphium* sp.			*Echinoparyphium indicum*
	Range	x̄±SE	n	Range
BL	2586-3143	2865	2	5388-6200
BW	432-606	519	2	1310-1370
FORE	652-709	681	2	-
OSL	104-111	107±2	3	49-99
OSW	86-96	92±3	3	66-99
PHL	69-77	73±5	2	72-82
PHW	64-67	66±2	2	49-69
VSL	264-288	276±7	2	-
VSW	246-288	267±22	2	-
CSL	146-153	149±4	2	148-330
CSW	89-96	93±4	2	82-138
ATL	241-248	244±4	2	260-340
ATW	145-181	163±18	2	230-290
PTL	-	253	1	280-370
PTW	-	156	1	230-310
OVL	-	164	1	280-620
OVW	-	157	1	109-140
E	-	14	1	7-10
EL	71-101	87±5	6	82-95
EW	51-62	57±9	6	42-49
BW%	17-20	18±2	2	18%
FO%	23-26	24±2	2	25*
T%	-	23.26	1	27%*
OS:VS	1:2.4-2.6	1:2.5±0.2	2	1:4.5*

*Inferred from line drawing in Mehra 1980

Table 1.13. Morphometric comparison of *Leyogonimus polyoon* collected from Europe (Sey 1968) and North America (Present study). All metrics from Sey (1968) inferred from line drawing.

Source	European (Sey 1968)	North American (Present study)		
	$\bar{x}$	$\bar{x}$±SE	Range	n
BL	1280	906±47	576-1218	17
BWL	563	353±24	206-532	14
BD	-	329±59	215-411	3
FO	563	283±14	200-360	17
OsL	127	79±3	58-93	16
OsW	136	63±3	42-78	14
OSD	-	37±11	17-58	4
PH	14	30±6	13-60	8
PHL	75	49±2	37-59	13
PHW	66	42±3	25-53	11
VSL	84	66±5	53-94	8
VSW	89	66±6	52-89	7
VSD	-	59*	-	1
TL	237 (230-244)	148±2	146-149	2
TW	136 (132-141)	78±12	66-89	2
CL	-	146±11	126-164	3
CW	-	63±11	42-78	3
OVL	230	151±8	128-168	5
OVW	220	132±12	101-160	5
OVLL[2]	-	65±5	46-80	13
OVLW[2]	-	56±3	43-75	11
E	100+	100+	-	-
EL	-	25±1	18-30	55
EW	-	14±1	11-16	55
BW%	44	39±2	27-61	14
BD%	-	39±4	33-47	3
FO%	44	32±2	22-49	17
OS:VS	1:1.6	1:1.2±0.1	1:1-1.3	3

[1]TL and TW indicate testes length and width

[2]OVLL and OVLW denote length and width of individual lobes of the ovary

Table 1.14. Morphological comparison of *Maritrema obstipum* between recent and previous studies.

Feature	Chung et al. 2011	Etges, 1953	Current study		
	$\bar{x}$ (Range)	Range	$\bar{x}$±SE	Range	n
BL	451 (400–495)	228–517	277±33	239–341	3
BW	265 (260–270)	119–303	173±44	121–259	3
FORE	279*	–	103±6	95–114	3
OSL	39	37–64	29±3	22–35	4
OSW	39	–	32±4	26–39	4
PHL	29*	17–29	24±4	21–27	2
PHW	23*	24–47	18±1	17–19	2
VSL	36	31–71	29±5	19–39	4
VSW	39	–	26±4	21–33	3
CSL	154 (126–178)	124–211	158±15	112–192	5
CSW	43*	18–45	36±3	32–46	5
TL[1]	–	51–93	53±3	44–68	7
TW[1]	–	–	61±5	43–74	7
TEND	112.8*	–	65±4	61–68	2
E	100+	–	100+	–	3
EL	20	19–25	19±1	16–22	27
EW	13	11–14	11±1	9–14	23
BW%	57*	53*	60±8	50–76	3
FO%	62*	32*	37±2	33–40	3
T%	25*	40*	23±3	20–25	2
OS:VS	1:1*	1.2:1*	1:0.84±0.02	1:0.8–088	3

* inferred from line drawing

[1]TL and TW indicate testes length and width

Table 1.15. Morphological comparison of *Sphaeridiotrema pseudoglobulus* McLaughlin, Scott, & Huffman, 1993[1] (McLaughlin et al. 1993) and *Sphaeridiotrema globulus* Rudolphi, 1814[2] (Price 1934) to *S. pseudoglobulus* in the present study

Source	*S. pseudoglobulus*[1]		*S. globulus*[2]		*S. pseudoglobulus* (Present)		
	Range	$\bar{x}$±SD	Range	$\bar{x}$ ±SD	Range	$\bar{x}$ ±SE	n
BL	900–1380	1100±100	600–1200	900±100	470–1030	854±65	9
BW	600–950	780±100	500–1020	700±900	300–581	480±42	7
BD	–	–	–	–	591–644	618±27	2
FORE	–	369*	342–605*	441±126*	152–591	368±56	10
OSL	120–182	138±16	96–168	133±16	57–132	101±8	11
OSW	125–216	173±22	139–221	177±18	51–11	104±14	8
OSD	–	–	–	–	77–125	108±16	3
PHL	72–120	96±12	81–156	107±14	42–15	73±10	9
PHW	62–120	94±12	72–156	106±18	28–89	59±9	9
VSL	240–480	347±54	168–432	313±78	155–346	238±23	9
VSW	336–475	419±34	312–480	421±37	180–428	271±25	10
VSD	–	–	–	–	–	230*	1
CSL	252–384	307±43	–	–	76–198	149±17	6
CSW	48–84	69±11	–	–	33–63	50±5	6
PTL	96–288	160±41	120–228	197±48	120–227	155±20	5
PTW	250–408	349±42	206–408	297±49	82–144	119±14	4
TEND	–	27*	26–53*	46±13*	0–18	12±2	10
OVL	110–197	140±22	86–144	113±14	124–163	139±12	3
OVW	120–216	173±27	96–182	136±17	101–137	120±11	3
E	5–15	9±3	6–50	23±10	1–7	4±1	12
EL	103–125	116±5	91–108	97±4	94–129	109±4	12
EW	62–84	71±5	53–72	63±4	62–83	73±2	10
BW%	–	75*	71–88*	78±7*	55–64	59±1	7
BD%	–	–	–	–	62–63	63±0.0	2
FO%	–	36*	32–43*	38±6*	25–57	46±4	9
T%	–	3*	2–5*	40±1*	1–4	2±0.0	7
OS:VS	–	1:2.2*	1:2.5–3.4*	1:3±0.4*	1:1.9–4.1	2.97±0.26	8

*Inferred from line drawing.

Table 1.16. Morphometric comparison of undescribed Psilostomidae species.

Feature	Psilostomidae sp. (A)			Psilostomidae sp. (B)			Psilostomidae sp. (C)		
	Range	x̄±SE	n	Range	x̄±SE	n	Range	x̄±SE	N
BL	922–1012	967±46	2	774–1196	991±38	13	498–746	614±43	7
BW	–	360	1	219–376	312±20	8	179–311	246±19	6
BD	–	258	1	189–506	307±46	6	–	199	1
FORE	235–259	247±12	2	163–275	218±10	13	112–174	151±10	7
OSL	71–91	81±10	2	49–94	72±5	10	51–73	60±4	5
OSW		67	1	49–77	61±4	7	45–70	61±4	7
PHL	46–58	52±6	2	43–61	54±4	6	35–67	48±4	7
PHW	42–58	50±9	2	39–56	48±3	6	32–57	42±4	7
VSW	–	236	1	134–217	170±9	13	139–168	155±5	6
VSD	–	182	1	159–374	244±40	5	–	152	1
CSL	–	–	–	108–228	157±12	13	120–172	146±11	4
CSW	–	–	–	50–121	80±6	13	56–66	62±2	5
SVL1	–	61.7	1	–	55	1	24–55	41±9	3
SVW1	–	56.7	1	–	76	1	28–47	38±6	3
SVL2	–	–	–	–	60	1	53–59	57±2	3
SVW2	–	–	–	–	61	1	45–53	49±3	3
ATL	107–142	124±18	2	78–150	112±8	11	55–116	82±10	6
ATW	129–134	131±3	2	122–192	154±11	7	105–162	123±9	6
ATD	–	–	–	108–147	132±8	4	–	96	1
PTL	138–152	145±7	2	94–134	113±5	10	50–92	71±7	7
PTW	131–157	144±14	2	110–191	148±12	7	94–136	111±6	6
PTD	–	–	–	116–138	127±6	3	–	108	1
OVL	–	83	1	66–87	79±3	10	53–80	69±7	4
E	–	10	1	1–10	5±1	14	1–3	1±1	7
EL	60–85	69±3	9	60–88	75±2	40	71–97	80±5	5
EW	34–56	43±3	9	31–58	48±1	40	37–56	47±3	5
TEND	106–137	121±16	2	159–333	272±16	12	66–198	127±22	6

Table 1.17. Comparison of body proportions for undescribed Psilostomidae species

Feature	Psilostomidae sp. (A)			Psilostomidae sp. (B)			Psilostomidae sp. (C)		
	Range	x̄±SE	n	Range	x̄±SE	n	Range	x̄±SE	n
BW%	–	39	1	26—44	34±2	8	0.35–0.48	0.4±0.02	6
BD%	–	25	1	19—48	2±4	6	–	0.34	1
FO%	25–26	26±0	2	15—28	22±1	13	0.23–0.3	0.25±0.01	7
T%	11–13	12±1	2	15—38	27±2	12	0.11–0.27	0.2±0.02	6
E%	6–8	7±0	9	5—11	8±0	36	0.1–0.13	0.11±0.01	5
OS:VS	–	1:2.6	1	1:1.7—3.3	1:2.4±0.2	10	1:2.2–2.7	1:2.5±0.2	4

Table 1.18. Comparison of *Zygocotyle lunata* from different waterfowl hosts collected in present study.

Feature	*A. platyrhynchos*			*A. collaris*			*A. americana*			*A. sponsa*			*A. affinis*		
	x̄±SE	Range	n	x̄±SE	Range	n	x̄±SE	Range	n	x̄±SE	Range	n	x̄±SE	Range	n
BL	6335±206	6129-6540	2	5023±636	4387-5658	2	5604	-	1	4839	-	1	5090	-	1
BW	2034±41	1987-2115	3	1452±232	1221-1684	2	1669	-	1	1427	-	1	1228	-	1
OSL	485±37	448-521	2	403±80	324-483	2	431	-	1	382	-	1	325	-	1
OSW	456±59	397-514	2	367±64	304-431	2	427	-	1	350	-	1	310	-	1
TDW[1]	281	-	1	310±45	265-355	2	301	-	1	-	-	-	-	-	-
DL[2]	221±12	196-244	4	180±26	131-224	4	180	-	1	-	-	-	176±1	175-176	2
DW[2]	122±12	103-151	4	125±7	108-137	4	-	-	-	-	-	-	107±2	105-108	2
VSL	1520±153	1224-1733	3	1178±219	959-1396	2	1376	-	1	821	-	1	1148	-	1
VSW	1057±66	931-1148	3	861±126	735-986	2	852	-	1	832	-	1	758	-	1
PaL[3]	-	-	-	434±4	431-437	2	-	-	-	-	-	-	443	-	1
PaW[3]	-	-	-	204±1	203-205	2	-	-	-	-	-	-	113	-	1
ATL	561±57	454-646	3	388	388	1	333	-	1	-	-	-	-	-	-
ATW	512±33	447-555	3	354±30	324-384	2	293	-	1	-	-	-	-	-	-
PTL	627±52	526-691	3	517	517	1	420	-	1	-	-	-	-	-	-
PTW	520±72	425-661	3	382±11	371-392	2	288	-	1	-	-	-	-	-	-
OVL	220	213-226	2	231±27	204-257	2	-	-	-	-	-	-	244	-	1
OVW	254±15	240-269	2	264±6	259-270	2	-	-	-	-	-	-	179	-	1
E	52±26	24-102	3	62±10	52-72	2	114	-	1	103	-	1	26	-	1
EL	134±4	122-150	7	139±2	135-146	6	141±3	136-146	4	133±1	133-134	2	142±2	140-143	3
EW	72±2	66-80	7	84±6	63-100	6	88±2	83-92	4	75±2	73-77	2	86±6	77-95	3
BW%	32±1	30-33	2	30±1	028-30	2	30	-	1	30	-	1	24	-	1
OS:VS	1:2.28±0.47	1:1.81-2.76	2	1:2.35±0.07	1:2.29-2.42	2	1:2	-	1	1:2.4	-	1	1:2.5	-	1

[1]Total oral diverticula width
[2]Individual oral diverticula length and width
[3]Muscular ventral sucker papillae length and width

Table 1.19. Morphometric comparison of *Zygocotyle lunata* from this study those from prior studies.

Feature	Ostrowski de Núñez et al. (2011)		Sutton & Lunaschi (1987)	Digiana (1997)	Present study		
	Mice	Chickens	*A. sibiliatrix*	*C. melancorypha*			
	x̄ (Range)	x̄ (Range)	x̄	x̄	x̄±SE	Range	n
BL	4690 (4064–5872)	3632 (3504–3792)	9110	6110	5189±295	3730–6540	9
BW	1666 (1056–2704)	1360 (1168–1504)	2930	1500	16340±113	1121–2115	9
OSL	–	334*	–	–	389±30	248–520	9
OSW	–	367*	–	–	365±30	206–514	9
TDW[1]	–	234*	–	–	292±18	257–355	5
DL[2]	–	167*	–	–	194±12	131–244	11
DW[2]	–	117*	–	–	120±3	103–151	10
VSL	1236 (1040–1568)	1164 (1120–1248)	1700	1590	1246±90	821–1733	10
VSW	965(672–1520)	856 (752–912)	1240	1110	883±48	735–1147	10
PaL[3]	–	–	–	–	396±26	333–443	5
PaW[3]	–	–	–	–	171±22	113–205	5
ATL	547 (432–720)	256 (192–320)	–	380	455±55	328	6
ATW	744 (480–1280)	416 (336–528)	–	490	420±38	293–555	7
PTL	544 (448–720)	280 (192–320)	–	380	528±55	351–690	6
PTW	698 (480–1088)	452 (400–480)	–	470	433±44	288–661	7
OVL	310 (240–512)	160 (144–176)	250	260	229±8	204–257	6
OVW	402 (240–800)	228 (192–272)	530	340	243±14	179–270	6
E	–	–	–	–	62±11	24–114	10
EL	136 (113–157)	131 (119–138)	140	131–138	139±2	122–150	29
EW	69 (57–94)	69 (57–82)	93	73–82	79±2	61–100	29
BW%	–	38*	–	–	29±1	24–33	8
OS:VS	–	1:2.5*	–	–	1:2.4±0.2	1:1.8–3.6	9

*inferred from line drawing
[1]Total oral diverticula width
[2]Individual oral diverticula length and width
[3]Muscular ventral sucker papillae length and width

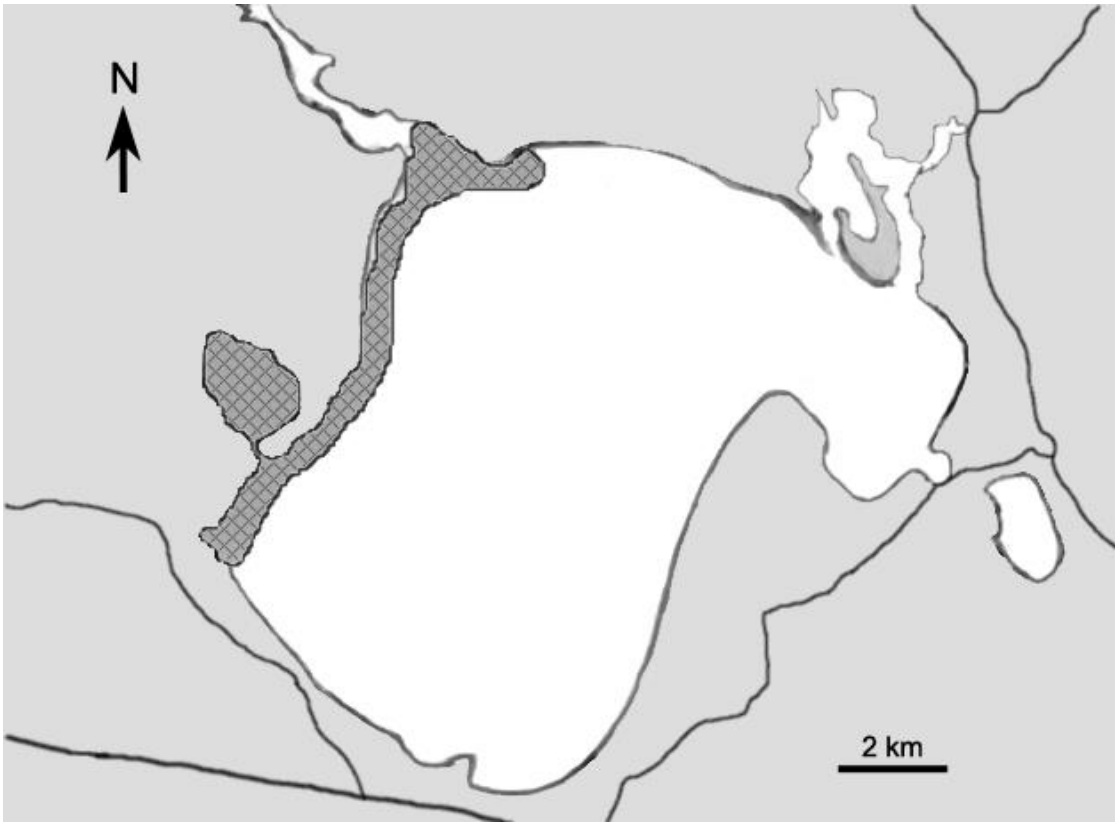

Figure 1.1. Collection sites at Lake Winnibigoshish, Minnesota shown in shaded area. Scale bar 2 km. Map adapted from Google Maps

```
                          10•        20•        30•        40•        50•
Echinoparyphium sp. ACTAACAGATTCCCTTAGTAACGGCGAGTGAACAGGGATAAGCCCAGCAC
E. recurvatum       ..................................................
E. speotyto         ..................................................

                          60•        70•        80•        90•       100•
Echinoparyphium sp. CGAAGCCTGTGGCCGTTTGGCCCCTAGGCAATGTGGTGTTCAGGTTAGCT
E. recurvatum       ..................................................
E. speotyto         ..................................................

                         110•       120•       130•       140•       150•
Echinoparyphium sp. CGCGGGGATGCTGCTCCACCCTAAGTCCTATAATGAGTAAGGTTACTCGG
E. recurvatum       ..................................................
E. speotyto         ..................................................

                         160•       170•       180•       190•       200•
Echinoparyphium sp. ACGTGGCCCACAGAGGGTGAAAGGCCCGTGGGGGTGGAGACTCAGATTGG
E. recurvatum       ..A...............................................
E. speotyto         ..A...............................................

                         210•       220•       230•       240•       250•
Echinoparyphium sp. CCAGTATCTCCCTGAGCAGACCTTGGAGTCGGGTTGTTTGTGAATGCAGC
E. recurvatum       ..................................................
E. speotyto         ..................................................

                         260•       270•       280•       290•       300•
Echinoparyphium sp. CCAAAGCGGGTGGTAAACTCCATCCAAGGCTAAATACTTGCACGAGTCCG
E. recurvatum       ..................................................
E. speotyto         ..................................................

                         310•       320•       330•       340•       350•
Echinoparyphium sp. ATAGCGAACAAGTACCGTGAGGGAAAGTTGAAAAGTACTTTGAAGAGAGA
E. recurvatum       ..................................................
E. speotyto         ..................................................

                         360•       370•       380•       390•       400•
Echinoparyphium sp. GTAAACAGTGCGTGAAACCGCTCAGAGGTAAACGGGTGGAGTTGAACTGC
E. recurvatum       ..................................................
E. speotyto         ..................................................

                         410•       420•       430•       440•       450•
Echinoparyphium sp. AAGCTCTGAGGATTCAGCTGGTGAGTTTGGCATGAGCTTGGTCATGTGGG
E. recurvatum       ..................................................
E. speotyto         ..................................................
```

Figure 1.2. The 28S rDNA nucleotide sequence data for three *Echinoparyphium* species [*Echinoparyphium* sp., *E. recurvatum*, and *E. speotyto*]. A dot (.) indicates that at that site the sequence is identical to the *Echinoparyphium* (A) sequence. Placement of a hyphen (-) indicates alignment gaps.

```
                          460•       470•       480•       490•       500•
Echinoparyphium sp. TTGTGTGTTCGGGTCTGCTTAGCTGCAGGTCCTCGCCTTTGGTGGGGATG
E. recurvatum       ..................................................
E. speotyto         ..................................................

                          510•       520•       530•       540•       550•
Echinoparyphium sp. CGCGTATCGCTTATCAAGCGTTGTGCGCCCGTTCTTGTCGAACCTGCTCG
E. recurvatum       ..................................A...G.........
E. speotyto         ..................................C...G.........

                          560•       570•       580•       590•       600•
Echinoparyphium sp. CCAGTGCACTTTCTCAGAGTGTTCACCACGACCGGCGTTGTCGTCTGACT
E. recurvatum       ..............................................G..
E. speotyto         ..............................................G..

                          610•       620•       630•       640•       650•
Echinoparyphium sp. GGTGCGGTTAAACCGGCCTTGTAGGGTCCTTGTGGCCTTGCTTGGTCGGG
E. recurvatum       ........................................C........
E. speotyto         ........................................C........

                          660•       670•       680•       690•       700•
Echinoparyphium sp. ATGGCAGGTAGCCCGTTGTGTACTTCGGTGTGCTTCGGGTGTAATAGCCG
E. recurvatum       ..................................................
E. speotyto         ..................................................

                          710•       720•       730•       740•       750•
Echinoparyphium sp. ACTGCATCGGTTCTGTGCGATACGTCGGAGACGGCGGCTTGTTGTGCGTG
E. recurvatum       ..................................................
E. speotyto         ..................................................

                          760•       770•       780•       790•       800•
Echinoparyphium sp. CGGGCGTGCCTGTTGCGCTGGCGGCTCTGGGTCTGGTTGCCTTGTTGCTT
E. recurvatum       ..................................................
E. speotyto         ..................................................

                          810•       820•       830•       840•       850•
Echinoparyphium sp. GTAAATGCAAGCCAGGTGATGGCCCGGGGTCGTTTGGTGTGCGGTTGCGT
E. recurvatum       ........................T.........................
E. speotyto         ..................................................

                          860•       870•       880•       890•       900•
Echinoparyphium sp. TCGTGGCACTTTAAAGGGCCAACAGTCTGTGGTGTAGTGGTAGACTATCC
E. recurvatum       ......................T...........................
E. speotyto         ......................T...........................

                          910•       920•       930•       940•       950•
Echinoparyphium sp. ACCTGACCCGTCTTGAAACACGGACCAAGGAGAGTAACATGTGCGCGAGT
E. recurvatum       ..................................................
E. speotyto         ..................................................
```

```
                          960•       970•       980•       990•      1000•
Echinoparyphium sp. CATTGGGCGTTACGAAACCCAAAGGCGAAGTGAAAGTAAAGGTTCGGCTT
E. recurvatum       ..................................................
E. speotyto         ..................................................

1010•     1020•     1030•     1040•     1050•
Echinoparyphium sp. GTCCGGACTGAGGTGAGATCCTGTCGTTTCTCACGCGTGGTACTACCAAG
E. recurvatum       ...T..............................................
E. speotyto         ...T.....................----------

                          1060•     1070•     1080•     1090•     1100•
Echinoparyphium sp. CATCGAGCGGCAGGCGCATCACCGGCCCGTCCCATGGCGTAGTGGCGGCT
E. recurvatum       ................................----------
E. speotyto         --------------------------------------------------

                          1110•     1120•   1128•
Echinoparyphium sp. TCGGCTTGCTCATCGTCGGGGCGGAGCA
E. recurvatum       ----------------------------
E. speotyto         ----------------------------
```

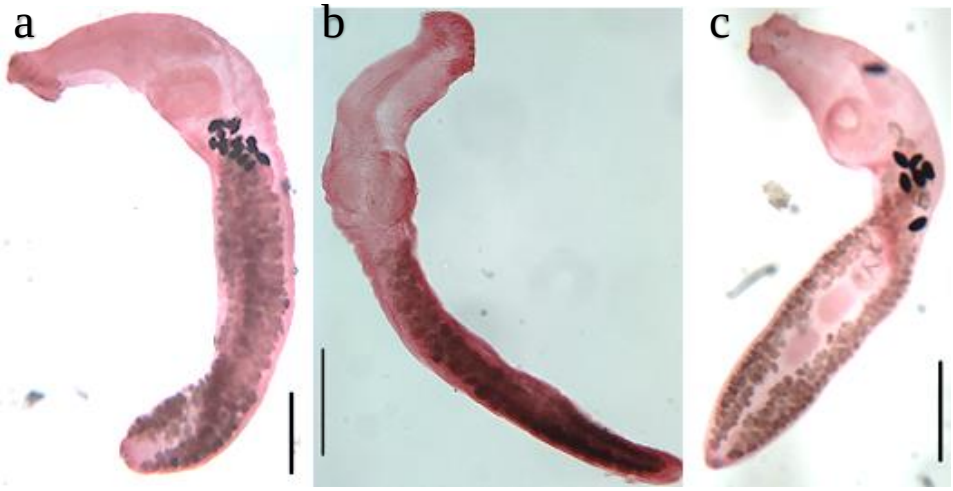

Figure 1.3. The morphology of *E. recurvatum* at 40x—scale bar denotes 400µm (a); *E. speotyto* at 100x—scale bar denotes 450µm (b); and *Echinoparyphium sp.* at 40x—scale bar denotes 600µm (c).

```
                        10•        20•        30•        40•        50•
Echinoparyphium sp. CCAACTGTGTGAATTAATGTAAACTGCATACTGCTTTGAACATCGACATC
E. speotyto         ..................................................

                        60•        70•        80•        90•       100•
Echinoparyphium sp. TTGAACGCATATTGCGGCCATGGGTTAGCCTGTGGCCACGCCTGTCCGAG
E. speotyto         ..................................................

                       110•       120•       130•       140•       150•
Echinoparyphium sp. GGTCGGCTTATAAACTATCACGACGCCCAAAAAGTCGTGGCTTGGGTTTT
E. speotyto         ..................................................

                       160•       170•       180•       190•       200•
Echinoparyphium sp. GCCAGCTGGCGTGATTTCCTCTGTGAGCAATCATGTGAGGTGCCAGATCT
E. speotyto         ............................T.....................

                       210•       220•       230•       240•       250•
Echinoparyphium sp. ATGGCGTTTCCCTAATGTATCCGGACGCATCCTTGTCTCGGCTGAAGGCC
E. speotyto         ....................................T...........

                       260•       270•       280•       290•       300•
Echinoparyphium sp. GTGGTGGGGTGCGGTGGCGGAATCGTGGTTTAATTTGGCTATGCCCCGTT
E. speotyto         A..................................G..............

                       310•       320•       330•       340•       350•
Echinoparyphium sp. TTCAGCATGTTTTGGCGATCCCCTAGTCGGCATGCATATGAATACGGGTG
E. speotyto         ...........AC......A.....................G..T......


                       360•       370•       380•       390•       400•
Echinoparyphium sp. GAGCTATGATCGGGTTGGTACTCCGTTATCAGTGTGTTTGGCGCTTCCAG
E. speotyto         ....................................C........T..

                       410•       420•       430•       440•       450•
Echinoparyphium sp. TCGGCATACTTATGATCTCGGAGGTAATTCCATACCAGGCACGTTCCGTT
E. speotyto         ....................G.A.........................

                       460•       470•       480•       490•       500•
Echinoparyphium sp. ACTGTCGCTCCATTGCTGGTTTTTGGCTGGCTTGGGCAATGCATCTGATG
E. speotyto         .......T.............GAA...................C....

                    504•
Echinoparyphium sp. TTAC
E. speotyto         ....
```

Figure 1.4. Internal transcribed spacer (ITS) rDNA nucleotide sequence data for *Echinoparyphium* sp. and *E. speotyto*. A dot (.) indicates that the sequence at that site is identical to the *Echinoparyphium* (A) sequence. Placement of a hyphen (-) indicates alignment gaps.

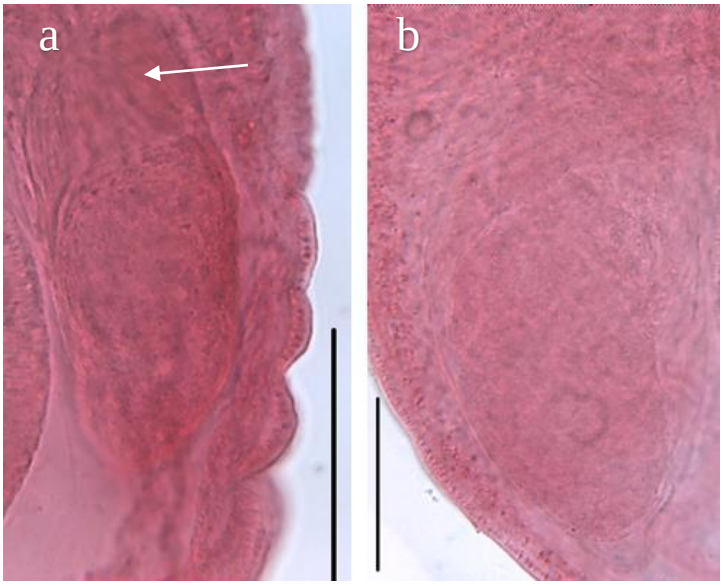

Figure 1.5. Comparison of cirrus and related-structures of *E. speotyto* (a) and *E. recurvatum* (b) at 400x. Well-defined pars prostatica denoted by arrow. Scale bar denotes 100µm.

```
                10•        20•        30•        40•        50•
L. polyoon GATTCCCCTAGTAACTGCGAGTGAACAGGGATTAGCCCAGCACCGAAGCC

                60•        70•        80•        90•       100•
L. polyoon TGTGGCCATTTGGTCACTAGGCAATGTGGTGTTTTGGTTGTTCCGCAAAG

               110•       120•       130•       140•       150•
L. polyoon GTGCTGCTCCACCCTAAGTCCATCAATGAGTACGGTAGTACGGACATGGC

               160•       170•       180•       190•       200•
L. polyoon CCACAGAGGGTGAAAGGCCCGTGGGGGTGGAGATCATGTAGGCCAGTGCC

               210•       220•       230•       240•       250•
L. polyoon TTTCTGGATAGACCATGGAGTCGGGTTGTTTGTGAATGCAGCCCAAAGCG

               260•       270•       280•       290•       300•
L. polyoon GGTGGTAAACTCCATCCAAGGCTAAATACAAGCACGAGTCCGATAGCGAA

               310•       320•       330•       340•       350•
L. polyoon CAAGTACCGTGAGGGAAAGTTGAAAAGTACTTTGAAGAGAGAGTAAACAG

               360•       370•       380•       390•       400•
L. polyoon TGCGTGAAACCGGTCAGAGGTAAACGGGTGGAGTTGAACTGCAAGCTCTG

               410•       420•       430•       440•       450•
L. polyoon GGAATTCAGCTGGTGAGTGTGGTTTGAGCTTGGTCAAATTGGTTGGGCCC

               460•       470•       480•       490•       500•
L. polyoon TGGAGTCTGCGTAGCAGCAGGCCCTCGCCTTTCGGGTGGGGGTGCGCGAT

               510•       520•       530•       540•       550•
L. polyoon ACACTTATCAAGTGTTGTGCGCTTCAGGTGTTCCTCGGGCCAACTCGCCA

               560•       570•       580•       590•       600•
L. polyoon GTGCACTTTCCCGGAGTAGTCATCACGACCGGCATCGCTGTCTGGCTGTT

               610•       620•       630•       640•       650•
L. polyoon GTGGTTAAACCGCTCTCGCATTGTCCTTGTGGCTCTGCTTGATCGGGATG

               660•       670•       680•       690•       700•
L. polyoon GCAGGTAGCTCGTTGACTTGCTTGTGGCTTGCCGCAGGCGCTGGGTCTTT

               710•       720•       730•       740•       750•
L. polyoon GAGTGTAATCAGCTGACCACATCGGTTCTGTGCAGTATGTCGGAGACGGC

               760•       770•       780•       790•       800•
L. polyoon GGCTTTTGTGTGTGCGTGCGTGCCTGTCCGGCCAAGGTGTCCGAGTTTGG
               810•       820•       830•       840•       850•
L. polyoon TTGTTATGTTGCCTGTTCACGCAGGCCTGACAATAGCTCGGATGCTTCTG
```

Figure 1.6. The 28S rDNA nucleotide sequence data for *Leyogonimus polyoon*.

```
                860•       870•       880•       890•       900•
L. polyoon GTTGGCGGTTGCGTGCGTGGCACAGTTCATGGGCCAATAGTCTGTGATGT

                910•       920•       930•       940•       950•
L. polyoon AGTGGTAGACTATCCACCTGACCCGTCTTGAAACACGGACCAAGGAGAGT

                960•       970•       980•       990•      1000•
L. polyoon AACAAGTGCGCGAGTCATTGGGCGTTACGAAACCCAAAGGCGCAGTGAAA

               1010•      1020•      1030•       140•      1050•
L. polyoon GTAAAGGTCTGGCTTGTCCAGGCTGAGGTGAGATCCTGTCGTTTCCTCAT

               1060•      1070•      1080•      1090•      1100•
L. polyoon GCGTGGTACCGCCAAGCTTCGAGCGGCAGGCGCATCACCGGCCCGTCCCA

              1106•
L. polyoon TGACAA
```

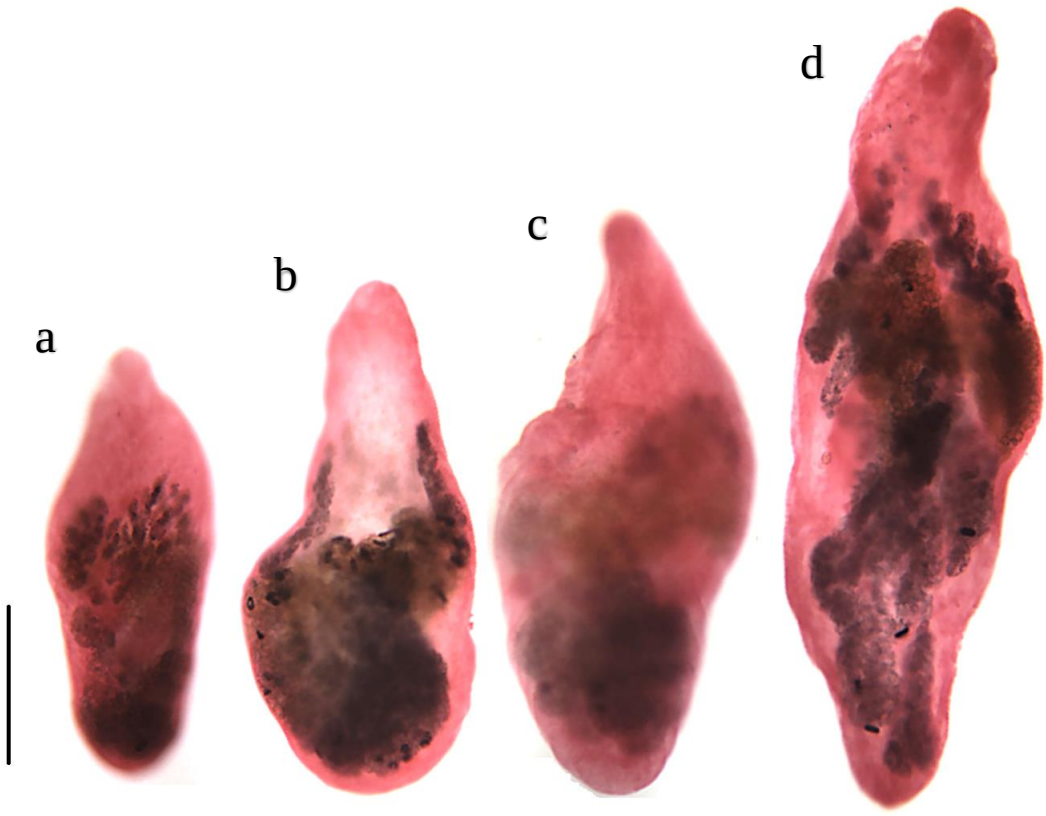

Figure 1.7. Different morphotypes of *Leyogonimus polyoon*. (a) ventro-dorsal view showing elongate-oval body form. (b) rotated slightly, showing distention of body at level of uterus. (c) lateral view showing rounded body form. (d) ventro-dorsal view of larger morphotype. Extension of uterus to level of ventral sucker visible. Scale bar denotes 250µm.

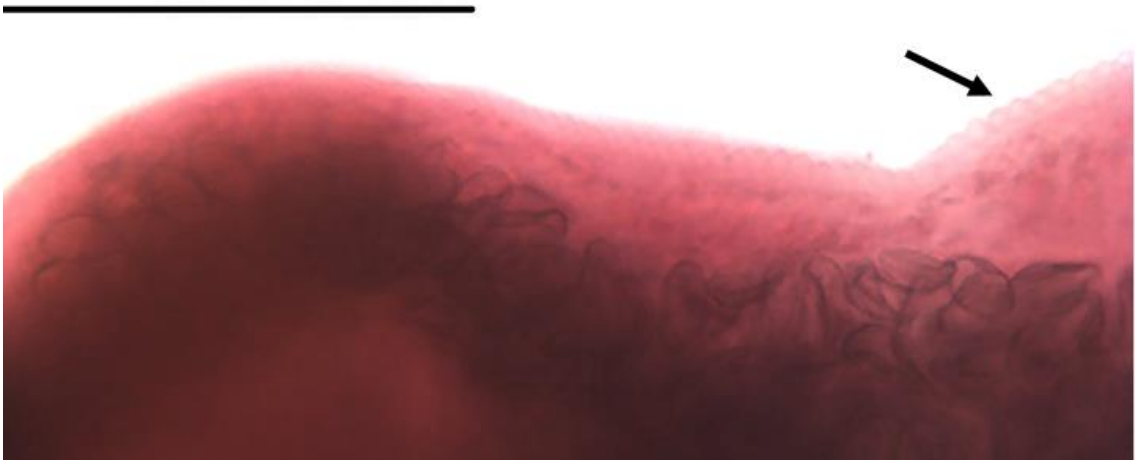

Figure 1.8. Tegument of *Leyogonimus polyoon* at 400x to observe tegumental structure. Arrow indicates tegumental scale-like spines. Scale bar indicates 150 μm.

Figure 1.9. *Maritrema obstipum* from *A. collaris* at 400x. (a) anterior of body in focus. (1) denotes pronounced cirrus; (2) denotes sinistral ceca. (b) posterior of body. Scale bar indicates 100 μm.

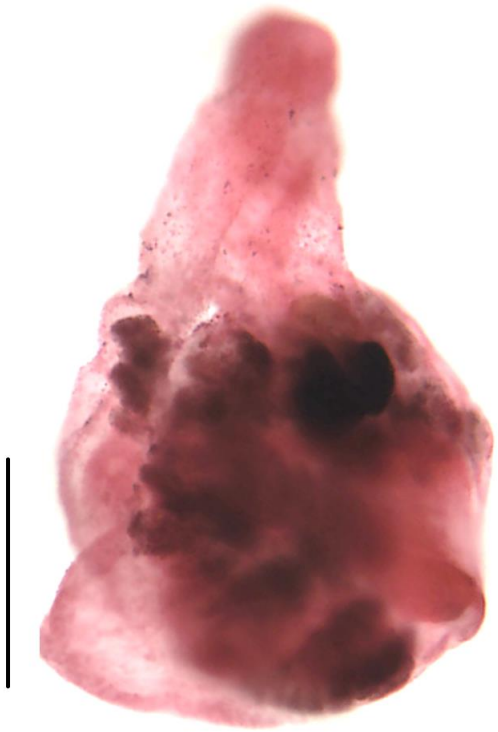

Figure 1.10. *Sphaeridiotrema pseudoglobulus* from *A. affinis* at 100x. Scale bar indicates 350 μm.

```
                        10•        20•        30•        40•        50•
Psilostomidae (A) -----AGGATTCCCTTAGTAACGGCGAGTGAACAGGGAAAAGCCCAGCAC
Psilostomidae (B) TAACC.....................................C.....
Psilostomidae (C) -----------.....................................

                        60•        70•        80•        90•       100•
Psilostomidae (A) CGAAGCCTGTGGCCGTTTGGCCTCTAGGCAATGTGGTGTTCAGGTCAGCT
Psilostomidae (B) .........A..T..................................
Psilostomidae (C) .........A..T..................................

                       110•       120•       130•       140•       150•
Psilostomidae (A) CGCGGAGGTACTGCTCCACCCTAAGTCCTATAATGAGTAAGGTTACTCGG
Psilostomidae (B) ...............................................
Psilostomidae (C) ...............................................

                       160•       170•       180•       190•       200•
Psilostomidae (A) ACGTGGCCCACAGAGGGTGAAAGGCCCGTGGGGGTGGAGACTCAGATTGG
Psilostomidae (B) ...............................................
Psilostomidae (C) ...............................................

                       210•       220•       230•       240•       250•
Psilostomidae (A) CCAGTATCTCCCTGAGTAGACCTTGGAGTCGGGTTGTTTGTGAATGCAGC
Psilostomidae (B) ................G..............................
Psilostomidae (C) ................G..............................

                       260•       270•       280•       290•       300•
Psilostomidae (A) CCAAAGCGGGTGGTAAACTCCATCCAAGGCTAAATACTAGCACGAGTCCG
Psilostomidae (B) ......T.............................A..........
Psilostomidae (C) ......T.............................A..........

                       310•       320•       330•       340•       350•
Psilostomidae (A) ATAGCGAACAAGTACCGTGAGGGAAAGTTGAAAAGTACTTTGAAGAGAGA
Psilostomidae (B) ...............................................
Psilostomidae (C) ...............................................

                       360•       370•       380•       390•       400•
Psilostomidae (A) GTAAACAGTGCGTGAAACCGCTCAGAGGTAAACGGGTGGAGTTGAACTGC
Psilostomidae (B) ...............................................
Psilostomidae (C) ...............................................

                       410•       420•       430•       440•       450•
Psilostomidae (A) AAGCTCTGAGAATTCAACTGGTGAGTATGGCATGAGCTGGGCATATTGGT
Psilostomidae (B) .....................................T........
Psilostomidae (C) .....................................T........
```

Figure 1.11. The 28S rDNA nucleotide sequence data for three unidentified Psilostomidae species. A dot (.) indicates that at that site the sequence is identical to Psilostomidae (A) sequence. Placement of a hyphen (-) indicates alignment gaps.

```
                        460•       470•       480•       490•       500•
Psilostomidae (A) TGACGGTCCGGGTCTGCTGAGTTGCAGGTCCTCGCCTTTTGGTGGGGATG
Psilostomidae (B) .......T.............C............................
Psilostomidae (C) .......T..........C..C............................

                        510•       520•       530•       540•       550•
Psilostomidae (A) CGCGAATCACTTGCCAAGTGTTGTGCGCCCGGACTGTATCGGACCTGCTT
Psilostomidae (B) .....TG...........................................
Psilostomidae (C) .................................................

                        560•       570•       580•       590•       600•
Psilostomidae (A) GCCAGTGCACTTTCTCAGAGTAATCACCACGACCGGCGTTGCTGTCTGGC
Psilostomidae (B) .................................................
Psilostomidae (C) .........................................C.......

                        610•       620•       630•       640•       650•
Psilostomidae (A) TGTTGTAGTTAAACCGGCCTTGTAGAGTCCTTGTGGCTTTGCTTGG-TCG
Psilostomidae (B) ................................................-...
Psilostomidae (C) ....................C........................C...

                        660•       670•       680•       690•       700•
Psilostomidae (A) GGACGGCAGGTAGCCCGTTGTGTACTTCTGTGCGTTTCGGGTGTAATCGC
Psilostomidae (B) ...T..................C....T....T.C...............
Psilostomidae (C) ...T..................C....T....T.C....A..........

                        710•       720•       730•       740•       750•
Psilostomidae (A) TGACTGCATCAGTCCTGTGCGGTACGTCGGAGACGGCGGCTTGTTGTGTG
Psilostomidae (B) ............T.....................................
Psilostomidae (C) ............T.....................................

                        760•       770•       780•       790•       800•
Psilostomidae (A) TGCGTGCGTACTTGTTATGCTGGCGGGGCTGAGTCTGGTTGCCGTGTTGC
Psilostomidae (B) ........................T..........................
Psilostomidae (C) ..........................C..........................

                        810•       820•       830•       840•       850•
Psilostomidae (A) TCGCTAATGCAAGCCCGGTGATGGCTCGGCGTCGTTCGGTGTGCAGTTGC
Psilostomidae (B) .T..A.....................T..T.............G.....
Psilostomidae (C) .T..A.....................T..T.............G.....

                        860•       870•       880•       890•       900•
Psilostomidae (A) GTGCGTGGCACTATTCAGGGCCAATAGTCTGTGGTGTAGTGGTAGACTAT
Psilostomidae (B) ............A....................................
Psilostomidae (C) ............C.G..................................

                        910•       920•       930•       940•       950•
Psilostomidae (A) CCACCTGACCCGTCTTGAAACACGGACCAAGGAGAGTAACATGTGCGCGA
Psilostomidae (B) .........................................A.....
Psilostomidae (C) .........................................A.....
```

```
                        960•      970•      980•      990•     1000•
Psilostomidae (A) GTCATTGGGCGTTACGAAACCCAAAGGCGCAGTGAAAGTAAAGGTTCGGC
Psilostomidae (B) .................................................
Psilostomidae (C) .................................................

                       1010•     1020•     1030•     1040•     1050•
Psilostomidae (A) TTGTCCGGACTGAGGTGAGATCCTGTCGTTTCTCACGCGCGGTACTACCA
Psilostomidae (B) ..........................C........................
Psilostomidae (C) ..........................C........................

                       1060•     1070•     1080•     1090•     1100•
Psilostomidae (A) AGCATCGAGCGGCAGGCGCATCACCGGCCCGTCCCATGGCGTGGTAGCAG
Psilostomidae (B) ........................................A.AG..G.
Psilostomidae (C) ........................................A.AG..G.

                       1110•     1220•          1135•
Psilostomidae (A) CCTTGTGCTTGCTCACCGTCGGGGCGGAGCATGAG
Psilostomidae (B) ........----------------------------
Psilostomidae (C) ...............T...................
```

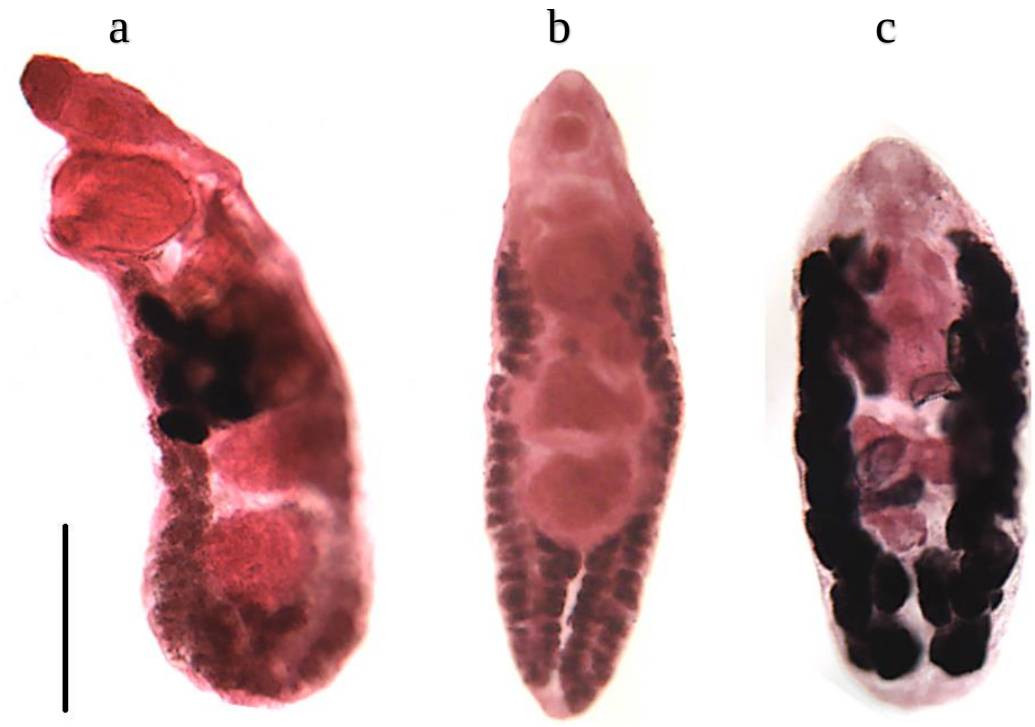

Figure 1.12. Psilostomidae species A-C (From left to right) at 100x. Scale bar indicates 250 μm.

```
                  10•        20•        30•        40•        50•
Z. lunata TTTGGTCACTAGGCAATGTGGTGTTTAGGTCGTCCTTTGGAGATGTTACC

                  60•        70•        80•        90•       100•
Z. lunata TCACTTCAAGTCCAGCAATGAGTATGGTAATTCTGACTTGGCCCAGAGAG

                 110•       120•       130•       140•       150•
Z. lunata GGTGAAAGGCCCGTGGGGGTGAGGTTCAGCTGTGATAACGTCTCCCTAGG

                 160•       170•       180•       190•       200•
Z. lunata TAGACCTTGGAGTCGGGTTGTTTGTGATTGCAGCCCAAAGTGGGTGGTAA

                 210•       220•       230•       240•       250•
Z. lunata ACTCCATCCAAGGCTAAATACTTACACGAGTCCGATAGCGAACAAGTACC

                 260•       270•       280•       290•       300•
Z. lunata GTGAGGGAAAGTTGAAAAGTACTTTGAAGAGAGAGTAAACAGTGCGTGAA

                 310•       320•       330•       340•       350•
Z. lunata ACCGCTCAGAGGTAAACGGGTGGAGTTGAACTGCAAGCTCTGAGAATTCA

                 360•       370•       380•       390•       400•
Z. lunata GCTGGTGAGTGTGGTTTGGGCTTGGTCAAAGTGATTGGCCTAGTGGGTCT

                 410•       420•       430•       440•       450•
Z. lunata GCTCAGCTGCAGGTCCCTGCCTTCGGGTGGGGATGTGCGAGGCACTTGTC

                 460•       470•       480•       490•       500•
Z. lunata AAGTGTTGCGCGCCCACAAGGTAACTCGGATCAGCTCGCCAGTGCACTTT

                 510•       520•       530•       540•       550•
Z. lunata CTCGGAGTGTTCACCACGACCGGCGCTGCTGCCTGTCTGATATGGCCAAA

                 560•       570•       580•       590•       600•
Z. lunata CCGGTCTTGCATTGTCCTTGTGGCTTTGCTTGGTCGGGATGGCAGGTAAC

                 610•       620•       630•       640•       650•
Z. lunata TCGTTGGCTTGCGTGTCGGCTTCGGTTGGCATGCGTTTGGCTTTCGAGCG

                 660•       670•       680•       690•       700•
Z. lunata TAATCAGCTGGCTATGTCAGTACTGTGCAGTGCGTCGGAGACGGCGGCTT

                 710•       720•       730•       740•       750•
Z. lunata GTTGTGGGCGTTCGTGCTTGCTCATTGACGGTTCCGAGTTTGATTGTTAT

                 760•       770•       780•       790•       800•
Z. lunata GTTGCCTGTCTCTGATAGGCCTGGTAATAGCTCGGTTCTGCTTGGTGGGC
```

Figure 1.13. The 28S rDNA nucleotide sequence data for *Zygocotyle lunata*.

```
                 810•       820•       830•       840•       850•
Z. lunata GGTTGCGGATGCTTTACATTTCAGGGCCAACAGTCTGTGGTGTAGTGGTA

                 860•       870•       880•       890•       900•
Z. lunata GACTATCCACCCGACCCGTCTTGAAACACGGACCAAGGAGAGTAACATGT

                 910•       920•       930•       940•       950•
Z. lunata GCGCGAGTCATTGGGCGTTACGAAACCCAAAGGCGCAGTGAAAGTAAAGG

                 960•       970•       980•       990•      1000•
Z. lunata CTCGGCTTGTCTGGGCTGAGGTGAGATCCTGTCGTTTCTCACGCAAGGTA

               1010•      1020•      1030•      1040•      1050•
Z. lunata CTACCAAGCGTTTGAGCGGCGGGCGCATCACCGGCCCGTCCCATGGCGTG

          1054•
Z. lunata GACA
```

```
                10•        20•        30•        40•        50•
Z. lunata CTCTAAAAAAAACAGAAGTCTTAACATCCAAACCAACCATAAACATATGA

                60•        70•        80•        90•       100•
Z. lunata TGAGCCCAAACAACACTCCCCAAACAAACAATAGAAGCCATAGCAAACAC

               110•       120•       130•       140•       150•
Z. lunata CAGACCATAATAACCAAACAAAGAATCTtGATTACTTAACCTCATACAAA

               160•       170•       180•       190•       200•
Z. lunata TATGTCTTACAGCACCGAAACCTGGCAAAATTAACACATAAACCTCAGGA

                212•
Z. lunata TGCCCAAAAAAA
```

Figure 1.14. The mitochondrial cytochrome oxidase (CO1) nucleotide sequence data for *Zygocotyle lunata*.

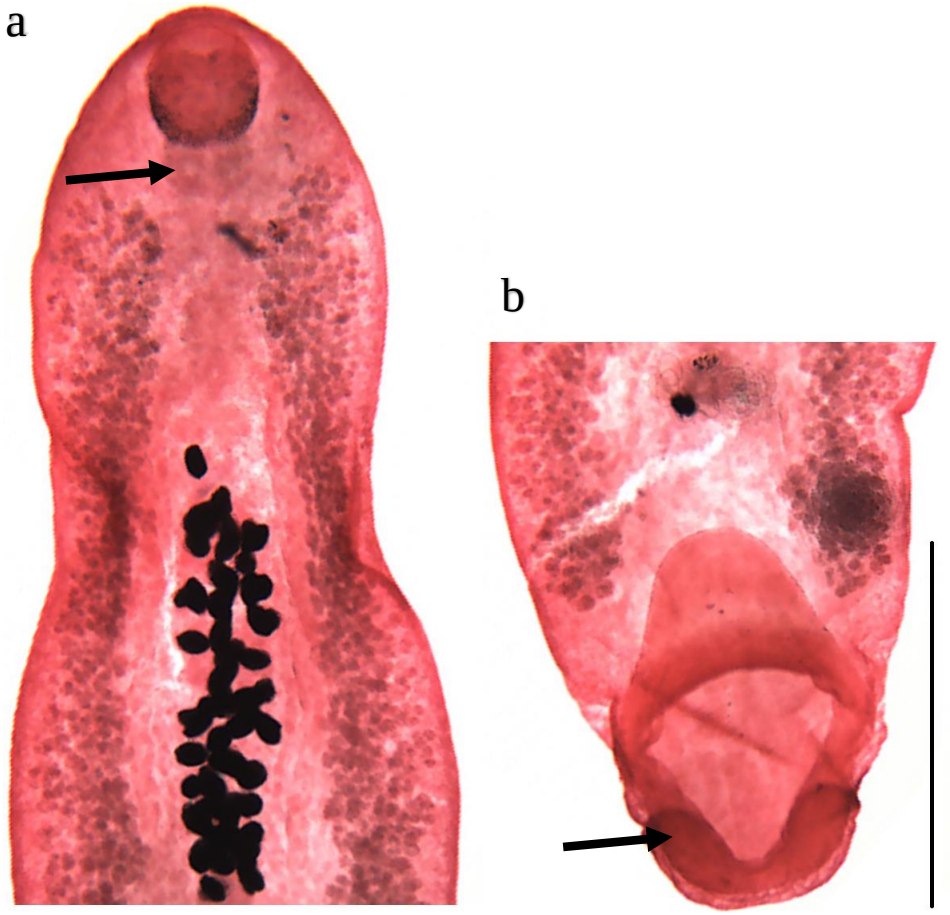

Figure 1.15. *Zygocotyle lunata* from *A. collaris* at 40x. (a) anterior segment of body of body. Arrow points to oral diverticula. (b) posterior segment of body. Arrow point to muscular papillae on ventral sucker. Scale bar indicates 1500 μm.

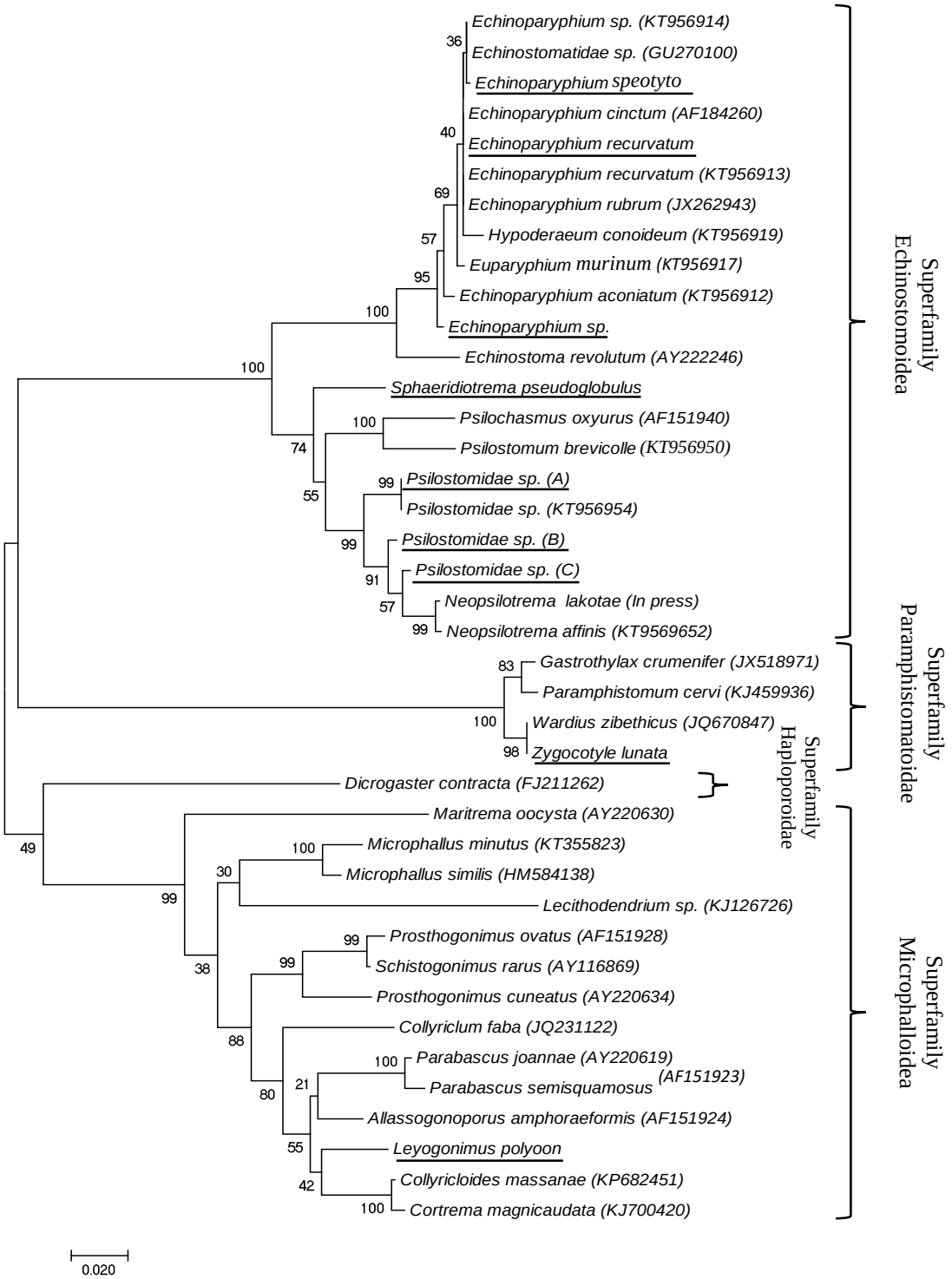

Figure 1.16. ML phylogeny for 28S rDNA sequences utilizing 500 bootstraps. Node support given out of 100. Underlined species indicate sequences obtained in the present study. The scale bar denotes the number of expected substitutions per site.

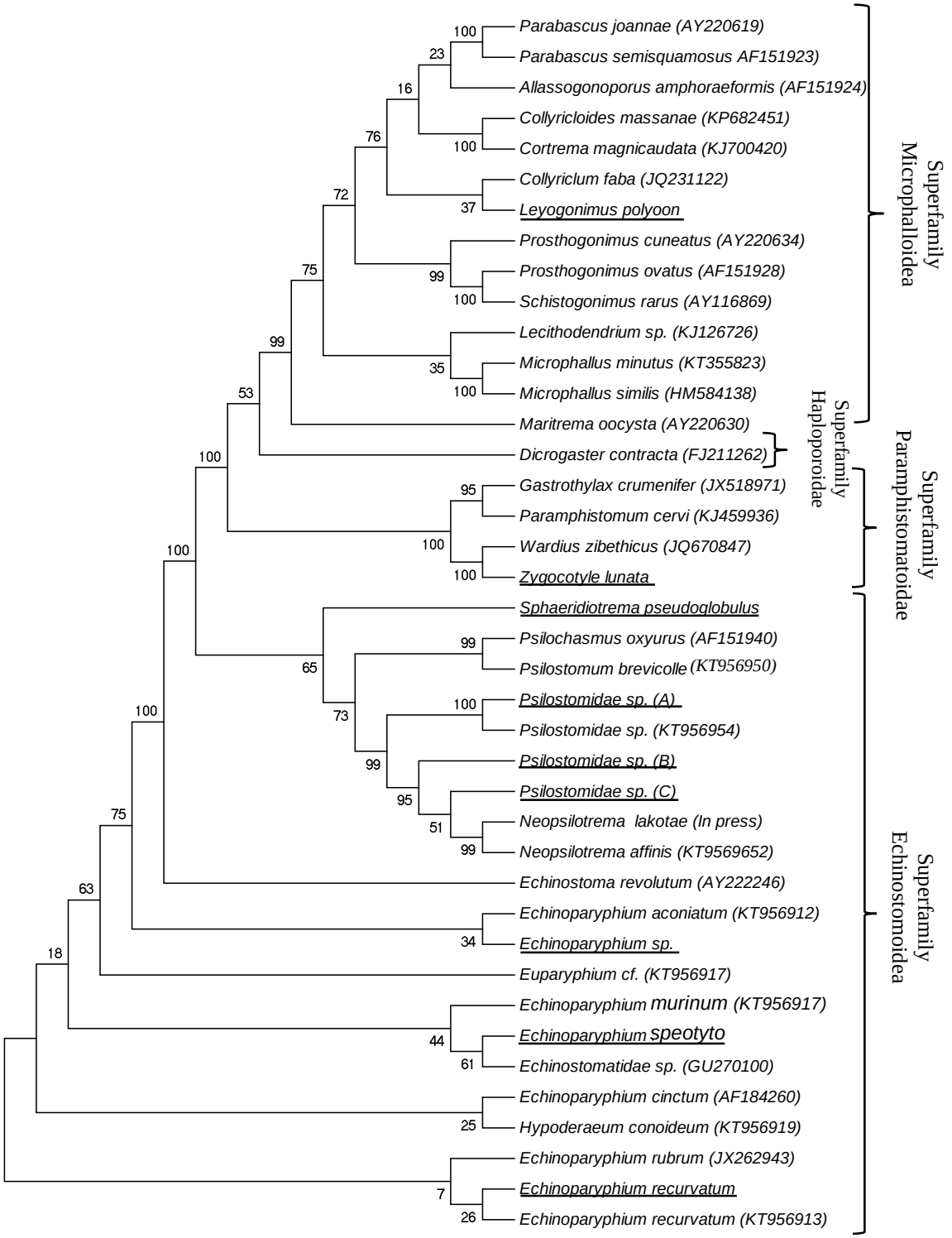

Figure 1.17. Consensus MP phylogeny of 28S rDNA sequences with 500 bootstraps. Node support given out of 100. Underlined species indicate sequences obtained in the present study.

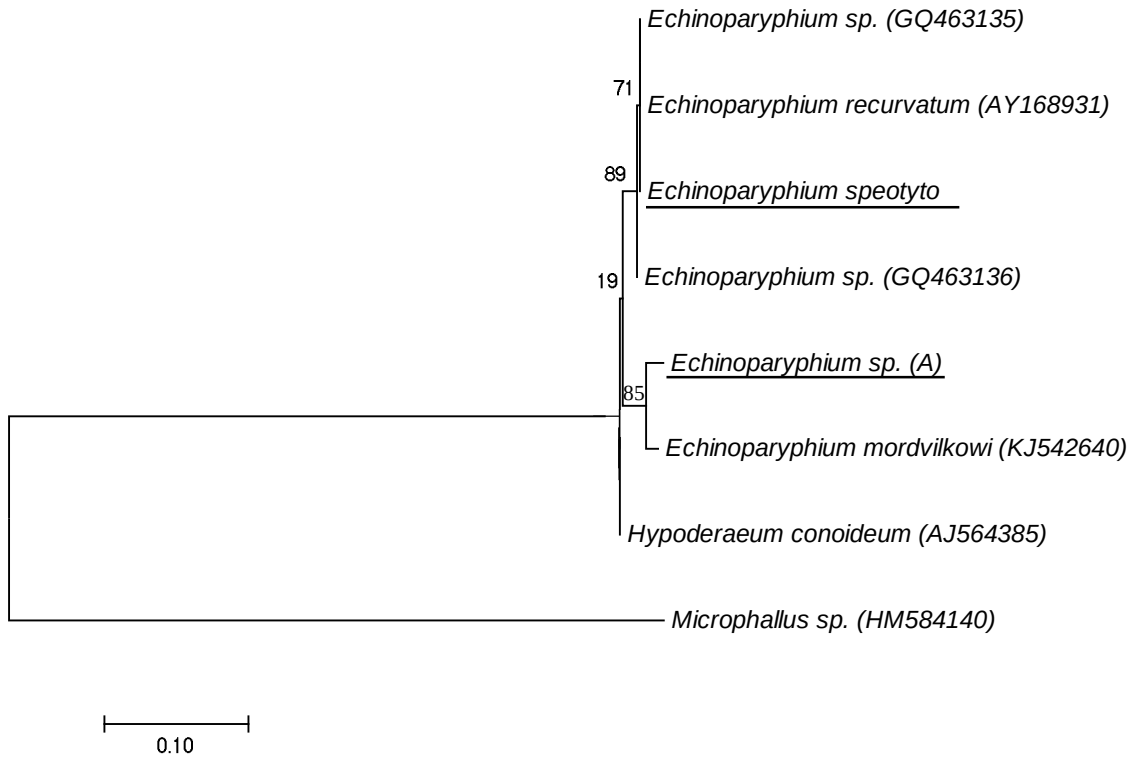

Figure 1.18. ML phylogeny for ITS sequences using 500 bootstraps. Node support given out of 100. Underlined species indicate sequences obtained in the present study. Scale bar denotes the number of expected substitutions per site.

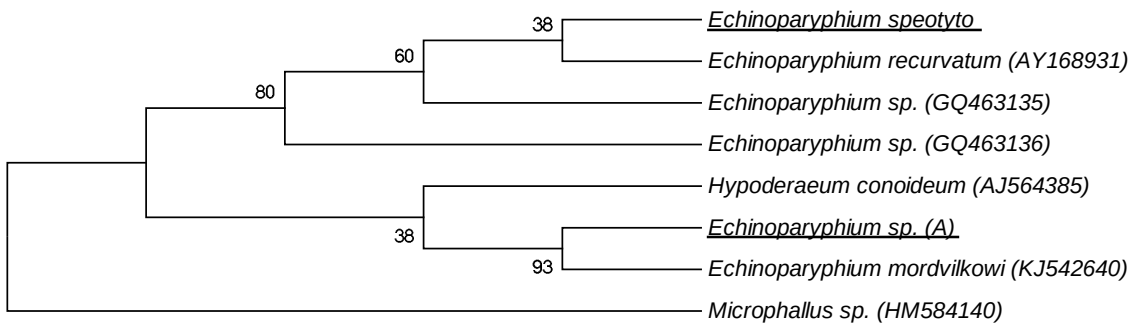

Figure 1.19. MP consensus phylogeny for ITS sequences using 500 bootstraps. Node support given out of 100. Underlined species indicate sequences obtained in the present study.

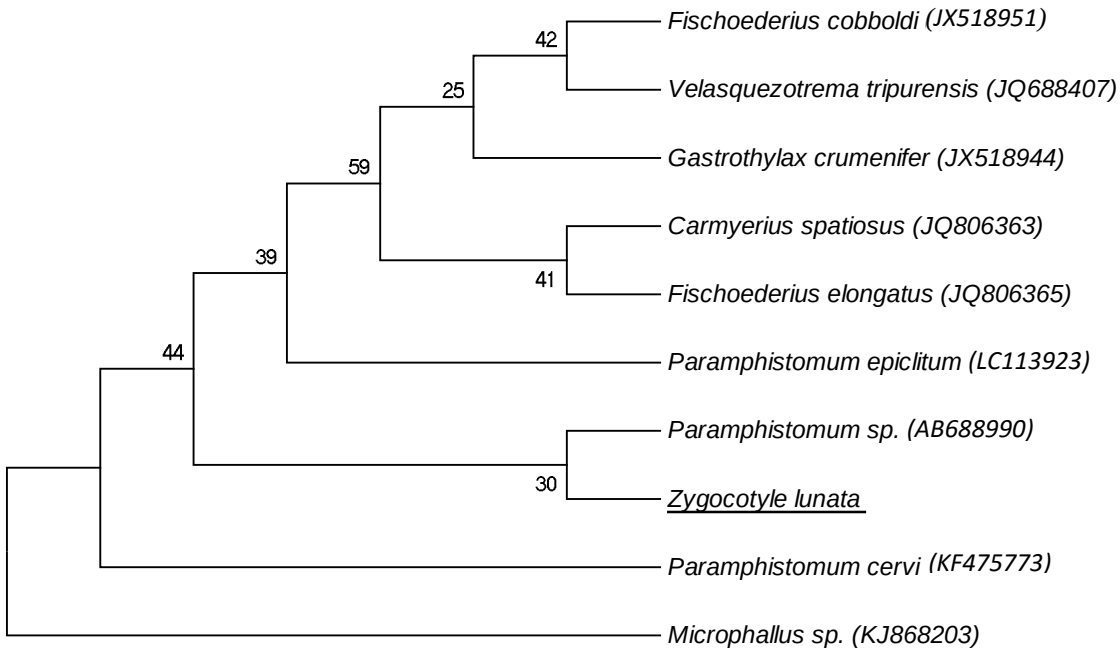

Figure 1.20. Consensus ML phylogeny for CO1 mtDNA sequences utilizing 500 bootstraps. Node support given out of 100. Underlined species indicate sequences obtained in the present study. The. scale bar denotes the number of expected substitutions per site.

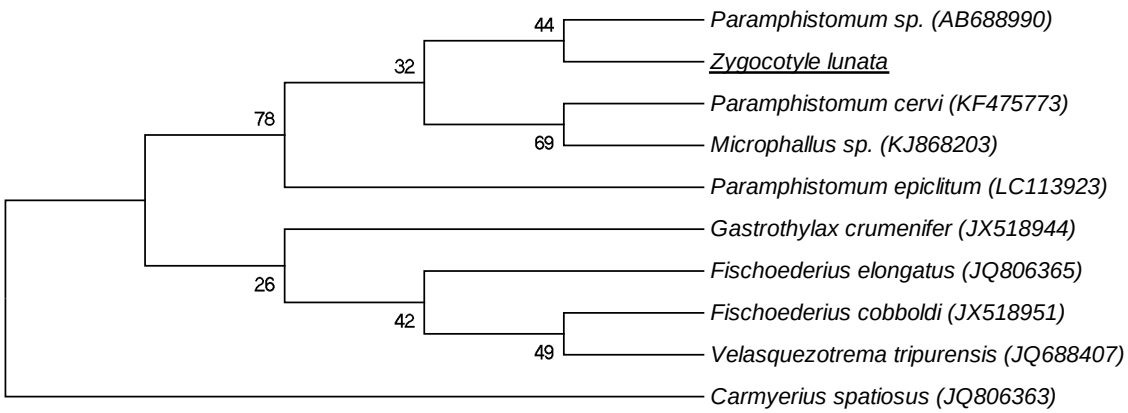

Figure 1.21. Consensus MP phylogeny of CO1 mtDNA sequences from 500 bootstraps. Node support given out of 100. Underlined species indicate sequences obtained in the present study.

Chapter 2: The identification and description of *Neopsilotrema lisitsynae* in North America.

Abstract

Neopsilotrema lisitsynae Kudlai, Pulis, Kostadinova, & Tkach, 2016 (*in press*) (Digenea: Psilostomidae) was originally known only from specimens collected in Ukraine (Kudlai et al. *in press*). This study documents the presence of *N. lisitsynae* in North American waterfowl for the first time. A survey of hunter-shot waterfowl from Lake Winnibigoshish, MN, in the fall 2012 and spring 2013 yielded 4 novel hosts for *N. lisitsynae*: *Anas platyrhynchos*, *Anas discors*, *Aythya collaris* and *Aythya affinis*. These worms were found primarily in the anterior to middle stretches of the small intestine with fewer individuals throughout the remainder of the gastrointestinal tract, but none were found within the cecae. A wider range of body measurements was associated with adults from North American hosts compared to the Ukrainian specimens described in Kudlai et al. (*in press*); in addition, the specimens described here suggests host-specific morphometric variation. Body spines were not evident through scanning electron microscopy; however, a few sporadic tuberculations were found on the tegument anterior to the ventral sucker along with strong tegumental folding and concentrated regions of tuberculations were found surrounding the genital pore. Diagnostic ratios of morphometric measures, adjusting for post-testicular vitelline fields, were shown to be statistically valid for *N. lisitsynae* identification between hosts while raw metrics were

more variable. These ratios were generated for a wide variety of psilostomids providing increased resolution for identification of cryptic psilostomids. Nucleotide information from 28S ribosomal DNA sequences showed one shared variable nucleotide site amongst the eleven individuals from the four birds collected in the fall and two from mallards harvested in the spring. Genetic differences did not appear to associate with worm body size, host species or collection season.

Introduction

Neopsilotrema Kudlai, Pulis, Kostadinova, & Tkach, 2016 (Family Psilostomidae) is a recently described genus of avian trematodes found in North America and eastern Europe. Body forms of psilostomids are well conserved with a general appearance somewhat similar to echinostomatids, but lacking a cephalic collar or associated collar spines (Kostadinova 2005b). Intergeneric diagnosis relies on the body size and shape, the presence of tegumental spines, a bipartite seminal vesicle, post-testicular field length, a medial genital pore opening, and a larger ventral sucker in comparison to the oral sucker. Currently, only three species have been described within the genus based upon genetic data and adult worm morphology (*Neopsilotrema affine, Neopsilotrema lakotae, Neopsilotrema lisitsynae*). Analysis of 28S rDNA was shown to accurately identify these three *Neopsilotrema* species (Kudlai et al. *in press*). One additional species was redescribed into the genus based on morphology (*Neopsilotrema marilae* Price, 1943) (Kudlai et al. *in press*). *N. affine* and *N. lakotae* from North Dakota and Minnesota were described as cryptic with the most reliable identification method being genetics *N.*

lisitsynae was described as a morphologically distinct species from Ukraine based on a few specimens that were collected for morphometric and genetic analysis of 28S rDNA sequences. To date, no large-scale morphometric analysis within this genus has been performed.

This study examined the morphometric variation among 397 *N. lisitsynae* individuals collected from various of North American waterfowl, which was compared to the same measures from the Ukrainian specimens. In addition, ultrastucture analysis was performed on the North American *N. lisitsynae* using images derived from scanning electron microscopy. Lastly, the 28S rDNA sequences of *N. lisitsynae* from each definitive host species collected here were compared to each other to confirm the species diagnosis and evaluate the potential existence of intraspecific genetic variation.

Materials and Methods

Sample collection

Intestines of waterbirds from Lake Winnibigoshish in Minnesota, USA, were received from waterfowl hunters in fall 2012 and spring 2013 (Table 1.1; Fig. 1.1). Upon collection, intestines were frozen and transported to Minnesota State University, Mankato until a time when parasites could be collected through dissection of the intestinal tissue. Small intestine tissue was segmented into 15cm linear sections, while cecae and large intestines were not subdivided into smaller segments prior to examination. Parasites were removed from the intestinal contents with the aid of a binocular dissecting microscope.

Collected worms were stored in 10% buffered formalin or frozen for morphological or molecular analysis, respectively.

Morphological analysis

Individual worms were prepared for light microscopy by staining them with Semichon's acetocarmine before they were dehydrated in ascending concentrations of ethanol. Upon dehydration, worms were cleared using xylene and mounted in Kleermount® (Carolina) or Canada balsam. Specimens were observed using an Olympus CH2 microscope and digital images were captured with a trinocular-mounted Moticam 10MP camera. Characteristics of the worms were measured using Moticam Images Plus 2.0 ML software (Motic). Statistical analysis of measurement data was carried out using a Kruskal-Wallis, nonparametric, one-way analysis of variance using SigmaPlot software (Systat).

For scanning electron microscopy, three individual worms that had been removed from an *A. affinis* duck were rinsed in phosphate buffered saline (PBS), treated with 1% osmium tetraoxide, then exposed to ascending concentrations of acetone (50%, 70%, 85%, 95%, absolute). Worms were critically dried using Polaron CPD7501 critical dryer, mounted on aluminum stubs, and coated with gold using a Cressington 108 auto sputter coater. A JEOL JSM6510LV scanning electron microscope was used for specimen visualization and image capture.

Abbreviations used for body measurements are as follows: body length—BL; body width—BW; body depth—BD; forebody length—FORE; oral sucker length—OSL; oral sucker width—OSW; prepharynx length—PL; pharynx length—PHL; pharynx width—PHW; ventral sucker length–VSL; ventral sucker depth–VSD; cirrus-sac length–CSL; cirrus-sac width–CSW; anterior seminal vesicle length–SVL1; anterior seminal vesicle width–SVW1; posterior seminal vesicle length–SVL2; posterior seminal vesicle width–SVW2; anterior testis length–ATL; anterior testis width–ATW; anterior testis depth–ATD; posterior testis length—PTL; posterior testis width—PTW; posterior testis depth—PTD; distance between posterior margin of posterior testis to posterior extremity of body—TEND; ovary length—OVL; egg number—E; egg-length—EL; and egg-width—EW. Proportions based on Kostadinova (2005a) were generated for: maximum body width to body length—BW%; maximum depth to body length—BD%; forebody length to body length—FO%; length of post-testicular field to body length—T%; and oral sucker to ventral sucker—OS:VS. All measurements given in text, tables and figures are in µm.

Molecular analysis

DNA of individual worms was extracted using a ZR Genomic DNA™-Tissue MiniPrep kit (Zymo Research) and eluted in 35 µL of water. The 28S rDNA locus was amplified with the primer pair DIG (5’-AAG CAT ATC ACT AAG CGG-3’) and 1200R (5’-GCA TAG TTC ACC ATC TTT CGG-3’) from Tkach et al. (2003) and Atopkin PCR amplifications were done using 0.25 µL of each primer (10µm), 7.5 µL of GoTaq® green mastermix (Promega), 50 ng of template DNA and raised to a volume of 15 µL with

ddH_2O. Run conditions for PCR were 94 ºC for 2 minutes followed by 35 cycles of 30 seconds at 94 ºC, 30 seconds at 50 ºC, and 1 minute at 72 ºC. After 35 cycles the temperature was set to 72 ºC for 10 minutes. 1200 basepair (bp) amplicons were run on a 1% agarose gel, gel excised, and purified using ZR Gel DNA Recovery Kit (Zymo Research). Recovered amplicons were cycle-sequenced using a modified protocol from Whalen (2011): BigDye™ terminators using 1 µL of BigDye™, 1 µL of 5x BigDye™ reaction buffer, 2 µL of either DIG or 1200R primer and 24 ng of PCR product, with the following run conditions: an initial 5 minutes at 95 ºC followed by 99 cycles of 30 seconds at 95 ºC, 20 seconds at 50 ºC for DIG or 53 ºC for 1200R and 4 minutes at 60 ºC. Sequencing products was run on an ABI Prism 377 DNA sequencer after clean up using a ZR Sequencing Clean-up kit (Zymo Research) or ethanol precipitation. Sequence electropherograms were refined using BaseFinder (Giddings et al. 1998) to aid base calling. When possible, contiguous sequences were assembled and aligned using Mega7; one alignment of 1108 nucleotides was generated based upon the shortest, contiguous sequence (Kumar & Hedges 2016).

Results

Hosts

Amongst North American waterfowl examined, *A. discors*, *A. platyrhynchos*, *A. affinis*, and *A. collaris* contained *N. lisitsynae* (Table 2.1) These worms were primarily within the first 60cm of the small intestine (n> 400 in some birds) with the number of worms decreasing through the remainder of the small and large intestine (n< 20 worms). None were found to reside within the cecae.

Morphometrics

A wider range of metrics were found for all structures examined in the North American samples compared to the worms described from Ukraine (Table 2.2; Fig. 2.1), with 4 relatively distinct morphotypes being identified frequently. Analysis of variance (Kruskal-Wallis) tests for both base metrics and ratios comparing worms from the different host species support the presence of a potential host effect on morphometric variation in all raw metrics and proportions measured except BD, CSL, EW, BW, and OS:VS (Tables 2.3, 2.4, 2.5) with indication of *N. lisitsynae* individuals from lesser scaup typically being larger than in other hosts ($p<0.01$ in most cases).

Due to the subspherical nature of the ovary in the worms collected in Minnesota, only a length measurement was taken, in contrast to Kudlai et al. (*in press*) who used both ovary length and width. The ovary was found in a dextral, medial, or sinistral position in the specimens from North America (Fig. 2.2). Tegumental spines were present on only a few specimens (est. 33%), while most *N. lisitsynae* in the present study had no evidence of spines (Fig. 2.3, 2.5).

The large number of individuals that were oriented in a lateral position on their slides required that measurements of depth be taken for most structures in hopes they provided diagnostic value. When viewed laterally, body depth tapered briefly before truncation. No morphometric variation was detected between worms form the birds collected in the spring when compared to those from the fall (data not shown).

Non-gravid adults made up 35% of the sample; the most gravid adults (E> 5) were among the largest worms found (BL> 1000), while the smallest adults identified were non-gravid (BL= 364.5).

Diagnostic ratios

Measurements for two regions of the individual worms (TEND and FORE) consistently varied the greatest regardless of host and maturity of the worm. In order to account for this variation, several additional proportions were generated utilizing the body length of the worms (Table 2.6; Fig. 2.4). The adjusted proportions of AF and ABD of the *N. lisitsynae* from Minnesota differed across hosts or age of worms, which was similar to raw morphometric values. While ABW, FBW, AFoBW, FBD, and AFoBD did not vary highly between hosts or age of worms (Table 2.7).

Adjusted diagnostic proportions based on line drawings of the members of *Neopsilotrema* described by Kudlai et al. (*in press*) appeared different than *N. lisitsynae* in the present study; however, statistical support for any differences is untenable because of the low sample size (n=1) and lack of variation in the measures taken from the line drawings. The AF, ABW, FBW, ABD, FBD, and AFoBD adjusted proportions of *N. lisitsynae* in the present study seemed to be different from the *Neopsilotrema* species examined with ABW and ABD values for *N. lakotae* being larger than the mean ± SE for *N. lisitsynae*, while all other adjusted ratios trended toward being larger in *N. lisitsynae*. Differences in ABW, FBW, and AFoBW were present between Ukrainian and North American worms

(Table 8a). Further, Ukrainian *N. lisitsynae* were closer to other *Neopsilotrema* species in regards to ABW, and FBW. Lateral proportions of Ukrainian *N. lisitsynae* could not be compared due to the lack of an available line drawing. The adjusted proportions from line drawings were compared between several species of psilostomids, showing at least one adjusted proportion diverging per species within a genus, which indicates potential diagnostic utility for species diagnosis. (Table 2.8a; Table 2.8b).

Ultramicroscopy

The tegument anterior to the ventral sucker on both ventral and lateral sides was smooth with few sporadic, small pits and tuberculations and many larger tegumental folds. No papillae, scales, spines or pits associated with spines could be seen on the tegument. The medial segment of the tegument remained smooth with limited tegumental folds and no external perturbations. The posterior segment of the tegument contained more folds then the medial, but less than the anterior, ventral, tegument (Fig. 2.5). The opening of the excretory pore was visible on the posterior end surrounded by a concentrated area of folds and no apparent external perturbations.

The ventral sucker did not show strong external muscular striation, rather it remains contiguous with tegumental tissue. This is consistent with the appearance of the ventral sucker when viewed with light microscopy, which showed a sizable amount of tegument separating the exterior walls of the ventral sucker from the external tegument. The ventral

sucker was strongly flexed on all specimens and contained a large amount of debris (Figs. 2.5-2.6).

The uterine opening of the genital pore was found to range from 14.85 to 20.1 µm in width with small tuberculations on the opening. These openings do not extend beyond the immediate tegument (<1 micrometer from the opening). The cirrus opening (5.3 to 8.4 µm diameter) of the genital pore was located between 9.61 to 12.9 µm from the uterine opening (Fig. 2.7).

Molecular Data

Thirteen 28S rDNA sequences (Fig. 2.8) were obtained with nine being contiguous. Noncontiguous sequences were not used for analysis. One nucleotide was found to vary (C-T transition) at nucleotide position 979 in the alignment of individual *N. lisitsynae*, including one heterozygous sequence. A ring-necked duck contained a 'C' genotype and a heterozygous individual. Blue-winged teal and lesser scaup only contained the "C' genotype. No pattern of this variation seemed to be associated with the various body forms.

Attempts were made to amplify the cytochrome c oxidase (CO1) mitochondrial DNA locus using the previously described MPLAT and JB primer sets (Morgan & Blair 1998; Moszczynska et al. 2009). Neither primer sets yielded PCR products for *N. lisitsynae*,

under a wide variety or reaction conditions even though these pairs have worked well for other trematode species.

Discussion

N. lisitsynae was described only from Eurasian teal in the Ukraine; however, other members of the genus *Neopsilotrema* have been reported from Minnesota, USA (Kudlai et al. *in press*). The geographical range of *N. lisitsynae* can now be expanded to include North America with the addition of four new waterfowl hosts: *A. platyrhynchos*, *A. discors*, *A. collaris*, and *A. affinis*.

The 28S DNA sequences examined did not show host- or season-specific variation; however, the variable nucleotide at position 979 in some mallard and ring-necked duck samples was unusual. The variable nucleotide could happen if the original PCR template DNA contained of a mix of the two sequences. In other words, a portion of the template DNA must have contained the T and the remainder contained both genotypes were found in a mallard from the fall, while only the 'T' genotype was found within mallards collected in the spring.

Typically, intraspecific divergence is not present within the 28S rDNA region, rather variation is typically associated with discrete species (Tkach et al. 1999). The absence of both genotypes within all bird species and seasons was most likely due to the smaller

sample size for lesser scaup, blue-winged teal, and spring-collected worms. Further work is required on more variable loci to identify potential population variation.

Care was given to examine both extreme and average sized individuals genetically; however, no genotypic pattern could be seen across different morphologies. Rather, both extremes (large and small) contained each genotype, as did the average-sized worms, indicating the presence of one synonymous species. This supports a need for future study using more variable loci to investigate the presence of a genetic marker specific to these morphotypes to aid future diagnostic efforts (Morgan & Blaire 1998; Sorensen et al. 1998; Moszczynska et al. 2009; Tkach et al. 2016).

Morphometric variation was detectable between hosts, with worms from mallard and lesser scaup being largest, most elongated, and contained the most eggs; however, it's possible this pattern is due to the age of worms rather than the hosts they came from. The largest individuals possessed the most eggs, however, most non-gravid adults were equitable to adults with fewer eggs. Perhaps, given enough time, the less gravid individuals may have continued to grow in size. Conversely, the difference in size may be due to host specific or competition-related effects on development. If the variation is due to competition, it is unlikely due intraspecific competition, as the larger individuals were found within hosts with the greatest intensity of *N. lisitsynae* (data not shown). Dubois & Rausch (1950) showed members of Family Strigeidae to have a high degree of variation dependent on the definitive host. It is quite likely that *N. lisitsynae* may undergo similar

changes as the worms from mallard and lesser scaup differed from *N. lisitsynae* found in other waterfowl.

Proportions that relate the size of various body regions have been utilized for both genus and species diagnoses. The proportions described by Kostadinova et al. (2005a), such as BW%, were found to be diagnostic for most genera diagnoses including families with conserved morphology such as Psilostomidae. Proportions based on Kostadinova (2005a) have been shown effective in species diagnosis in *Neopsilotrema*, such as the use of BW% between *N. affine* and *N. lisitsynae* from Ukraine (Kudlai et al. *in press*). The variation within proportions based on Kostadinova (2005a) for the specimens in this study was too great for their reliable use as diagnostic instruments. For instance, BW% between *N. affine* and *N. lisitsynae* from the present study overlapped strongly. Adjusted proportions, where the adjustments are made to a measurement to account for maturity or proportional growth differences, have been used in other taxa, namely Family Strigeidae, which is a known cryptic group. Adjustments were made to account for overall size of the worms on the assumption of different developmental stages. For instance, forebody length and the post-testicular field, appeared to increase at a greater rate than other regions as the worms mature, which skews the relationship between body length measures that do not show the same stage dependent growth pattern.

Measurement of body features from *N. lisitsynae* collected from different definitive hosts were generally statistically different, which could lead to the conclusion that these worms

were not conspecific; however, the use of the adjusted ratios accounts for variation in a way that would support the conspecific nature of these worms. This finding argues that adjusted proportions may provide an additional set of metrics for support of morphological diagnosis of *Neopsilotrema* members. In addition, *N. affine* and *N. lakotae*, which have been described as cryptic and morphologically indistinguishable, are able to be distinguished using the diagnostic ratios described here; however, this is based on ratios calculated from line drawing *N. affine* and *N. lakotae*, which may underrepresent variation among individuals and interfere with the use of these proportions. Identification of the potential range of these proportions needs to be identified in future studies to confirm their accuracy on other species.

Lateral measurements along the midline of a frontal plane were required for 52% of the specimens examined rather than measuring along the midline of a sagittal plane due to strong muscular flexing that bent individuals on the dorsal-ventral axis. Lateral measurements have been shown to be useful for diagnosing heterophyids, and strigeids amongst many other taxa (Martin 1958; Fischthal & Kunts 1963; Mizelle & Donahue 1944; Manter 1963), but have not been used for *Neopsilotrema* and other closely related genera (i.e. *Psilotrema*). Organ width versus depth did not appear to vary highly between dorsal and lateral views. Further, measurements of adjustment proportions of body depth were apparently different than other morphologically similar psilostomids (Tables 2.8a; 2.8b). The low level of variability between lateral and ventro-dorsal measurements supports the use of lateral measurements for diagnostic purposes for *N. lisitsynae*.

However, the lack of lateral measurements for many psilostomid species prevents complete analysis of potential diagnostic utility.

The wider range of morphology detected in the present study contrasts with the morphology previously described; the wider range of morphology is likely due to combination of worm age-, locality- and host-specific variability. Kudlai et al. (*in press*) found *N. lisitsynae* to infect Eurasian teal (*Anas crecca*), compared to the four identified hosts found in North America. The original description listed a concise metric range, our study found a larger amount of intraspecific variation, potentially due to the larger sample size. While a greater range of measurements was found, the means of all traits examined were equitable to those from Kudlai et al. (*in press*). This study's morphometric patterns showed sizable overlap with other described *Neopsilotrema* species; however, gross morphology of *N. lisitsynae* has been shown to be morphologically distinct from *N. affine*, *N. lakotae*, and *N. marilae*.

Three notable differences have been identified from the original description of *Neopsilotrema* when compared to the details of *N. lisitsynae* described herein: egg number, presence of tegumental spines, and ovary position. The genus *Neopsilotrema* is currently described as containing up to 5 eggs (*N. lisitsynae* – up to 4 eggs) and have fine tegumental spines. The most gravid adults in the present study contained up to 9 eggs, while most gravid adults only held 0 to 4 eggs.

Examination with 1000x light microscopy often did not show any sign of spines, while ultrastructure analysis, showed no sign of tegumental spines or scales or associated structure. It is possible spines were lost due to storage of worms prior to analysis because the intestines and worms were frozen prior to dissection rather than being immediately heat-killed and fixed. Prior studies have shown smaller spines to be lost easily; however, it is usual to be able to find pits or scars associated with spines if spines were indeed present during life. The loss of spines could also be accounted for due to phenotypic plasticity within the species, improper fixation, or chemical exposure (Meaney et al. 2001; Cribb 2005). Although spine loss is a possibility, the tubercles seen on ultrastructure analysis may be taking up stain which may appear spine-like on light microscopy. The concentrated area of tegumental folds appeared in regions associated with muscular structures. The contracted musculature is the most likely cause for the folds seen. Further studies of this species should be undertaken to account for these possibilities and until further information is gathered the presence of spines on *N. lisitsynae* should not be considered a valid diagnostic trait.

Ovary location was also found to be sinistral in some specimens in contrast to the previously described dextral-medial position; this is not entirely unusual as this has been reported to vary in intraspecifically in some *Psilotrema* Oschmarin, 1963 species. Both traits appear to be plastic traits of the species and should not be regarded strongly for species diagnosis.

The morphological differences noted require expansion of the description of *Neopsilotrema* Kudlai, Pulis, Kostadinova, & Tkach, 2016 to include: small (BL= up to 1600 expanded from 875), elongate (BW= 17-66% expanded from 27-57%) body forms, short forebody lengths (FO= 16-38%, expanded from 21-38%), increased egg number (E= 0-9, expanded from 0-5), and presence or absence of tegumental spines. The increase in body size further supports the difference from *Gyrosoma* Byrd, Bogitsh & Maples, 1961 (BL> 1mm vs < 1mm). The increased body size, elongate form, and egg number places *Neopsilotrema* closer to *Psilostomum* Looss,1899; however, differences between *Neopsilotrema* and *Psilostomum* are apparent in relative sucker size (OS:VS= 1:1.3 vs 1:1) and post-testicular field distance (T%= 14-47% vs 7-15%).

Further work on morphological traits at each stage of the life cycle of *N. lisitsynae* is needed in order to further show potential diagnostic traits for both generic and species diagnoses. As *N. lisitsynae* was identified from waterfowl from Lake Winnibigoshish, the lake may yield other life cycle stages for future study.

References

Atopkin, D. M. (2011). Genetic characterization of the *Psilotrema* (Digenea: Psilostomatidae) genus by partial 28S ribosomal DNA sequences. *Parasitology International*, 60 (4), 541–543.

Bunkley-Williams, L., Dyer, W. G., & Williams, E. H. (1996). Some Aspidogastrid and digenean trematodes of Puerto Rican marine fishes. *Journal of Aquatic Animal Health*, *8*(1), 87–92.

Cribb, T. H. (2005). Family Apocreadiidae Skrjabin, 1942. In: A. Jones, R. A. Bray, D. I. Gibson (Eds.), *Keys to the Trematoda Vol. 2* (pp. 621–639). Wallingford - London: CABI Publishing and The Natural History Museum.

Dubois, G., & Rausch, R. (1950). A contribution to the study of North American strigeids (Trematoda). *The American Midland Naturalist*, 43(1), 1–31.

Fischthal, J. H., & Kuntz, R. E. (1963). Trematode parasites of fishes from Egypt. Part V. Annotated record of some previously described forms. *The Journal of Parasitology, 49*(1), 91–98.

Giddings, M. C., Severin, J., Westphall, M., Wu, J., & Smith, L. M. (1998). A software system for data analysis in automated DNA sequencing. *Genome Research*, 8(6), 644–665.

Iskova, H. (1985). *Fauna of Ukraine in 40 volumes. Vol 34: Trematodes Issue 4*. Kiev: Naukova Dumka (In Russian).

Kostadinova, A. (2005a). Family Echinostomatidae Looss, 1899. In: A. Jones, R. A. Bray, D. I. Gibson (Eds.), *Keys to the Trematoda Vol. 2* (pp. 9–64). Wallingford - London: CABI Publishing and The Natural History Museum.

Kostadinova, A. (2005b). Family Psilostomidae Looss, 1900.In: A. Jones, R. A. Bray, D. I. Gibson (Eds.), *Keys to the Trematoda Vol. 2* (pp. 99–118). Wallingford - London: CABI Publishing and The Natural History Museum.

Kudlai, O., Pulis, E. E., Kostadinova, A., & Tkach, V.V. (*in press*). *Neopsilotrema* n. g. (Digenea: Psilostomidae) and three new species from ducks (Anseriformes: Anatidae) in North America and Europe. *Systemtatic Parasitology.*

Kumar, S., & Hedges, S. B. (2016). Advances in time estimation methods for molecular data. *Molecular Biology and Evolution*, 33(4), 863–869.

Martin, W. E. (1958). The life histories of some Hawaiian heterophyid trematodes. *The Journal of Parasitology, 44*(3), 305–318.

Meaney, M., Fairweather, I., Brennan, G., Ramasamy, P., & Subramanian, P. (2001). *Fasciola gigantica*: Tegumental surface alterations following treatment in vitro with the sulphoxide metabolite of triclabendazole. *Parasitology Research Parasitol Res., 88*(4), 315–325.

Morgan, J. A. T., & Blair, D. (1998). Relative merits of nuclear ribosomal internal transcribed spacers and mitochondrial CO1 and ND1 genes for distinguishing among *Echinostoma* species (Trematoda). *Parasitology*, 116(03), 289–297.

Moszczynska, A., Locke, S. A., McLaughlin, J. D., Marcogliese, D. J., & Crease, T. J. (2009). Development of primers for the mitochondrial cytochrome c oxidase I gene in digenetic trematodes (Platyhelminthes) illustrates the challenge of barcoding parasitic helminths. *Molecular Ecology Resources*, 9, 75–82.

Price, E. W. (1942). A new trematode of the family Psilostomidae from lesser scaup duck, *Marila affinis. Proceedings of the Helminthological Society of Washington*, 9, 30–31.

Oshmarin, P. G. (1963). *Parasitic worms of mammals and birds*. USSR: Publishing House of the USSR Academy of Sciences. (In Russian)

Sorensen, R. & Minchella, D. (1998). Parasite influences on host life history: *Echinostoma revolutum* parasitism of *Lymnaea elodes* snails. *Oecologia*, 115, 188–195.

Tkach, V. V., Grabda-Kazubska, B., Pawlowski, J., & Świderski, Z. (1999). Molecular and morphological evidence for close phylogenetic affinities of the genera *Macrodera, Leptophallus, Metaleptophallus* and *Paralepoderma* (Digenea, Plagiorchiata). *Acta Parasitology*, 44,170–179.

Tkach, V. V., Littlewood, D. T., Olson, P. D., Kinsella, J. M., & Swiderski, Z. (2003). Molecular phylogenetic analysis of the Microphalloidea Ward, 1901 (Trematoda: Digenea). *Systematic Parasitology Syst Parasitol*, 56(1), 1–15.

Tkach, V. V., Kudlai, O., & Kostadinova, A. (2016). Molecular phylogeny and systematics of the Echinostomatoidea Looss, 1899. *International Journal of Parasitology*, 46(3), 171–185.

Whalen, S. (2011). Analysis of the genetic structure of *Bithynia tentaculata* snail populations in Wisconsin and Minnesota. (Master's thesis). Minnesota State University, Mankato, MN.

Table 2.1. Seasonal prevalence of *N. lisitsynae* in waterfowl harvested at Lake Winnibigoshish, MN.

Bird species	Common name	Fall		Spring	
		n	%	n*	%
Anas platyrhynchos	Mallard	10	70%	11	27.3%
Anas discors	Blue-winged teal	15	87%	2	0
Aythya collaris	Ring-necked duck	13	15.4%	7	0%
Aythya affinis	Lesser scaup	10	60%	1	100%

Table 2.2. Morphometric comparison between Ukraine (Kudlai et al *in press*) and North America *N. lisitsynae* samples.

Source	Ukraine		North America (Present study)		
	Range	$\bar{x}$	Range	$\bar{x}$±SE	n
BL	810-875	833	365-1632	828±10	395
BW	238-263	250	108-378	233±4	188
BD	-	-	84-344	196±3	214
FORE	168-182	173	67-327	184±3	331
OSL	63-76	72	19-104	58±1	359
OSW	71-81	75	27-110	68±1	379
PL	0	0	0	0	100
PHL	52-56	54	23-97	52±1	368
PHW	53-56	55	20-76	45±1	366
CSL	182-220	204	97-351	191±3	321
CSW	80-98	87	41-180	70±1	338
SVL1	50-58	55	32-72	49±2	37
SVW1	49-71	60	42-79	55±2	40
SVL2	75-111	90	55-108	78±2	50
SVW2	64-84	74	44-96	66±2	48
VSW	159-187	169	66-254	142±2	391
VSD	-	-	74-288	175±3	232
ATL	81-96	89	53-181	94±2	282
ATW	105-119	110	53-178	112±2	161
ATD	-	-	53-181	115±2	125
PTL	76-96	87	50-159	94±2	266
PTW	85-116	99	67-171	113±2	158
PTD	-	-	62-188	118±2	109
TEND	303-342	323	91-724	282±5	319
OVL	61-89	78	52-129	86±1	307
E	-	-	1-9	3±1	266
EL	76-88	82	48-107	75±1	628
EW	46-50	48	30-70	51±1	677
BW%	27-33	30	17-66	30±0	186
BD%	-	-	14-36	24±0	207
FO%	23-27	25	12-37	22±0	328
T%	37-40	39	15-47	32±0	313
OS:VS	1:2.0-2.5	2.2	1.4-3.9	2.4±0.1	354

Table 2.3. Comparison of body forms and structures of North American *N. lisitsynae* between hosts

Feature	*A. collaris*			*A. platyrhynchos*			*A. discors*			*A. affinis*			P-value
	$\bar{x}$ ±SE	Range	n	$\bar{x}$ ±SE	Range	n	$\bar{x}$ ±SE	Range	n	$\bar{x}$ ±SE	Range	n	
BL	726±73	581-817	3	768±18	365-1125	90	774±9	462-1040	200	989±22	484-1632	103	*
BW	199±25	174-223	2	21±7	107-313	58	217±4	136-275	74	271±7	160-378	55	*
BD	211±30	18-240	2	183±7	83-263	36	195±3	100-264	128	207±6	116-344	48	0.08
FORE	178±6	172-184	2	168±6	66-326	77	179±2	112-261	168	206±4	103-279	84	*
OSL	57±5	50-66	3	54±1	19-76	82	55±1	31-75	189	69±2	47-104	85	*
OSW	45±2	43-47	2	63±2	27-93	88	64±1	39-98	198	78±2	51-110	91	*
PHL	46±5	41-57	3	48±1	23-62	84	49±1	36-97	194	60±1	37-93	87	*
PHW	36±2	32-40	3	42±1	19-75	84	44±1	30-60	193	50±1	34-61	86	*
VSW	122±6	112-133	3	143±4	65-215	90	128±2	83-215	198	170±4	98-254	100	*
VSD	152	-	1	182±4	113-231	48	162±3	74-214	141	212±6	143-278	42	*
TEND	214±2	164-243	3	228±7	90-358	70	270±4	138-405	168	355±13	150-724	78	*

* denotes a p-value of <0.001

Table 2.4. Comparison of gonad and gonad related structures within North American *N. lisitsynae* between hosts.

Feature	*A. collaris*			*A. platyrhynchos*			*A. discors*			*A. affinis*			P-value
	$\bar{x} \pm$SE	Range	n	$\bar{x} \pm$SE	Range	n	$\bar{x} \pm$SE	Range	n	$\bar{x} \pm$SE	Range	n	
CSL	149±14	135-162	2	187±5	104-270	71	190±4	99-265	158	197±6	97-351	90	0.36
CSW	53±3	50-58	3	61±2	41-84	69	69±2	45-180	179	80±1.60	48-111	87	*
SVL1	44	-	1	44±2	32-56	12	49±2	41-65	15	56±4	39-72	9	0.003
SVW1	45	-	1	51±2	53-62	15	55±3	42-68	14	65±4	45-79	10	0.007
SVL2	85	-	1	70±3	58-86	16	83±3	55-94	20	93±3	77-108	13	0.002
SVW2	58	-	1	61±2	52-3	16	65±3	44-82	20	78±1	66-96	11	0.002
ATL	83±1	82-84	2	88±3	55-132	67	92±2	53-181	150	108±3	60-167	63	*
ATW	100±12	89-111	2	101±4	53-138	46	110±3	64-178	66	127±4	68-175	47	*
ATD	111	-	1	114±6	76-181	24	112±2	53-137.9	84	137±7	91-181	16	0.003
PTL	68±4	64-71	2	87±3	50-130	62	90±2	55-143	137	109±3	71-159	65	*
PTW	95	-	1	101±3	67-133	42	108±2	71-143	66	130±3	89-171	49	*
PTD	101	-	1	110±6	62-166	21	115±2	77-146	71	140±7	104-188	16	0.002
OVD[1]	79±1	79-80	2	81±2	60-112	56	84±1	52-107	172	94±2	61-129	77	*
E	3±1	2-4	3	2±1	1-4	53	3±1	1-7	147	3±1	1-9	63	*
EL	68±3	60-78	7	79±2	56-107	78	75±1	48-97	379	75±1	48-94	164	0.004
EW	49±2	42-53	6	50±1	30-70	90	51±1	32-69	405	52±1	30-69	176	0.06

[1]Diameter at greatest distance.
* denotes a p-value of <0.001

Table 2.5. Comparison of morphometric proportions in North American *N. lisitsynae* between hosts.

	A. collaris			*A. platyrhynchos*			*A. discors*			*A. affinis*			P-value
Proportion	$\bar{x}$ ±SE	Range	n	$\bar{x}$ ±SE	Range	n	$\bar{x}$ ±SE	Range	n	$\bar{x}$ ±SE	Range	n	
BW%	32±4	27-36	2	30±1	21-41	55	31±1	17-66	74	28±1	17-51	55	0.22
BD%	26±3	23-29	2	23±1	17-33	35	23	15-36	122	22±1	14-36	48	*
FO%	20±2	17-22	3	22	14-31	76	23	14-37	167	21	12-31	82	*
T%	29±1	28-30	3	28±1	18-37	68	34	16-46	165	33±1	15-46	77	*
OS:VS	2.2±0.3	1.7-2.7	3	2.4±0.1	1.4-3.60	85	2.4±0. 1	1.4-3.9	183	2.5±0.1	1.4-3.8	83	0.07

* denotes a p-value of <0.001

Table 2.6. Equations for calculating adjusted diagnostic proportions

Adjusted proportion	Formula
Adjusted forebody (AF)	F/(L-T)
Adjusted body width (ABW)	W/(L-T)
Forebody-body width (FBW)	Fo/ABW[1]
Adjusted Forebody-body width (AFoBW)	F/D
Adjusted body depth (ABD)	F/W
Forebody-body depth (FBD)	D/(L-T)
Adjusted Forebody-body depth (AFoBD)	Fo/ABD[1]

[1] Fo denotes forebody:body length

Table 2.7. Diagnostic proportion comparison for *N. lisitsynae* individuals recovered from various hosts.

Adjusted proportion	*A. collaris*			*A. platyrhynchos*			*A. discors*			*A. affinis*			P-value
	$\bar{x}$ ±SE	Range	n	$\bar{x}$ ±SE	Range	n	$\bar{x}$ ±SE	Range	n	$\bar{x}$ ±SE	Range	n	
AF	0.3±0.02	0.25-0.32	3	0.31±0.01	0.25-0.38	50	0.33	0.25-0.39	137	0.31	0.24-0.39	59	*
ABW	0.4±0.01	0.39-0.42	2	0.42±0.01	0.29-0.6	44	0.44±0.01	0.25-0.60	58	0.41±0.01	0.25-0.58	47	0.36
FBW	0.82	0.82	1	0.78±0.03	0.51-1.16	44	0.82±0.02	0.56-1.17	60	0.75±0.02	0.50-1.06	44	0.1
AFoBW	0.58	0.58	1	0.53±0.02	0.37-0.73	33	0.54±0.01	0.35-0.75	58	0.51±0.02	0.31-0.75	43	0.31
ABD	0.38±0.04	0.33-0.42	2	0.31±0.01	0.23-0.42	24	0.36±0.01	0.22-0.53	103	0.30±0.01	0.23-0.43	32	*
FBD	0.86±0.09	0.77-0.95	2	0.95±0.04	0.59-1.40	28	0.95±0.02	0.56-1.39	104	0.99±0.03	0.64-1.36	33	0.59
AFoBD	0.6±0.06	0.54-0.66	2	0.7±0.03	0.46-1.2	20	0.63±0.01	0.40-0.91	100	0.65±0.02	0.40-0.87	29	0.07

[1]F denotes forebody length.

[2]Fo denotes proportion of forebody to body length

Table 2.8a. Adjusted diagnostic proportion comparison between *Neopsilotrema* and *Psilotrema* species. Values from *N. lisitsynae* collected in Minnesota for the present study are the mean proportion±SE for the population of worms measured; values for the other species are based on measurements taken from line drawings in papers describing those species.

Proportion	*Neopsilotrema*					*Psilotrema*				
	N. lisitsynae (Present)	*N. lisitsynae* (Ukraine)[1]	*N. affine*[1]	*N. lakotae*[1]	*N. marilae*[2]	*P. brevis*[3]	*P. mediopora*[3]	*P. acutirostris*[3]	*P. simillimum*[4]	*P. oligoon*[4]
AF	0.32±0	0.33	0.4	0.28	0.38	0.28	0.3	0.26	0.31	0.36
ABW	0.42±0.01	0.5	0.62	0.49	0.67	0.47	0.43	0.54	0.53	0.5
FBW	0.79±0.01	0.66	0.64	0.56	0.56	0.6	0.7	0.48	0.53	0.72
AFoBW	0.53±0.01	0.4	0.51	0.45	0.47	0.51	0.43	0.37	0.35	0.6
ABD	0.34±0.01	-	-	0.7	-	-	0.35	-	0.26	-
FBD	0.96±0.01	-	-	0.4	-	-	0.86	-	1.24	-
AFoBD	0.64±0.01	-	-	0.31	-	-	0.52	-	0.96	-

[1]inferred from line drawings from Kudlai et al. (*in press*)

[2]inferred from line drawings from Price (1942)

[3]inferred from line drawings from Oshmarin (1963)

[4]inferred from line drawings in Iskova (1985)

Table 2.8b. Adjusted diagnostic proportion comparison between various Family Psilostominae species. Values for these species are based on measurements taken from line drawings in papers describing those species.

Proportion	*Psilostomum* (*Pm*)		*Psilochasmus* (*Pc*)		*Sphaeridiotrema*
	Pm. anserinum[3]	*Pm. brevicolle*[4]	*P. oxyurus*[4]	*Pc. longicirratus*[4]	*S. globulus*[4]
AF	0.4	0.23	0.33	0.36	0.33
ABW	0.45	0.27	0.25	0.29	0.8
FBW	0.9	0.86	1.31	1.22	0.41
AFoBW	0.66	0.73	1.05	0.98	0.41
ABD	-	-	-	-	-
FBD	-	-	-	-	-
AFoBD	-	-	-	-	-

[1]inferred from line drawings from Kudlai et al. (*in press*)

[2]inferred from line drawings from Price (1942)

[3]inferred from line drawings from Oshmarin (1963)

[4]inferred from line drawings in Iskova (1985)

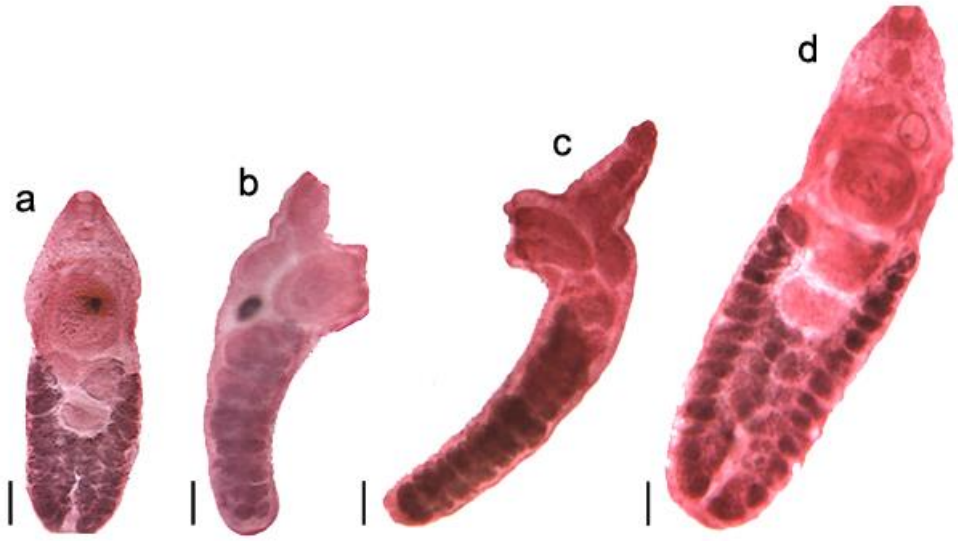

Figure 2.1.Three morphological variations of *N. lisitsynae* body form. (a and b) show the ventro-dorsal and lateral views of the small form. (c) shows the lateral view a midsized body form. (d) shows the ventro-dorsal view of the largest body form. All images taken at 100x. Scale bar 100 μm.

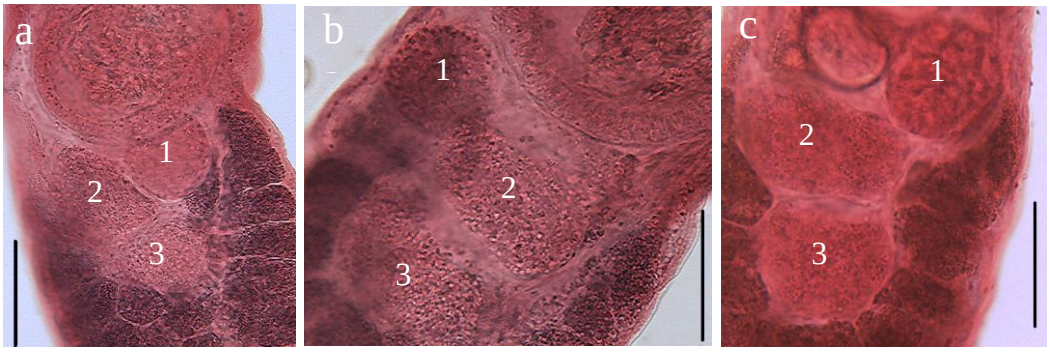

Figure 2.2. Genital structure of *N. lisitsynae* showing various ovary positions (1) compared to anterior (2) and posterior (3) testes positions. (a) Ovary located medial-sinistrally. Scale bar denotes 100µm (b) Ovary located dextrally. Scale bar denotes 120µm. (c) Ovary located sinistrally. Scale bar denotes 85µm.

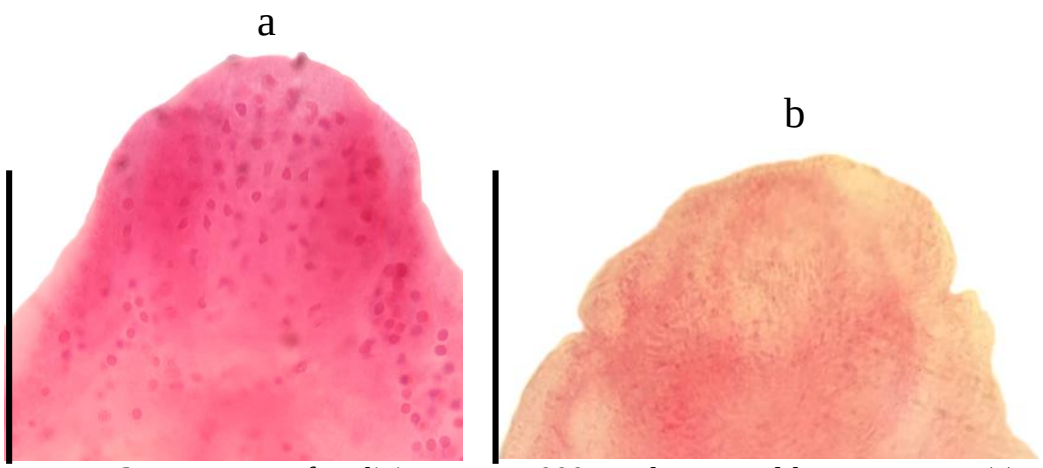

Figure 2.3. Tegument of *N. lisitsynae* at 1000x with a spine-like appearance (a) and no apparent spines (b). Scale bar denotes 60 μm.

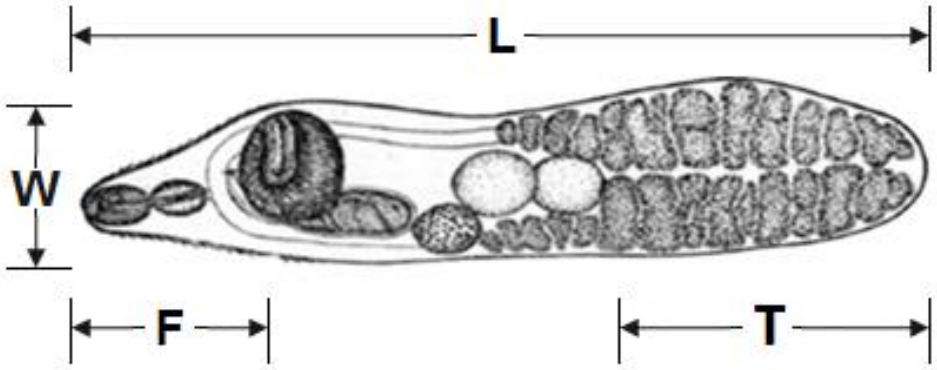

Figure 2.4. Diagram of body measurements needed for proportion analysis. Line drawing was adapted from Oshmarin (1963).

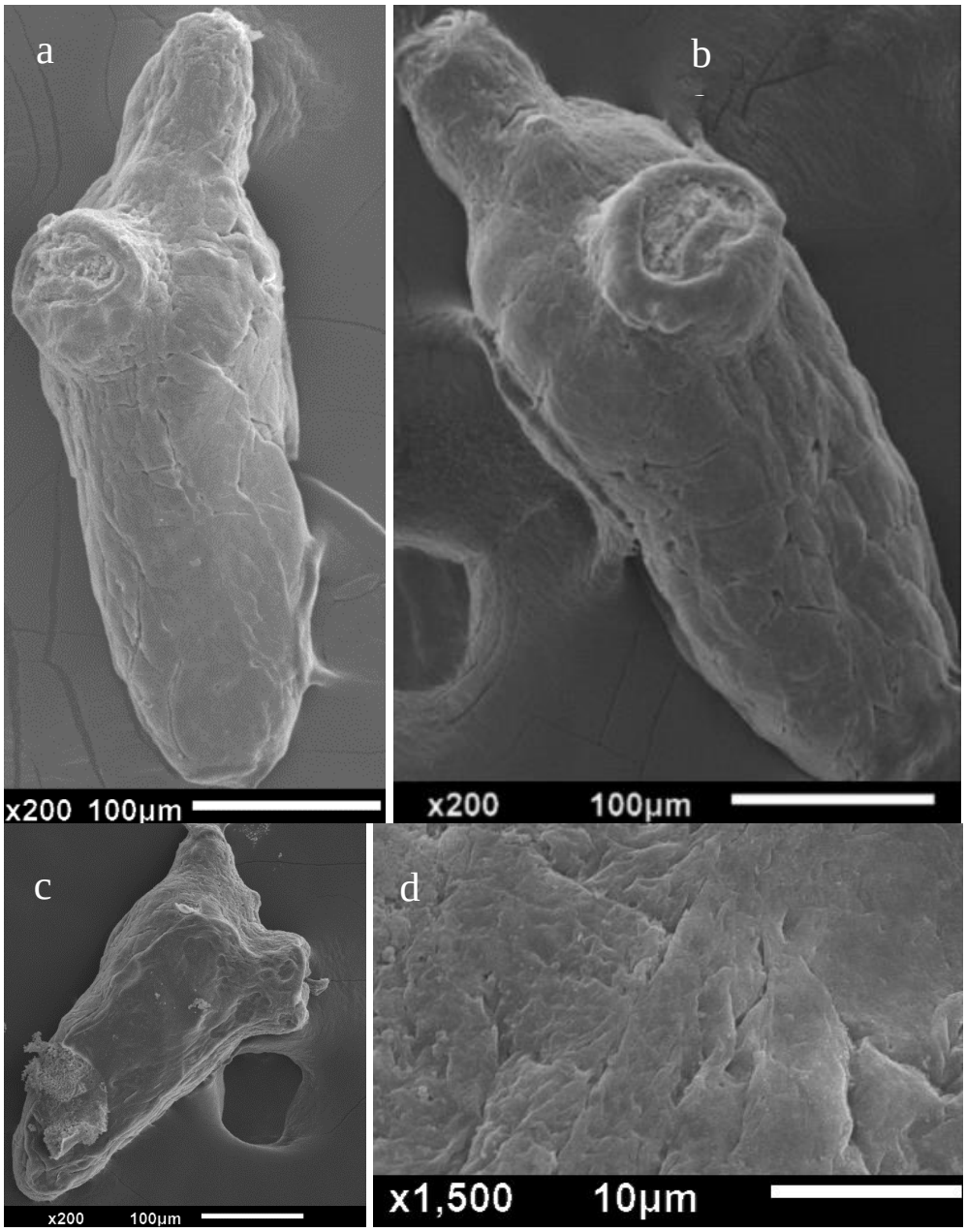

Figure 2.5. SEM view of *N. lisitsynae surface*. (a-b) Tegumental folding over whole worm at 200x. Anterior folds were most apparent when viewed laterally. Ventral sucker and genital pore can be seen on a-c specimens and the genital pore can be seen on b. (c) Enhanced view of anterior tegumental folds. (d) Magnified view of anterior tegument showing tegumental folds, pits and sporadic tuberculations, however, no spines or scales are visible.

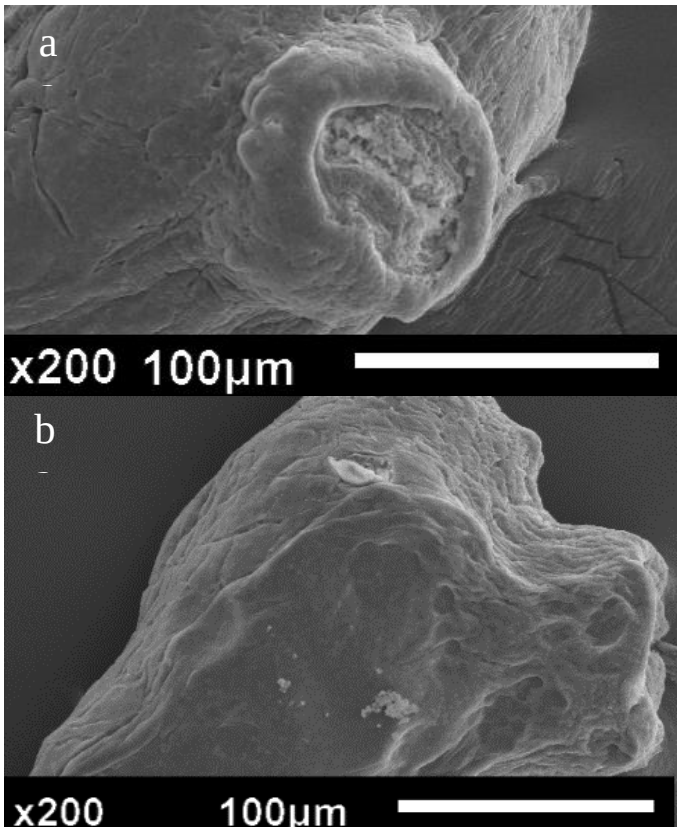

Figure 2.6. Ventral (a) and lateral (b) view of *N. lisitsynae* ventral sucker with no apparent external muscle striations, rather it appears smooth. Debris can be seen within the ventral sucker in the top image.

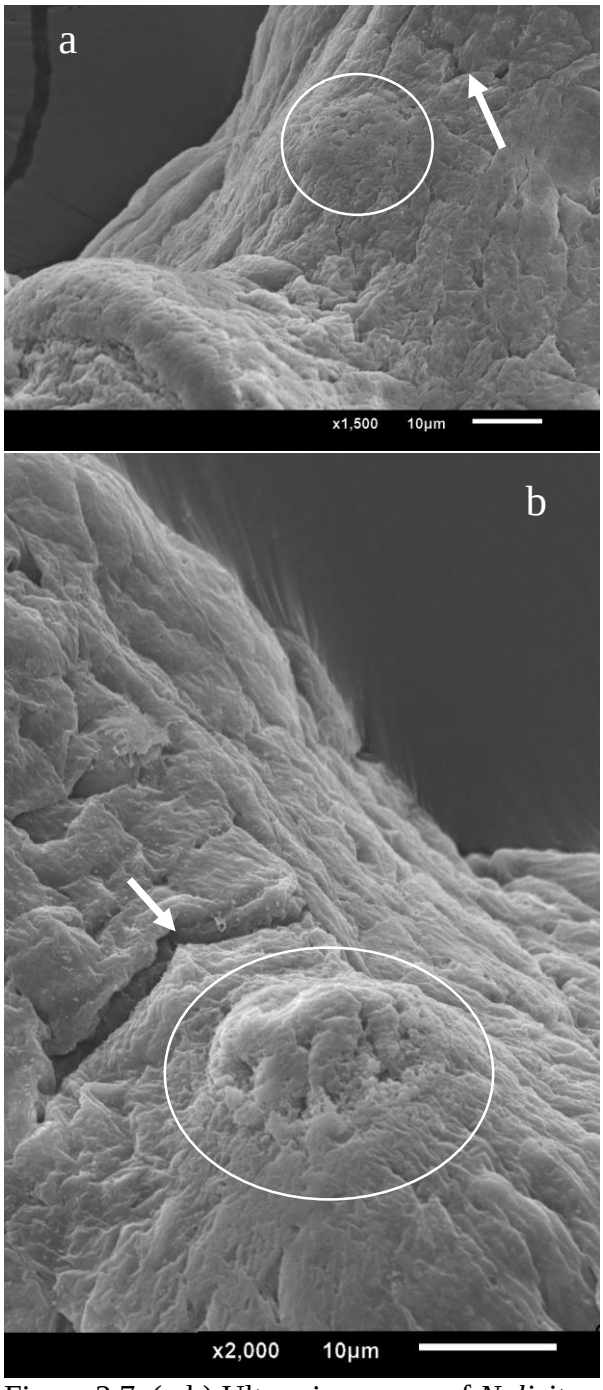

Figure 2.7. (a-b) Ultramicroscopy of *N. lisitsynae* external genital structures. Cirrus (circle) and uterine (arrow) genital pore openings are shown. Few, small tuberculations can be seen across the opening of the uterine opening. Scale bar 10µm in both images

```
                        10•       20•       30•       40•       50•
N. lisitsynae (T) ACTAACCAGGATTCCCTTAGTAACGGCGAGTGAACAGGGAAAAGCCCAGC
N. lisitsynae (Y) ...................................................
N. lisitsynae (C) ...................................................

                        60•       70•       80•       90•      100•
N. lisitsynae (T) ACCGAAGCCTGTGGTCGTTTGGCCTCTAGGCAATGTGGTGTTCAGGTCAG
N. lisitsynae (Y) ...................................................
N. lisitsynae (C) ...................................................

                       110•      120•      130•      140•      150•
N. lisitsynae (T) CTCGCGGAGGTACTGCTCCACCCTAAGTCCTATAATGAGTAAGGTTACTC
N. lisitsynae (Y) ...................................................
N. lisitsynae (C) ...................................................

                       160•      170•      180•      190•      200•
N. lisitsynae (T) GGACGTGGCCCACAGAGGGTGAAAGGCCCGTGGGGGTGGAGACTCAGATT
N. lisitsynae (Y) ...................................................
N. lisitsynae (C) ...................................................

                       210•      220•      230•      240•      250•
N. lisitsynae (T) GGCCAGTATCTCCCTGAGTGGACCTTGGAGTCGGGTTGTTTGTGAATGCA
N. lisitsynae (Y) ...................................................
N. lisitsynae (C) ...................................................

                       260•      270•      280•      290•      300•
N. lisitsynae (T) GCCCAAAGTGGGTGGTAAACTCCATCCAAGGCTAAATACTAGCACGAGTC
N. lisitsynae (Y) ...................................................
N. lisitsynae (C) ...................................................

                       310•      320•      330•      340•      350•
N. lisitsynae (T) CGATAGCGAACAAGTACCGTGAGGGAAAGTTGAAAAGTACTTTGAAGAGA
N. lisitsynae (Y) ...................................................
N. lisitsynae (C) ...................................................

                       360•      370•      380•      390•      400•
N. lisitsynae (T) GAGTAAACAGTGCGTGAAACCGCTCAGAGGTAAACGGGTGGAGTTGAACT
N. lisitsynae (Y) ...................................................
N. lisitsynae (C) ...................................................

                       410•      420•      430•      440•      450•
N. lisitsynae (T) GCAAGCTCTGAGAATTCAACTGGTGAGTATGGCATGAGCTGGGTATATTG
N. lisitsynae (Y) ...................................................
N. lisitsynae (C) ...................................................

                       460•      470•      480•      490•      500•
N. lisitsynae (T) GTTGACGGTCCGGGTCTGCTTAGCTGCAGGTCCTCGCCTTTTGGTGGGGA
N. lisitsynae (Y) ...................................................
N. lisitsynae (C) ...................................................
```

Figure 2.8. The 28S rDNA nucleotide sequence data for three isolates of *Neopsilotrema lisitsynae* that differ from each other at position 979. A dot (.) indicates that at that site the sequence is identical to *N. lisitsynae* (T) sequence. Where a base is ambiguous within a species, IUPAC codings are given. Placement of a hyphen (-) indicates alignment gaps.

```
                          510•       520•       530•       540•       550•
N. lisitsynae (T) TGCGCGAATCACTTACCAAGTGTTGTGCGCCCGGATTGTATCGGACCTGC
N. lisitsynae (Y) ..................................................
N. lisitsynae (C) ..................................................

                          560•       570•       580•       590•       600•
N. lisitsynae (T) TTGCCAGTGCACTTTCTCAGAGTAATCACCACGACCGGCGTTGCCGTCTG
N. lisitsynae (Y) ..................................................
N. lisitsynae (C) ..................................................

                          610•       620•       630•       640•       650•
N. lisitsynae (T) GCTGTTGTAGTTAAACCGGCCTTGTAGAGTCCTTGTGGCTTTGCTTGGTC
N. lisitsynae (Y) ..................................................
N. lisitsynae (C) ..................................................

                          660•       670•       680•       690•       700•
N. lisitsynae (T) GGGATGGCAGGTAGCCCGTTGTGCACTTTTGTGTGCTTCGGGTGTTATCG
N. lisitsynae (Y) ..................................................
N. lisitsynae (C) ..................................................

                          710•       720•       730•       740•       750•
N. lisitsynae (T) CTGACTGCATCAGTTCTGTGCGGTACGTCGGAGACGGCGGCTTGTTGTGT
N. lisitsynae (Y) ..................................................
N. lisitsynae (C) ..................................................

                          760•       770•       780•       790•       800•
N. lisitsynae (T) GTGCGTGCGTACTTGTTATGCTGGCGGGGCCGAGTCTGGTTGCCGTGTTG
N. lisitsynae (Y) ..................................................
N. lisitsynae (C) ..................................................

                          810•       820•       830•       840•       850•
N. lisitsynae (T) ATTGCAAAAGCAATCCCGGTGATGGCTTGGTGTCGTTCGGTGTGCAGTTG
N. lisitsynae (Y) ..................................................
N. lisitsynae (C) ..................................................

                          860•       870•       880•       890•       900•
N. lisitsynae (T) CGTGCGTGTCACTATGCAGGGCCAATAGTCTGTGGTGTAGTGGTAGACTA
N. lisitsynae (Y) ..................................................
N. lisitsynae (C) ..................................................

                          910•       920•       930•       940•       950•
N. lisitsynae (T) TCCACCTGACCCGTCTTGAAACACGGACCAAGGAGAGTAACATGTGCGCG
N. lisitsynae (Y) ..................................................
N. lisitsynae (C) ..................................................

                          960•       970•       980•       990•      1000•
N. lisitsynae (T) AGTCATTGGGCGTTACGAAACCCAAAGGTGCATTGAAAGTAAAGGTTCGG
N. lisitsynae (Y) ............................Y.....................
N. lisitsynae (C) ............................C.....................

                         1010•      1020•      1030•      1040•      1050•
N. lisitsynae (T) CTTGTCCGGACTGAGGTGAGATCCTGCCGTTTCTCACGCGCGGTACTACC
N. lisitsynae (Y) ..................................................
N. lisitsynae (C) ..................................................
```

```
                          1060•     1070•     1080•     1090•     1100•
N. lisitsynae (T) AAGCATCGAGCGGCAGGCGCATCACCGGCCCGTCCCATGGCGTAGAGGCG
N. lisitsynae (Y) ..................................................
N. lisitsynae (C) ..................................................

                          1110•     1120•     1130•     1140•     1150•
N. lisitsynae (T) ACCTTGTGTTTGCTCATCGTCGGGGCGGAGCATGAGCGTACATGTTGAGA
N. lisitsynae (Y) ..................................................
N. lisitsynae (C) ..................................................

                          1160•     1170•     1180•     1190•
N. lisitsynae (T) CCCGAAAGATGGTGAACTATGCTTGCGCAGGTTGAAGCCA
N. lisitsynae (Y) ....................................
N. lisitsynae (C) ....................................
```

Chapter 3: Identification of new species *Neopsilotrema itascae* n. sp. and reclassification of *Psilotrema mediopora* to *Neopsilotrema mediopora* n. comb.

Abstract

Neopsilotrema itascae n. sp. is an avian psilostomid digenean found within the anterior small intestine of *Aythya affinis* in North America. The larger *Neopsilotrema lisitsynae* Kudlai, Pulis, Kostadinova, & Tkach, 2016 (*in press*) described in Chapter 2 and *Psilotrema mediopora* Oschmarin, 1963, share a morphological overlap with *N. itascae*; however, *N. itascae* n. sp. differ from other members of *Neopsilotrema* with the presence of prominent vitelline ducts, which extend to the level of the ventral sucker before returning posterior to the Mehlis gland, a larger anterior seminal vesicle, a sub-spherical shape of the testes, and thinner, lateral vitelline bands. Sequences of 28S ribosomal DNA (rDNA) sequences were effective to identifiy species. Two nucleotides were found to differ from the closest genetic relatives, *N. lisitsynae* and *Neopsilotrema lakotae* Kudlai, Pulis, Kostadinova, & Tkach, 2016 (*in press*). Further, *N. itascae* n. sp. differs from *P. mediopora* in the number and size of eggs, as well as having more elongate, and larger gonads. *P. mediopora* was originally placed within *Psilotrema* Odhner, 1913 due to the presence of tegumental spines and ventral sucker that is smaller than the oral sucker. The recently described genus *Neopsilotrema* Kudlai, Pulis, Kostadinova, & Tkach, 2016 (*in press*) provides a better match for *P. mediopora* than its original placement in *Psilotrema* due to the shared location of the genital pore, similar sucker sizes, the presence of body

spines, similar egg size and number, and the length of post-testicular fields. *P. mediopora* was originally described with a unipartite seminal vesicle, but studies by Besprozvannykh (2003, 2007) utilizing a variety of *Psilotrema* species. from Oschmarin's (1963) collection described individuals of the genus to have bipartite seminal vesicles. The morphological similarity to *Neopsilotrema* and doubt over the nature of the unipartite seminal vesicle lends support to the transfer of *P. mediopora* from *Psilotrema* to *Neopsilotrema*.

Introduction

Psilostomids, members of Family Psilostomidae, share a highly conserved body form with generic differentiation relying on distinct proportions or presence of specific structures. *Neopsilotrema* Kudlai, Pulis, Kostadinova, & Tkach, 2016 (*in press*), a genus of avian psilostomids, was original described to contain minute (BL< 1mm), elongate oval (BW= 26-57%) body forms, an oral sucker that is smaller than the ventral sucker, along with the presence of tegumental spines and a bipartite seminal vesicle. However, analysis of a large number of *Neopsilotrema lisitsynae* (Chapter 2) expands the range of morphological forms to include larger (BL= up to 1600µm), more elongate (BW= 16-66%) body forms and uncertainty about the diagnostic value of tegmental spines.

Recent analysis of 28S ribosomal (r) DNA effectively diagnosed species within *Neopsilotrema* and closely related genera (Tkach et al. 2016). Within *Neopsilotrema*, the current reported level of interspecific variation is between 0.2–0.5%, on par with other

genera of Family Echinostomatidae (Georgieva et al. 2014; Kudlai et al. *in press*). However, some genera are known to vary at much higher interspecific rates, such as *Dicrogaster* Looss, 1902 and *Saccocoelium* Looss, 1902 [0.9-4.8%] (Blasco-Costa et al. 2009).

While 28S rDNA has been shown diagnostic for species identification, three of the four described *Neopsilotrema* members share sizable morphological overlap with one another. Utilization of proportions that relate the size of one body feature to another and that adjust for forebody length and post-testicular fields, regions that appear to change in their proportional size following maturity, effectively distinguish various *Neopsilotrema* species and members of other Psilostomidae genera (Chapter 2).

Following the recent description of *Neopsilotrema*, it is somewhat expected that previous species affiliations for similar species may be called into question when their traits more closely match those of the new genus rather than being extreme forms in their previous genus. This study describes *N. itascae* n. sp. from North American waterfowl along with an argument for the reclassification of *Psilotrema mediopora* to *Neopsilotrema* based upon historical evidence.

Materials and Methods

Sample collection

Intestines of waterbirds from Lake Winnibigoshish in Minnesota, USA, were received from waterfowl hunters in fall 2012 and spring 2013 (Table 1.1; Fig. 1.1). Upon collection, intestines were frozen and transported to Minnesota State University, Mankato until a time when parasites could be collected through dissection of the intestinal tissue. Small intestine tissue was segmented into 15cm linear sections, while cecae and large intestines were not subdivided into smaller segments prior to examination. Parasites were removed from the intestinal contents with the aid of a binocular dissecting microscope. Collected worms were stored in 10% buffered formalin or frozen for morphological or molecular analysis, respectively.

Morphological analysis

N. itascae n. sp. were prepared for light microscopy by staining them with Semichon's acetocarmine before they were dehydrated in ascending concentrations of ethanol. Upon dehydration, worms were cleared using xylene and mounted in Kleermount® or Canada balsam. Specimens were observed using an Olympus CH2 microscope and digital images were captured with a trinocular-mounted Moticam 10MP camera. Characteristics of the worms were measured using Moticam Images Plus 2.0 ML software (Motic). Statistical analysis of measurement data compared to *Neopsilotrema lisitsynae* was carried out with the non-parametric Mann-Whitney U-test using SigmaPlot software (Systat).

Abbreviations used for body measurements are as follows: body length–BL; body width–BW; body depth–BD; forebody length–FORE; oral sucker length–OSL; oral sucker width–OSW; pharynx length–PHL; pharynx width–PHW; ventral sucker length–VSL; ventral sucker depth–VSD; cirrus-sac length–CSL; cirrus-sac width–CSW; anterior seminal vesicle length–SVL1; anterior seminal vesicle width–SVW1; posterior seminal vesicle length–SVL2; posterior seminal vesicle width–SVW2; anterior testis length–ATL; anterior testis width–ATW; anterior testis depth–ATD; posterior testis length–PTL; posterior testis width–PTW; posterior testis depth–PTD; distance between posterior margin of posterior testis to posterior extreme of body–TEND; ovary length–OVL; ovary width–OVW; ovary diameter–OVD; egg number–E; egg-length–EL; and egg-width–EW. Proportions based on Kostadinova (2005a) were generated for: maximum body width to body length–BW%; maximum depth to body length–BD%; forebody length to body length–FO%; length of post-testicular field to body length–T%; and oral sucker to ventral sucker–OS:VS. Adjusted proportions, which were described in Chapter 2, were generated for: forebody to body length discounting the post-testicular field–AF; maximum body width to body length discounting the post-testicular field–ABW; forebody length to maximum body width–FBW; forebody to body length ratio to ABW–AFoBW; maximum body depth to body discounting the post-testicular field –ABD; forebody length to maximum body depth–FBD; and forebody to body length ratio to ABD–AFoBD. All measurements given in text, tables and figures are in micrometers.

SEM Analysis

For scanning electron microscopy, two individual worms that had been removed from an *A. affinis* duck were rinsed in phosphate buffered saline (PBS), treated with 1% osmium tetraoxide, then exposed to ascending concentrations of acetone (50%, 70%, 85%, 95%, absolute). Worms were critically dried using Polaron CPD7501 critical dryer, mounted on aluminum stubs, and coated with gold using a Cressington 108 auto sputter coater. A JEOL JSM6510LV scanning electron microscope was used for specimen visualization and image capture.

Molecular analysis

DNA of individual worms was extracted using a ZR Genomic DNA™-Tissue MiniPrep kit (Zymo Research) and eluted in 35 µL of water. The 28S rDNA locus was amplified with the primer pair DIG (5'-AAG CAT ATC ACT AAG CGG-3') and 1200R (5'-GCA TAG TTC ACC ATC TTT CGG-3') from Tkach et al. (2003) and AtopkinPCR amplifications were done using 0.25 µL of each primer (10µm), 7.5 µL of GoTaq® green mastermix (Promega), 50 ng of template DNA and raised to a volume of 15 µL with ddH_2O. Run conditions for PCR were 94 ^oC for 2 minutes followed by 35 cycles of 30 seconds at 94 ^oC, 30 seconds at 50 ^oC, and 1 minute at 72 ^oC. After 35 cycles the temperature was set to 72 ^oC for 10 minutes. 1200 base pair (bp) amplicons were run on a 1% agarose gel, gel excised, and purified using ZR Gel DNA Recovery Kit (Zymo Research). Recovered amplicons were cycle-sequenced using a modified protocol from Whalen (2011): BigDye™ terminators using 1 µL of BigDye™, 1 µL of 5x BigDye™ reaction buffer, 2 µL of either DIG or 1200R primer and 24 ng of PCR product, with the

following run conditions: an initial 5 minutes at 95 ºC followed by 99 cycles of 30 seconds at 95 ºC, 20 seconds at 50 ºC for DIG or 53 ºC for 1200R and 4 minutes at 60 ºC. Sequencing products was run on an ABI Prism 377 DNA sequencer after clean up using a ZR Sequencing Clean-up kit (Zymo Research) or ethanol precipitation.

Alignment and Phylogenetic Analysis

Sequence electropherograms were refined using BaseFinder (Giddings et al. 1998) to aid base calling. When possible, contiguous sequences were assembled and aligned using Mega7 (Kumar & Hedges 2016). Two alignments were performed using ClustalW on Mega7 with the parameters of 15 for a gap opening penalty and 6.66 for a gap extension penalty for all pairwise and multiple alignments. Sequences were trimmed to shortest sequence length. Additional sequences were taken from GenBank for comparison (Benson et al. 2012).

The first alignment was composed of 1025 nucleotides (nt) and compared sequences from Superfamilies Echinostomatoidea, Haploporoidae, Microphalloidea, and Paramphistomoidea to infer systematic placement within Family Psilostomidae (Tables 3.1-3.2). A second alignment (1062 nt) that included 4 described genera of Family Psilostomidae along with three additional species, which do not currently have generic placement, were used to infer placement within Family Psilostomidae. Transition weight was set to 0.5 under ClustalW 1.6.

Phylogenetic analyses were carried out using Maximum likelihood (ML) and maximum parsimony (MP) 500 bootstraps each in Mega7. Prior to analyses, Mega7 was used to identify best-fitting models of nucleotide substitution for maximum likelihood analysis. The first alignment utilized a general time reversible model with gamma distribution (GTR+G) (Lanave et al. 1984; Tavare 1986; Rodriguez et al. 1990). The second alignment used a Hasegawa-Kishino-Yano model, with gamma distributed among-site rate variation (HKY+G) (Hasegawa et al. 1985). ML phylogenies utilized nearest-neighbor-interchange (NNI) with a very strong branch swap filter. MP phylogenies utilized a subtree-pruning-regrafting (SPR) search method. Additionally, uncorrected p-distances were calculated using Mega7 for a raw estimate of genetic divergence within *Neopsilotrema* and other closely related taxa.

Results

Neopsilotrema itascae n. sp.

Type-host: *Aythya affinis* (Anseriformes: Anatidae)

Prevalence: 2 out of 10 lesser scaup

Type-locality: Lake Winnibigoshish, Minnesota, USA (47º30’17.73”N, 94º13’34.4958”W)

Site in host: Anterior to middle small intestine [Highest intensity 30–60cm; lower intensity 0–30 cm; None present in posterior small or large intestine]

Etymology: The species name is based upon the county of the type-locality

Genotype: (Fig, 3.1)

Description (Fig. 3.2; Fig. 3.3):

[Measurements in text based on dorso-ventral[1] and lateral[2] holotypes. Ranges, means, and standard error of adults given in Table 3.3]. Body small (BL = 1186[1]; 1386[2]), elongate-oval (BW = 22%[1]), shallow (BD =29%[2]), widest (259[1]) and deepest (397[2]) at ventral sucker. Ventral-dorsal body width did not taper until truncation; lateral depth tapers until up to one third depth then truncates; few individuals bulge slightly immediately prior to truncation. Forebody short (FO = 13%[1]; 19%[2]). Tegument typically smooth with many folds on anterior half of body, on some individuals very fine tegumental spines were present on the ventral and dorsal surfaces between anterior extremity and ventral sucker. Oral sucker subterminal, transversally oval from ventral-dorsal (75x78[1]); dorsal muscle of oral sucker longer than ventral muscle from lateral view (87x84[2]). Ventral sucker large, transversely oval or subspherical, strongly muscular in first quarter of body, rarely in second, from ventral view, 133x174[1]; from lateral view, 144 x 252[2]. Ventral sucker is fully immersed in the tegument. Ventral sucker near double the size of the oral sucker or greater (1:2.2[1]; 1:3[2]). Prepharynx short (6[1]; 12[2]), typically not present. Pharynx muscular, subspherical (54 x 63[1]; 59 x 56[2]). Esophagus short, bifurcating halfway between to or immediately anterior to ventral sucker, typically hidden by thick tegument folds. Cecae thin-walled, reaching near posterior margin of body, typically obscured by vitellarium.

Testes 2, entire, tandem, contiguous with or overlapping each other in third quarter of body at some distance from the ventral sucker. Testes subspherical on ventral and lateral view, posterior testis (154x162[1]) equitable or larger than anterior testis (126x123[1]; 128 x

118[2]). Testes width fill majority of body width at widest point (Fig. 3.4). Vas deferens pronounced. Cirrus-sac (142x74[1]; 249x82[2]) elongate-oval, antero-dorsal to ventral sucker, occasionally extending posterior to anterior margin of ovary. Internal seminal vesicle bipartite-saccular; bipartite nature indiscriminate in some individuals (Fig. 3.5). Anterior seminal vesicle subspherical (44x60[2]), smaller than elongate-oval, posterior, seminal vesicle (111x80[2]). Pars prostatica indistinct; prostatic cells few, small. Genital pore muscular, median, immediately below pharynx or ventral sucker on ventral view, while immediately anterior to end of forebody prior to ventral sucker on lateral view. Post testicular field long to very long representing 39%[1] (42%[2]) of body.

Ovary subspherical for both ventral (OVL=117[1]) and lateral (OVL=122[2]) views, typically dextral, rarely sinistral, and contiguous with or overlapping or slightly anterior testis, and contiguous or posterior to ventral sucker. Accurate width and depth measurements difficult due to overlapping vitellaria and associated ducts. Ovary not strongly pronounced ventrally, most visible laterally. Mehlis gland smaller, more pronounced than ovary, opposite at or slightly anterior to level of the ovary, not overlapping testis, often obscured by thick vitelline ducts. Laurer's canal and seminal receptacle not observed. Uterus short (5%[1]; 3%[2] of body length) containing 0 to 9 (3[1]; 0[2]) oval, operculated eggs (78 x 50-56), 7%[1] of body length. Metraterm was noted, but could not be observed well enough for description.

Vitellarium follicular in two lateral fields converging immediately post-testicular, vitelline reservoir dextral, ventral composed of well-defined groups of small vitelline

cells. From dorso-ventral view, thinner vitelline follicles extend lateral fields from posterior testis to anterior margin or slightly anterior to anterior testis, occasionally becoming less dense or discontinuous entirely at the level of each testes. Vitelline ducts distinct, long, reaching to posterior margin of ventral sucker before uniting and traveling posterior to Mehlis gland, occasionally looping to between genital pore and anterior margin of ventral sucker. Excretory system could not be identified, other than the excretory pore, which was terminal and surrounded by gland cells. Amongst the adults examined, there were no morphometric differences between gravid and non-gravid adults (data not shown).

SEM data

The oral sucker had wider longitudinal (3.8–4.9) muscle striations in comparison to transverse striations (2.2). Elongated transverse pits could be seen in direct association with transverse muscle, potentially related to protease activity (Fig. 3.6b).

Tegument appeared textured with many, small tuberculations anterior to the ventral sucker; however, no spines or spine-pits were visible. Fewer tegumental folds and pits could be seen on the anterior region of the tegument that on *N. lisitsynae* (Chapter 2) (Fig. 3.8). The cirrus opening of the genital pore, with a diameter of 6.9–7.0, was located immediately posterior to the uterine opening, which measured 5.7 (Fig. 3.7).

The ventral sucker had visible muscle striations on the interior margin with thick tegumental tissue surrounding most its periphery. The ventral sucker remained strongly

contracted and contained debris in all specimens. The top rim of the ventral sucker was covered in distinct nodules in an apparent random distribution. The ascending tegument on the ventral sucker's sides appeared strongly textured with many distinct tegumental folds (Fig. 3.6c.)

Molecular analysis

In both alignments for maximum likelihood and maximum parsimony phylogenies, *Neopsilotrema itascae* n. sp. was clustered closest to members of *Neopsilotrema* as a discrete clade (Fig. 3.9–3.12). The first alignment showed 0.2–0.3% (uncorrected p-distance [2-3 nt]) divergence in comparison to other *Neopsilotrema* species and 0.2-0.5% [2-5 nt] in the second alignment. These levels of divergence are much lower than those seen between *N. itascae* n. sp. and other genera. *Psilostomum* (5.9%) and *Psilochasmus* (6.1%) diverged identically in both alignments, however, the first alignment yielded 57 and 59 nucleotides difference, respectively, while the second yielded 62 and 65 differing nucleotides. Additionally, the undefined species of Psilostomidae sp. described in Chapter 1 diverged at lower levels than *Psilostomum* and *Psilochasmus* in both alignments 1, with values of 1.1-2.7% (11-22 nt) and 1.4-2.9%; (15-31 nt), respectively.

Discussion

Morphology and Morphometrics

N. itascae n. sp. apparently differs from *N. affine, N. lakotae,* and *Neopsilotrema marilae* in a more elongate (BW = 16-23% vs 38-57%), longer body (BL > 1050 vs < 800) with a much longer post-testicular field (T = 29-49% vs 14-22%) and typically a smaller sucker

ratio. Additionally, the testes are subspherical rather than pyramidal or transversely oval, the vas efferens is pronounced, the vitelline clusters are less dense, the vitelline fields reach the level of the ovary and have vitelline ducts extending up to the posterior margin of the ventral sucker, rarely extending to the anterior margin of the ventral sucker, rather than having vitelline fields, which reach the anterior margin of the ventral sucker or more anterior. Adjusted diagnostic ratios differ between *N. itascae* n. sp. and other *Neopsilotrema* species (Table 3.4) supporting diagnostic utility for those ratios, which are particularly applicable to comparisons involving closest morphological relatives of *N. itascae*: *Psilotrema mediopora* and *Neopsilotrema lisitsynae.*

N. itascae n. sp. is somewhat similar to *Neopsilotrema lisitsynae*, notably in body size and shape, egg number and size, and adjusted body proportions. Nonetheless, *N. itascae* n. sp. can be differentiated from *N. lisitsynae* by the pronounced vitelline duct system and vas deferens, sub-spherical testes, a larger anterior seminal vesicle, and the presence of a short prepharynx. Vitelline band width at testes also appears diagnostic; *N. itascae* n. sp. has smaller clusters of vitellarium on the lateral margins of the testes, occasionally with breaks, while *P. lisitsynae* has larger, unbroken clusters. In addition, lateral proportions show *N. itascae* n. sp. as the thicker species, with a brief an open region in the vitellaria near the posterior testis (Fig. 3.8). All measurements except for SVW1, SVL2, SVW2, PTD, EL, EW, FBW, FBD, and AFoBD were found to be statistically different when compared between *N. lisitsynae* and *N. itascae* with a Mann-Whitney U-test, further supporting morphological distinction between species.

Ultrastructure analysis revealed a rough tegument with few macroscopic perturbations, but none that would clearly account for spines. The nodules found on the ventral sucker could potentially be the remnants of spines, but further support for this point is needed; *N. lisitsynae* also did not have obvious tegumental spines based on ultrastructure analysis, in contrast to the generic description of *Neopsilotrema,* which lists tegumental spines as a trait of the genus (Chapter 2). The tegumental folding on the periphery of the ventral sucker are most likely associated with strong muscular contraction. The larger tuberculations and tegumental folds on and around the ventral sucker were not seen on *N. lisitsynae* indicating they may be unique to this species. The tegument of *N. lisitsynae* (Chapter 2) was very wrinkled, while *N. itascae* n. sp. appeared smoother. This may be due to the difference in body size; the more elongated worm has greater distance between muscular structures, potentially decreasing the appearance of wrinkles due to contraction.

The addition of this species supports previous modifications to the description for *Neopsilotrema*. Originally, *Neopsilotrema* was described as an elongate-oval (BW= 27-57%) with a long to very long forebody (FO= 21-38); however, evidence in Chapter 2 shows a more elongate form (BW =17-66%) with a short forebody (FO= 12-37%) for another member of this genus, *N. lisitsynae*. Both of those measures are similar to ones obtained in this study (BW= 16-23%; FO=11-21%). Additionally, uncertainty about the presence or absence of spines depending upon which *N. itascae* n. sp. individuals are examined and whether the individuals are examined with light microscopy or scanning

electron microscopy suggests a lack of diagnostic utility for spines among members of *Neopsilotrema*.

Phylogenetics

Maximum likelihood and maximum parsimony phylogenies support placing *N. itascae* n. sp. within *Neopsilotrema* in comparison to other Psilostomidae genera. The genetic divergence demonstrated by p-distance values from this study (0.2-0.3% for alignment 1; 0.2-0.5% for alignment 2) is equitable to interspecific divergence within the genus *Neopsilotrema* (0.2–0.5%) supporting placement of *N. itascae* n. sp. within *Neopsilotrema* (Kudlai et al. *in press*).

Morphologically similar *N. lisitsynae* and morphologically distinct *N. lakotae* were both found to diverge by 0.2% (2 nt). The genetic similarity of morphologically distinct members of *Neopsilotrema* was reported by Kudlai et al. (*in press*). These authors showed that the morphologically distinct *N. lisitsynae* and *Neopsilotrema affinis* pair were more similar genetically than the morphologically similar *N. affinis* and *N. lakotae* pair.

Status of *Psilotrema mediopora* Oschmarin, 1963.

Initial morphological examination of the *N. itascae* n. sp. specimens led to a potential diagnosis as *P. mediopora* Oschmarin, 1963. In comparison to *P. mediopora*, *N. itascae* n. sp. has smaller, more numerous eggs (EL= 75 *vs* 90; EN= 0-9 *vs* 0-1) and a larger body length (BL=1370 *vs* 1200). It is possible *P. mediopora* and *N. itascae* n. sp. are synonymous with differences between the isolates being due to regional, parasite-population factors and the use of different host birds; however, this seems unlikely as egg

size would not be expected to vary as much as worm size and egg number might. Unfortunately, there is no genetic information or voucher specimens available for *P. mediopora*. Genetic attributes of other members of *Psilotrema* have been compared to *Neopsilotrema* showing a close relationship, but only short sequences were used due to limitations of the available *Psilotrema* sequences (Tkach et al. 2016; Kudlai et al. *in press*). One of the diagnostic traits separating *Psilotrema* and *Neopsilotrema* is the presence or absence of a bipartite seminal vesicle. Life cycle studies based on Oschmarin's material by Besprozvannykh (2003, 2007) cast doubt on the absence of the bipartite seminal vesicle in members of *Psilotrema* originally described by Oschmarin (1963). In both Besprozvannykh's (2003, 2007) studies, the three *Psilotrema* species examined had a bipartite seminal vesicle.

Psilotrema mediopora described in *Anas clypeata* and *Anas platyrhynchos* in Ukraine, was initially placed within the genus *Psilotrema* based upon the presence of tegumental spines and the lack of an esophagus (Oschmarin 1963). However, *P. mediopora* morphology as described by Oschmarin (1963) diverges highly from the generic description of *Psilotrema* given by Odhner (1913) and Kostadinova (2005b) by having a more elongate body (BW= 26% vs 30-60%), smaller pharynx than oral sucker (66% vs ≥100%), and genital pore location (post-pharyngeal, medial vs pharynx-level, sinistral). Rather, the traits described by Oschmarin (1963) are descriptive of *Psilostomum*, Loos, 1899 and *Neopsilotrema* Kudlai, Pulis, Kostadinova, & Tkach, 2016. However, *P. mediopora* differs from *Psilostomum* in the post-testicular field distance (T> 15%),

having a much larger ventral sucker than oral sucker, possession of a short uterus (UT = 8.5%), the presence of tegumental spines, and confluent vitellarian fields posterior to testes.

P. mediopora differs from *Mehlisia* Johnston, 1913 in definitive host (avian *vs* monotremes and marsupials), body size (minute to small *vs* medium to large), egg size (EL = 90 *vs* >130), size of tegumental spines (small, fine *vs* large), testis shape (spherical *vs* s-shaped), and cirrus location (extending posterior to level of ovary *vs* anterior to ventral sucker). *P. mediopora differs from Psilorchis* Thapar & Lal, 1936 in the presence of confluent vitelline fields, uterus length (short *vs* long), presence of tegumental spines, location of cirrus (extending posterior to level of ovary *vs* anterior to ventral sucker). Differences from *Apopharynx* Luhe, 1909 include the genital pore location (post-cecal fork *vs* level of oral sucker), while variation from *Psilotornus* Byrd & Prestwood, 1969 is apparent in the more anterior location of the ventral sucker (FO= 11-21% *vs* 43-55%), elongate body form (BW= 16-23% *vs* 30-46%), and location of testes (T= 29-49% *vs* 7-15%).

Rather, *P. mediopora* closely matches *Neopsilotrema* in the minute to small, elongate to elongate-oval body (BW=26% *vs* 20%-57%), forebody long (19% *vs* 16%-38%), sucker ratio (oral sucker much smaller than ventral sucker), absent prepharynx, presence of contiguous, tandem, subspherical testes in third quarter of body (T= 37% *vs* 14-45%), medial, post-pharyngeal genital pore location, and few, large eggs (E=7% *vs* 5-13%). P.

mediopora was not originally described with a bipartite seminal vesicle, however, this could be due to misdiagnosis by Oschmarin (1963), as described by Besprozvannykh (2003, 2007) with other *Psilotrema* species The deviation from the generic description of *Psilotrema* supports the movement of *P. mediopora* to *Neopsilotrema.*

P. mediopora apparently differs from all other currently described members of *Neopsilotrema* as well. *N. lakotae* (^{L}), *N. affine* (^{A}), and *N. marilae* (^{M}) diverge from *P. mediopora* (^{P}) with smaller body length ($BL^{max} = 803^{L}$, 648^{A}, and 630^{M} vs $BL^{min} = 950^{P}$), oral sucker length ($OSL^{max} = 80^{L}$ vs $OSL^{min} = 98^{P}$), cirrus length ($CSL^{max} = 220^{L}$, 198^{A}, and 150^{M} vs $CSL^{min} = 350^{P}$), ovary length ($OVL^{max} = 75^{L}$ and 76^{A} vs $OVL^{min} = 95^{P}$), egg length ($EL^{max} = 78^{L}$ vs $EL^{min} = 90^{P}$), testes shape (subglobular^{L} and transversely oval^{A} vs spherical^{P}), and post-testicular field length ($BL^{max} = 22\%^{L}$, $22\%^{A}$, and $17\%^{M}$ vs $T^{min} = 37\%^{P}$). Additionally, adjusted proportions, as described in Chapter 2, seemed to vary from those found for other *Neopsilotrema* species.

In comparison to *N. lisitsynae*, many measurement ranges overlapped highly due to the expanded morphology of *N. lisitsynae* described in Chapter 2. That being said, in all raw morphometrics, except those associated with testes, *P. mediopora* was described as being larger than *N. lisitsynae*. In many cases, the average measurements of *P. mediopora* were found to be much larger (BL= 1200 *vs* 828; BW= 380 vs 233; BD= 340 vs 196). In addition, adjusted proportions of FBD, FBW, AFoBW, and AFoBD of *P. mediopora* were found to be below the $\bar{x} \pm$standard error of *N. lisitsynae.* However, the

morphometric comparisons are limited due to Oshmarin's (1963) description of *P. mediopora* and limited morphometric analysis of other members of *Neopsilotrema,* except for *N. lisitsynae*. The morphometric comparisons are limited due to small sample sizes used in prior studies which may not fully describe the measurement ranges for each species.

Genetic characterization of *P. mediopora* would greatly aid claims about this species' status. However, until *P. mediopora* can be genetically synonymized with *N. itascae* n. sp., *P. mediopora* should be transferred to *Neopsilotrema* as *N. mediopora* Oschmarin, 1963 n. comb.

Interestingly, the life cycle of *N. mediopora* n. comb. was originally described to use *Bithynia tentaculata* snails as the first intermediate host (Usinene 1980). Both the Ukrainian and Minnesota study regions, which possess *Neopsilotrema* species are in the current range of *B. tentaculata* (Roy & Herwig 2011) suggesting *Neopsilotrema* species may use *B. tentaculata* a first-intermediate host. The potential use of *B. tentaculata* by *Neopsilotrema* is further suggested by the common occurrence of other members of Family Psilostomidae utilizing *B. tentaculata* as well (Usinene 1980; Besprozvannykh 2003, 2007). The absence of any members of *Neopsilotrema* in historical trematode surveys of the Minnesota and recent reports of *Neopsilotrema* in areas of Minnesota with *B. tentaculata* is additional support for the potential use of *B. tentaculata* as a first intermediate host for *Neopsilotrema* (Kudlai et al. in press; Herrmann & Sorensen 2009).

Furthermore, and perhaps more importantly, larval stages of *Neopsilotrema* species are likely present among *B. tentaculata* snails at Lake Winnibigoshish, MN. No life cycle studies have been done on any of the described *Neopsilotrema* species, indicating the need to confirm the life cycle of *Neopsilotrema* species. Perhaps, Lake Winnibigoshish, MN, can provide the specimens to facilitate such a study.

Dichotomous key for Neopsilotrema

1a. Body elongate (BW= 16-26%); body length greater than 950µm; testes spherical or sub spherical……..…….2

1b. Body elongate oval, rarely elongate (BW= 17-66%); body length typically less than 900µm, rarely up to 1650µm; testes pyramidal to transversally oval……...……..3

2a. Body length typically 1200µm, up to 1240µm; body deep (BD= 28%), zero to one larger egg in original description (90 x 52µm); testes smaller, spherical equitable in size (80-115µm); cirrus larger (300 x 100µm); vitellaria extend to level of ovary…..…..……..…....*N. mediopora n. comb.* (Oschmarin 1963)

2b. Body length typically 1400µm, up to 1740µm; body shallow (BD= 11-21%), zero to 9 egg ($\bar{x}$= 3-4 eggs), smaller eggs (75x51µm); testes larger, spherical or subspherical, posterior (107-166 x 114-171µm) larger than anterior (85.3-166.3 x 119-165.9µm) cirrus typically smaller (240 x 77µm); distinct vitelline ducts extending up to or slightly beyond ventral sucker before ending at level of or immediately anterior to the level of the ovary. ……..……..…..... *N. itascae* n. sp. (Present study)

3a. Body more elongate-oval (BW= 38-57%), less than 800 µm; post-testicular field shorter (T< 25%); vitellaria extend beyond ventral sucker…….……..4

3b. Body more elongate (BW= 17-66%) , greater than 800 µm, rarely 365 to 1630 µm; Post-testicular field typically greater than 30% of body length, rarely as small as 15%; vitellaria stop at posterior margin of the ventral sucker; up to 9 eggs (75 x 50µm)…….…….*N. lisitsynae* (Kudlai et al. *in press*)

4a. Body typically less than 600 µm; forebody longer (FO= 31-38%); eggs typically larger than 80µm long and 50µm wide……...…….……..5

4b. Body minute, larger than 600 µm; forebody can be smaller (FO= 21-37%); posterior seminal vesicle small (52-65 x 53-81µm); egg size 70-78 x 43-50µm…….……..*N. lakotae* (Kudlai et al. *in press*)

5a. Eggs typically larger (85-90 x 50-60µm); oral sucker to ventral sucker ratio 1:2; oral sucker width 60µm; ventral sucker 115 x 150µm…….*N. marilae* (Price 1942)

5b. Eggs typically smaller (74-96 x 52-56µm); oral sucker to ventral sucker ratio 1:2.3-3.3; posterior testis smaller (76-111µm)…….....*N. affine* (Kudlai et al. *in press*)

References

Atopkin, D. M. (2011). Genetic characterization of the *Psilotrema* (Digenea: Psilostomatidae) genus by partial 28S ribosomal DNA sequences. *Parasitology International*, 60 (4), 541–543.

Benson, D. A., Cavanaugh, M., Clark, K., Karsch-Mizrachi, I., Lipman, D. J., et al. (2012). GenBank. *Nucleic Acids Research*, 41(D1).

Besprozvannykh, V. V. (2003). Life cycle of the trematode *Psilotrema acutilostris* (Psilostomidae) from the Primorye region. *Parazitologiya*, 37, 241-245 (In Russian).

Besprozvannykh, V. V. (2007). Trematodes *Psilotrema simillimum* and *Psilotrema oschmarini* sp. n. (Psilostomidae) and their life cycles in Primorye. *Zoologicheskii Zhurnal*, 86, 771-777 (In Russian).

Blasco-Costa, I., Balbuena, J. A., Kostadinova, A., & Olson, P. D. (2009). Interrelationships of the Haploporinae (Digenea: Haploporidae): A molecular test of the taxonomic framework based on morphology. *Parasitology International,* 58(3), 263–269.

Detwiler, J. T., Zajac, A. M., Minchella, D. J., & Belden, L. K. (2012). Revealing cryptic parasite diversity in a definitive host: Echinostomes in muskrats. *Journal of Parasitology, 98*(6), 1148–1155.

Galaktionov, K. V., Blasco-Costa, I., & Olson, P. D. (2012). Life cycles, molecular phylogeny and historical biogeography of the ‘pygmaeus’ microphallids

(Digenea: Microphallidae): Widespread parasites of marine and coastal birds in the Holarctic. *Parasitology,* 139(10), 1346–1360.

Georgieva, S., Faltýnková, A., Brown, R., Blasco-Costa, I., Soldánová, M., et al. (2014). *Echinostoma 'revolutum'* (Digenea: Echinostomatidae) species complex revisited: Species delimitation based on novel molecular and morphological data gathered in Europe. *Parasites Vectors Parasites & Vectors,* 7(1). doi: 10.1186/s13071-014-0520-8

Ghatani, S., Shylla, J., Roy, B., & Tandon, V. (2014). Multilocus sequence evaluation for differentiating species of the trematode Family Gastrothylacidae, with a note on the utility of mitochondrial CO1 motifs in species identification. *Gene*, 548, 277–284.

Giddings, M. C., Severin, J., Westphall, M., Wu, J., & Smith, L. M. (1998). A software system for data analysis in automated DNA sequencing. *Genome Research*, 8(6), 644–665.

Hasegawa, M., Kishino, H., & Yano, T. (1985). Dating of the human-ape splitting by a molecular clock of mitochondrial DNA. *Journal of Molecular Evolution*, 22(2), 160–174.

Heneberg, P., & Literák, I. (2013). Molecular phylogenetic characterization of *Collyriclum faba* with reference to its three host-specific ecotypes. *Parasitology International, 62*(3), 262–267.

Herrmann, K. K., & Sorensen, R. E. (2011). Differences in natural infections of two mortality-related trematodes in lesser scaup and American coot. *The Journal of Parasitology*, 97(4), 555–558.

Kanarek, G., Zalesny, G., Sitko, J., & Tkach, V. V. (2014). Phylogenetic relationships and systematic position of the families Cortrematidae and Phaneropsolidae (Platyhelminthes: Digenea). *Folia Parasitologica*, 61(6), 523-528.

Kanarek, G., Zaleśny, G., Czujkowska, A., Sitko, J., & Harris, P. D. (2015). On the systematic position of *Collyricloides massanae* Vaucher, 1969 (Platyhelminthes: Digenea) with notes on distribution of this trematode species. *Parasitology Research Parasitol Res*, 114(4), 1495-1501.

Kostadinova, A. (2005a). Family Echinostomatidae Looss, 1899. In: A. Jones, R. A. Bray, D. I. Gibson (Eds.), *Keys to the Trematoda Vol. 2* (pp. 9–64). Wallingford - London: CABI Publishing and The Natural History Museum.

Kostadinova, A. (2005b). Family Psilostomidae Looss, 1900.In: A. Jones, R. A. Bray, D. I. Gibson (Eds.), *Keys to the Trematoda Vol. 2* (pp. 99–118). Wallingford - London: CABI Publishing and The Natural History Museum.

Kudlai, O., Cutmore, S. C., & Cribb, T. H. (2015a). Morphological and molecular data for three species of the Microphallidae (Trematoda: Digenea) in Australia, including the first descriptions of the cercariae of *Maritrema brevisacciferum* Shimazu et Pearson, 1991 and *Microphallus minutus* Johnston, 1948. *Folia Parasitologica*, 62, doi: 10.14411/fp.2015.053

Kudlai, O., Stunzenas, V., & Tkach, V. V. (2015b). The taxonomic identity and phylogenetic relationships of Cercaria pugnax and C. helvetica XII (Digenea: Lecithoendriidae) based on morphological and molecular data. *Folia Parasitologica, 62,* doi: 10.14411/fp.2015.003

Kudlai, O., Pulis, E. E., Kostadinova, A., & Tkach, V.V. (*in press*). *Neopsilotrema* n. g. (Digenea: Psilostomidae) and three new species from ducks (Anseriformes: Anatidae) in North America and Europe. *Systemtatic Parasitology.*

Kumar, S., & Hedges, S. B. (2016). Advances in time estimation methods for molecular data. *Molecular Biology and Evolution,* 33(4), 863–869.

Lanave, C., Preparata, G., Saccone, C., & Serio, G. (1984). A new method for calculating evolutionary substitution rates. *Journal of Molecular Evolution*, 20(1), 86-93.

Olson, P. D., Cribb, T. H., Tkach, V. V., Bray, R. A., & Littlewood, D. T. J. (2003). Phylogeny and classification of the Digenea (Platyhelminthes : Trematoda). *International Journal of Parasitology*, (33), 733-755.

Price, E. W. (1942). A new trematode of the family Psilostomidae from lesser scaup duck, *Marila affinis. Proceedings of the Helminthological Society of Washington*, 9, 30–31.

Oshmarin, P. G. (1963). *Parasitic worms of mammals and birds*. USSR: Publishing House of the USSR Academy of Sciences (In Russian).

Rodríguez, F., Oliver, J., Marín, A., & Medina, J. (1990). The general stochastic model of nucleotide substitution. *Journal of Theoretical Biology,* 142(4), 485-501.

Roy, C., & Herwig, C. (2010). Investigation of trematodes and faucet snails responsible for lesser scaup and american coot die-offs. In G. D. DelGiudice, M. Grund, J. S. Lawrence, & M. S. Lenarz (Eds.), *Summaries of Wildlife Research Findings 2010* (pp. 20-27). St. Paul: Minnesota Department of Natural Resources.

Tavare, S. (1986). Some probabilistic and statistical problems in the analysis of DNA sequences. *Lectures on Mathematics in the Life Sciences (American Mathematical Society)*, 17, 57– 86.

Tkach, V. V., Pawlowski, J., & Mariaux, J. (2000). Phylogenetic analysis of the suborder Plagiorchiata (Platyhelminthes, Digenea) based on partial lsrDNA sequence. *International Journal for Parasitology*, 30(1), 83-93.

Tkach, V. V., Littlewood, D. T., Olson, P. D., Kinsella, J. M., & Swiderski, Z. (2003). Molecular phylogenetic analysis of the Microphalloidea Ward, 1901 (Trematoda: Digenea). *Systematic Parasitology Syst Parasitol*, 56(1), 1–15.

Tkach, V. V., Kudlai, O., & Kostadinova, A. (2016). Molecular phylogeny and systematics of the Echinostomatoidea Looss, 1899. *International Journal of Parasitology*, 46(3), 171–185.

Usinene, B. (1980). Study of the biology of trematode larvae of the genus *Psilotrema* Odhner, 1911. In B. Kapsukas (Ed), *Voprosy parazitologii vodnykh bespozvonochnykh zhivotnykh Tematicheskii Sbornik* (pp. 110-111). Leningrad: Institute of Zoology and Parasitolgoy Academy of Sciences (In Russian).

Whalen, S. (2011). Analysis of the genetic structure of *Bithynia tentaculata* snail populations in Wisconsin and Minnesota. (Master's thesis). Minnesota State University, Mankato, MN.

Zheng, X., Chang, Q., Zhang, Y., Tian, S., Lou, Y., et al. (2014). Characterization of the complete nuclear ribosomal DNA sequences of *Paramphistomum cervi*. *The Scientific World Journal, 2014*, doi: 10.1155/2014/751907

Table 3.1 Accession numbers of GenBank sequences of Superfamilies Echinostomatoidea and Haploporoidae used for 28S rDNA analysis.

Family	Genus species	Accession #	Reference
Superfamily Echinostomatoidea			
Echinostomatidae	*Echinostoma revolutum*	AY222246	Olsen et al. 2003
Psilostomidae	*Neopsilotrema affinis*	KT956953	Tkach et al. 2016
Psilostomidae	*Neopsilotrema lakotae*	*in press*	Kudlai et al. *in press*
Psilostomidae	*Psilochasmus oxyurus*	AF151940	Tkach et al. 2000
Psilostomidae	*Psilostomidae sp.*	KT956953	Tkach et al. 2016
Psilostomidae	*Psilostomidae sp.*	KT956955	Tkach et al. 2016
Psilostomidae	*Psilostomidae sp.*	KT956954	Tkach et al. 2016
Psilostomidae	*Psilostomum brevicolle*	KT956950	Tkach et al. 2016
Superfamily Haploporoidae			
Haploporidae	*Dicrogaster contracta*	FJ211262	Blasco-Costa et al. 2009

Table 3.2. Accession numbers of GenBank sequences of Superfamilies Microphalloidea and Paramhphistomoidea used for 28S rDNA analysis.

Family	Genus species	Accession #	Reference
Superfamily Microphalloidea			
Collyriclidae	*Collyriclum faba*	JQ231122	Heneberg & Literak 2013
Collyriclidae	*Collyricloides massanae*	KP682451	Kanarek et al. 2015
Cortrematidae	*Cortrema magnicaudata*	KJ700420	Kanarek et al. 2014
Lecithodendriidae	*Lecithodendrium sp.*	KJ126726	Kudlai et al. 2015
Microphallidae	*Maritrema oocysta*	AY220630	Tkach et al. 2003
Microphallidae	*Microphallus minutus*	KT355823	Kudlai et al. 2015
Microphallidae	*Microphallus similis*	HM584138	Galaktionov et al. 2012
Prosthogonimidae	*Prosthogonimus ovatus*	AF151928	Tkach et al. 2000
Prosthogonimidae	*Schistogonimus rarus*	AY116869	Tkach et al. 2003
Prosthogonimidae	*Prosthogonimus cuneatus*	AY220634	Tkach et al. 2003
Pleurogenidae	*Allasogonoporus amphoraeformis*	AF151924	Tkach et al. 2000
Pleurogenidae	*Parabascus joannae*	AY220619	Tkach et al. 2003
Pleurogenidae	*Parabascus semisquamosus*	AF151923	Tkach et al. 2000
Superfamily Paramhphistomoidea			
Gastrothylacidae	*Gastrothylax crumenifer*	JX518971	Ghatani et al. 2014
Paramphistomidae	*Paramphistomum cervi*	KJ459936	Zheng et al. 2014
Zygocotylidae	*Zibethicus wardius*	JQ670847	Detwiler et al. 2012

Table 3.3. Morphometric comparison of new *Neopsilotrema* species. to North American *N. lisitsynae*. Statistical significance of differences between *N. itascae* and *N. lisitsynae* are designated by superscript symbol.

	N. itascae n. sp			*N. mediopora* n. comb		*N. lisitsynae* (Chapter 2)	
Feature	Range	$\bar{x}$ ±SE	n	Range	$\bar{x}$	Range	$\bar{x}$ ±SE
BL†	1069-1741	1370±27	31	950-1240	1200	365-1632	828±10
BW§	210-313	266±10	12	330-380	380	108-378	233±4
BD†	315-448	399±9	15	NA	340*	84-344	196±3
FORE†	142-273	216±6	30	NA	225*	67-327	184 ±3
OSL†	69-97	81±2	31	95-103	98	19-104	58±1
OSW†	65-87	76±2	18	68-80	75	27-110	68±1
PL$^{\emptyset}$	8-32	22±2	26	NA	0*	0.00	0
PHL†	52-85	63±2	31	65-67	65	23-97	52±1
PHW†	48-65	57±1	22	60-65	60	20-76	45±1
CSL†	142-323	239±10	29	-	300	97-351	191±3
CSW†	61-94	78± 2	30	-	100	41-180	70±1
SVL1†	48-75	62±2	15	-	-	32-72	49±2
SVW1$^{\infty}$	36-71	54±2	15	-	-	42-79	55±2
SVL2$^{\infty}$	62-119	80±3	18	-	-	54-108	78±2
SVW2$^{\infty}$	53-82	67±2	18	-	-	44-96	66±2
VSW$^{\infty}$	115-200	148±4	31	145-160	152	66-254	142±2
VSD†	206-272	239±4	22	-	240*	74-278	175±3
ATL†	86-167	130±4	28	80-115*	95	53-181	94±2
ATW†	119-166	141±5	10	80-115*	95	53-178	112±2
ATD†	111-174	130±5	17	-	103*	53-181	115±2
PTL†	106-166	133±4	20	80-115*	95	50-159	94±2
PTW†	115-171	142±7	8	80-115*	95	67-171	113±2
PTD$^{\infty}$	51-148	118±9	13	-	NA	612-188	118±2
TEND†	308-848	570±19	31	-	445*	91-724	282±5
OVL†	100-124	117±3	7	75-100	95	52-129	86±1
OVW$^{\emptyset}$	83-111	91±3	8	-	-	-	-
E†	1-9	4±1	30	1	NA	1-9	3±1
EL$^{\infty}$	55-94	76±1	92	-	90	48-107	75±1
EW$^{\infty}$	34-64	51±1	102	-	52	30-70	51±1
BW%†	16-23	20±1	12	-	26*	17-66	30±0
BD%†	27-32	29±0	15	-	28*	14-36	24±0
FO%†	11-21	16±0	30	-	19*	12-37	22±0
T%†	29-49	41±1	31	-	37*	15-47	32±0
OS:VS†	1.44-2.41	1.89±0.06	18	-	1.55*	1.4-3.9	2.4±0.1
AF†	0.19-0.37	0.27±0.01	30	-	0.30*	0.25-0.39	0.32±0
ABW†	0.24-0.44	0.35±0.02	12	-	0.43*	0.25-0.60	0.42±0.01
ABD†	0.33-0.59	0.48±0.02	15	-	0.35*	0.22-0.53	0.34±0.01
FBW$^{\infty}$	0.57-1.09	0.75±0.05	11	-	0.70*	0.50-1.17	0.79±0.01
FBD$^{\infty}$	0.55-1.59	0.86±0.09	15	-	0.86*	0.56-1.40	0.96±0.01
AFoBW†	0.31-0.71	0.44±0.03	11	-	0.43*	0.31-0.75	0.53±0.01
AFoBD$^{\infty}$	0.3-1.27	0.57±0.09	15	-	0.52*	0.40-0.91	0.64±0.01

*estimated from original manuscript and associated line drawing

$^{\infty}$P-value < 0.05

§P-value = 0.05 to 0.005

†P-value < 0.005

$^{\emptyset}$Not tested due to values only available for *N. itascae* n.sp.

Table 3.4. Comparison of adjusted proportions among *Neopsilotrema* species.

Measure	*N. itascae* n. sp.	*N. lisitsynae*[1]	*N. affine*[2]	*N. lakotae*[2]	*N. marilae*[3]
AF	0.27±0.01	0.32±0	0.4	0.28	0.38
ABW	0.35±0.02	0.42±0.01	0.62	0.49	0.67
FBW	0.75±0.05	0.79±0.01	0.64	0.56	0.56
AFoBW	0.44±0.03	0.53±0.01	0.51	0.45	0.47
ABD	0.48±0.02	0.34±0.01	-	0.7	-
FBD	0.86±0.09	0.96±0.01	-	0.4	-
AFoBD	0.57±0.09	0.64±0.01	-	0.31	-

[1]Chapter 2
[2]inferred from line drawings from Kudlai et al. i*n press*
[3]inferred from line drawings from Price (1942)

```
                        10•        20•        30•        40•        50•
N. itascae      AACGGCGAGTGAACAGGGAAAAGCCCAGCACCGAAGCCTGTGGTCGTTTG

                        60•        70•        80•        90•       100•
N. itascae      GCCTCTAGGCAATGTGGTGTTCAGGTCAGCTCGCGGAGGTACTGCTCCAC

                       110•       120•       130•       140•       150•
N. itascae      CCTAAGTCCTATAATGAGTAAGGTTACTCGGACGTGGCCCACAGAGGGTG

                       160•       170•       180•       190•       200•
N. itascae      AAAGGCCCGTGGGGGTGGAGACTCAGATTGGCCAGTATCTCCCTGAGTGG

                       210•       220•       230•       240•       250•
N. itascae      ACCTTGGAGTCGGGTTGTTTGTGAATGCAGCCCAAAGTGGGTGGTAAACT

                       260•       270•       280•       290•       300•
N. itascae      CCATCCAAGGCTAAATACTAGCACGAGTCCGATAGCGAACAAGTACCGTG

                       310•       320•       330•       340•       350•
N. itascae      AGGGAAAGTTGAAAAGTACTTTGAAGAGAGAGTAAACAGTGCGTGAAACC

                       360•       370•       380•       390•       400•
N. itascae      GCTCAGAGGTAAACGGGTGGAGTTGAACTGCAAGCTCTGAGAATTCAACT

                       410•       420•       430•       440•       450•
N. itascae      GGTGAGTATGGCATGAGCTGGGTATATTGGTTGACGGTCCGGGTCTGCTT

                       460•       470•       480•       490•       500•
N. itascae      AGCTGCAGGTCCTCGCCTTTTGGTGGGGATGCGCGAATCACTTACCAAGT

                       510•       520•       530•       540•       550•
N. itascae      GTTGTGCGCCCGGACTGTATCGGACCTGCTTGCCAGTGCACTTTCTCAGA

                       560•       570•       580•       590•       600•
N. itascae      GTAATCACCACGACCGGCGTTGCCGTCTGGCTGTTGTAGTTAAACCGGCC

                       610•       620•       630•       640•       650•
N. itascae      TCGTAGAGTCCTTGTGGCTTTGCTTGGTCGGGATGGCAGGTAGCCCGTTG

                       660•       670•       680•       690•       700•
N. itascae      TGCACTTTTGTGTGCTTCGGGTGTTATCGCTGACTGCATCAGTTCTGTGC

                       710•       720•       730•       740•       750•
N. itascae      GGTACGTCGGAGACGGCGGCTTGTTGTGTGTGCGTGCGTACTTGTTATGC

                       760•       770•       780•       790•       800•
N. itascae      TGGCGGGGCCGAGTCTGGTTGCCGTGTTGATTGCAAAAGCAATCCCGGTG

                       810•       820•       830•       840•       850•
N. itascae      ATGGCTTGGTGTCGTTCGGTGTGCAGTTGCGTGCGTGTCACTATGCAGGG
```

Figure 3.1. The 28S rDNA nucleotide sequence data for the new species *Neopsilotrema. itascae* n. sp.

```
                        860•       870•       880•       890•       900•
N. itascae              CCAATAGTCTGTGGTGTAGTGGTAGACTATCCACCTGACCCGTCTTGAAA

                        910•       920•       930•       940•       950•
N. itascae              CACGGACCAAGGAGAGTAACATGTGCGCGAGTCATTGGGCGTTACGAAAC

                        960•       970•       980•       990•      1000•
N. itascae              CCAAAGGCGCAGTGAAAGTAAAGGTTCGGCTTGTCCGGACTGAGGTGAGA

                       1010•      1020•      1030•      1040•      1050•
N. itascae              TCCTGCCGTTTCTCACGCGCGGTACTACCAAGCATCGAGCGGCAGGCGCA
                       1060•      1070•      1080•      1090•      1100•
N. itascae              TCACCGGCCCGTCCCATGGCGTAGAGGCGACCTTGTGTTTGCTCATCGTC

                             1115•
N. itascae              GGGGCGGAGCATGAG
```

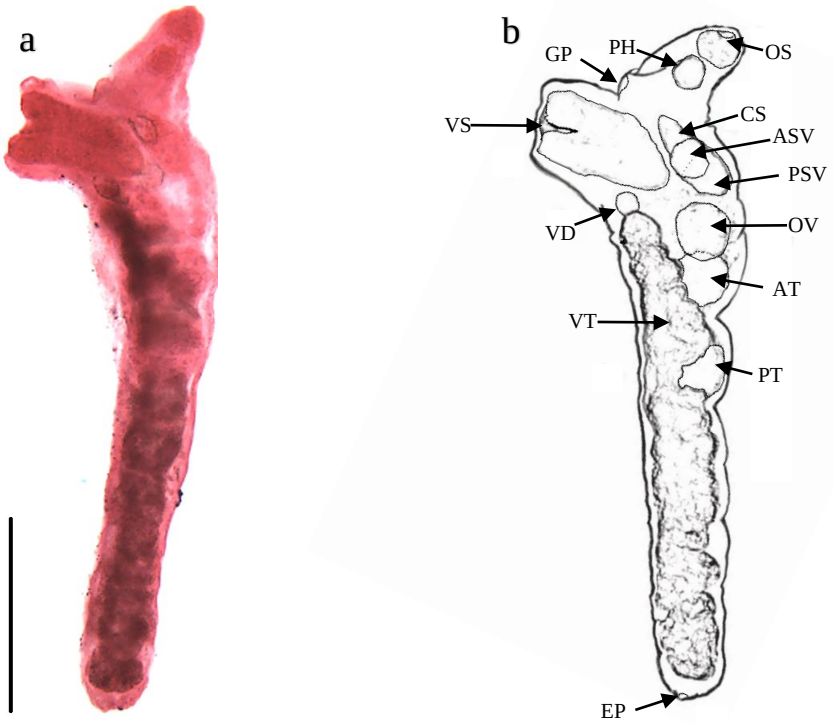

Figure 3.2. (a) Photograph of a lateral of *N. itascae* at 100x. (b) Line drawing of lateral holotype drawn at 100x [OS—oral sucker; PH—pharynx; VS—ventral sucker; GP—genital pore; CS—cirrus sac; ASV—anterior seminal vesicle inside cirrus sac; PSV—posterior seminal vesicle inside cirrus sac; OV—ovary; AT—anterior testis; PT—posterior testis; VD—vitelline duct; VT—vitelline fields; EP—excretory pore]. Scale bar 300μm.

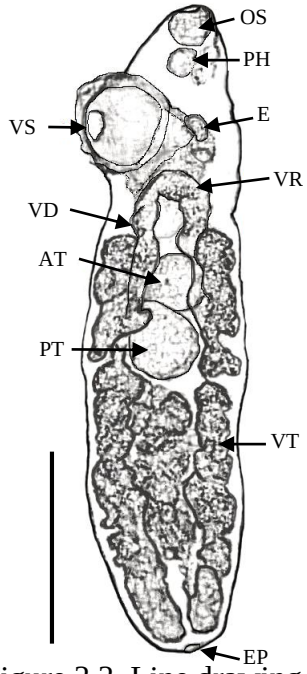

Figure 3.3. Line drawing of ventro-dorsal holotype of *N. itascae* drawn at 100x [OS—oral sucker; PH—pharynx; VS—ventral sucker; E—egg; AT—anterior testis; PT—posterior testis; VR—vitelline reservoir; VD—vitelline duct; VT—vitelline fields; EP—excretory pore]. Scale bar 300μm.

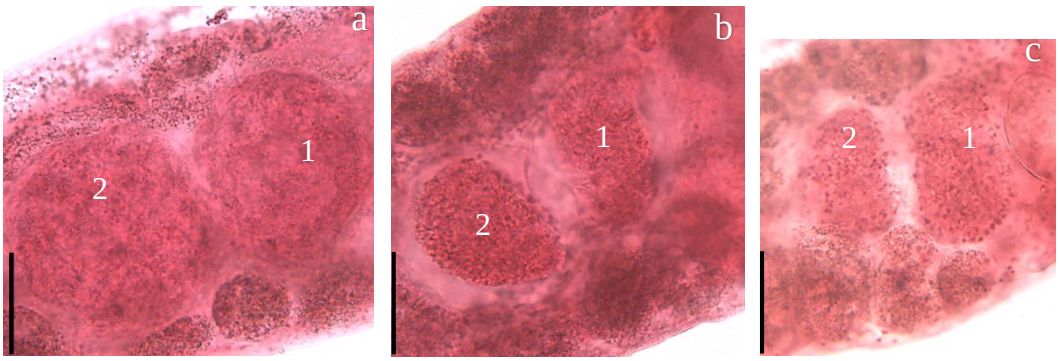

Figure 3.4. Anterior (1) and posterior (2) testes of (a) *N. itascae* and (b and c*) N. lisitsynae* showing the more spherical nature of *N. itascae* in comparison to *N. lisitsynae*'s more transverse nature. Scale bar 70 μm.

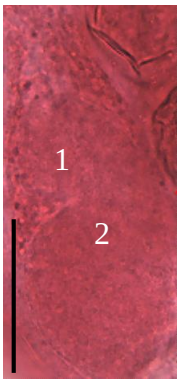

Figure 3.5. Cirrus sac of *N. itascae* at 400x. Anterior (1) and posterior (2) seminal vesicles marked. Scale bar denotes 80μm.

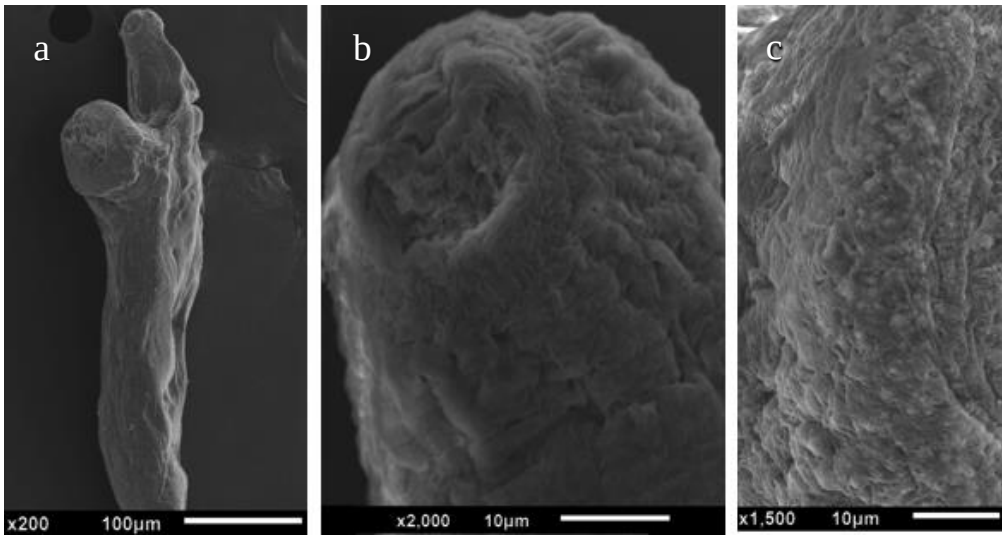

Figure 3.6. (a) Whole body view of *N. itascae*. (b) Muscular striations of oral sucker visible along with transverse pits on anterior margin. (c) White nodules on ventral sucker apparent on ventral margin along with tegumental folding on the external perimeter of the ventral sucker.

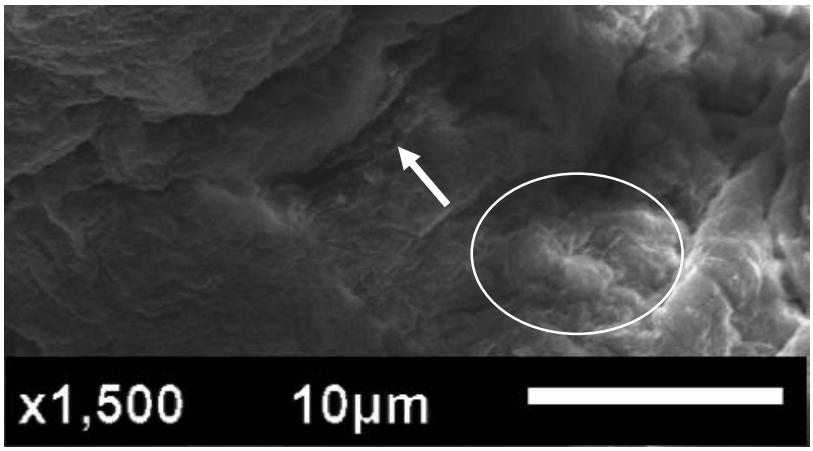

Figure 3.7. Genital pore location and structure. Cirrus opening circled. Uterus opening marked with an arrow.

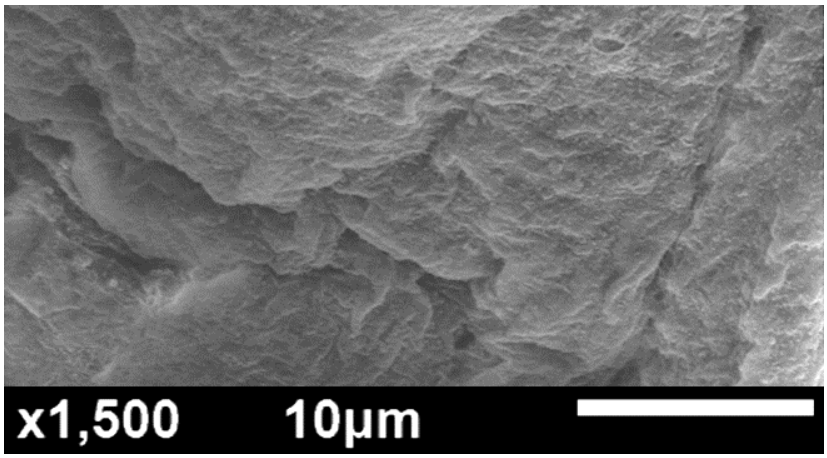

Figure 3.8. Tegumental structure showing rough appearance, along with sporadic, small pits. No apparent tegumental spines or associated structures can be seen.

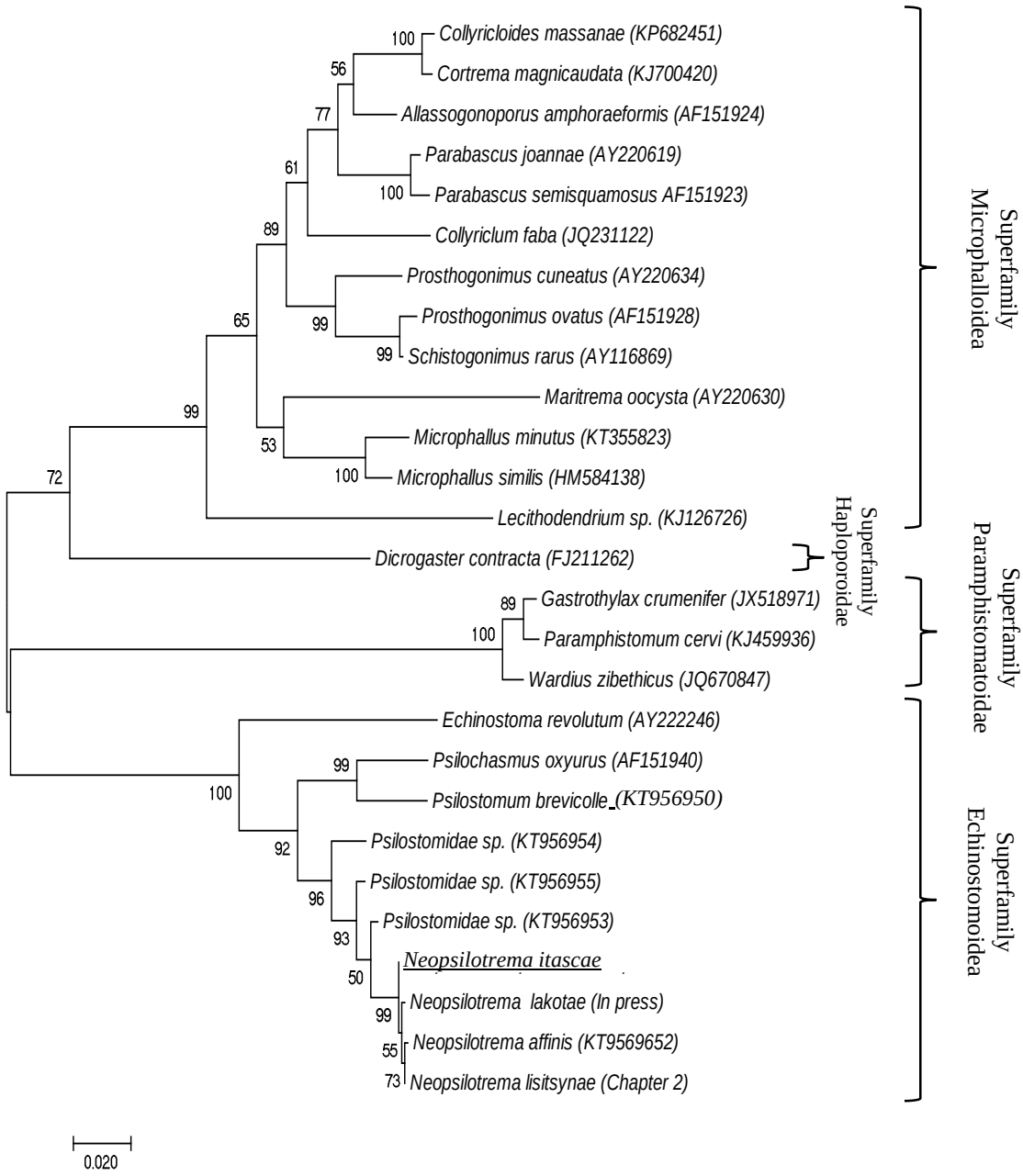

Figure 3.9. Maximum likelihood phylogeny of assorted digeneans to validate placement of *N. itascae* within Family Psilostomidae. Phylogeny generated using GTR+G model of nucleotide substitution with 500 bootstraps. Nodule support of branches given out of 100. The *N. itascae* n. sp. is underlined. The scale bar denotes the number of expected substitutions per site.

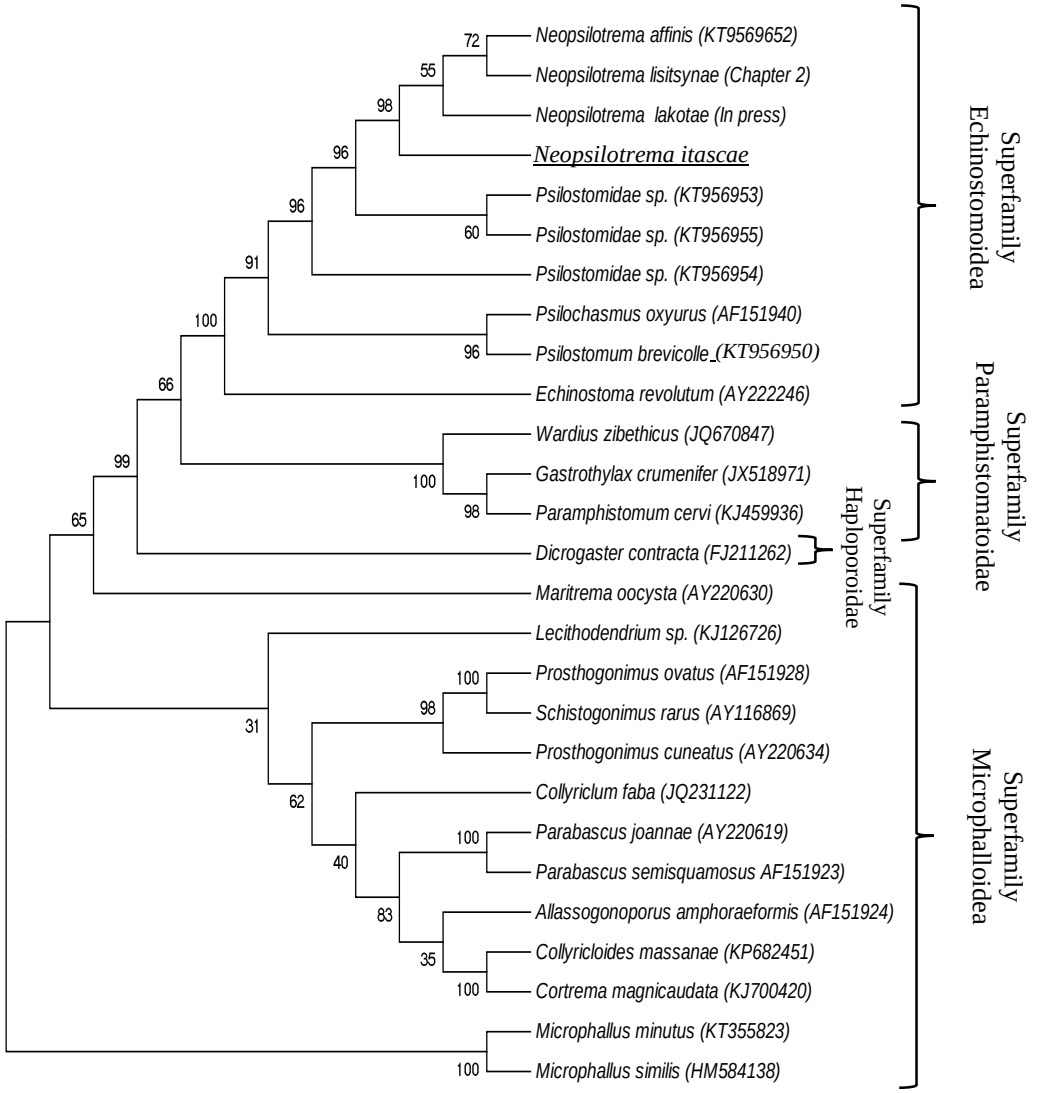

Figure 3.10. Consensus MP phylogeny using 500 bootstraps of assorted digeneans to validate placement of *N. itascae* within Family Psilostomidae. Phylogeny generated using 500 bootstraps. Nodule support of branches given out of 100. The *N. itascae* n. sp. is underlined.

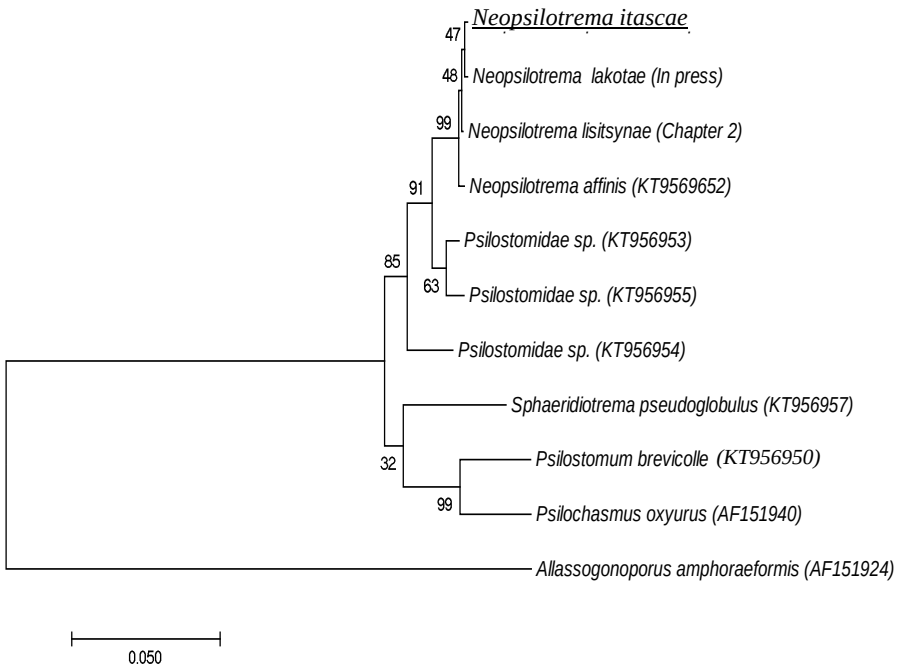

Figure 3.11. Maximum Likelihood phylogeny of Family Psilostomidae members generated 500 bootstraps based on HKY+G model of nucleotide substitution. Nodule support of branches given out of 100. The *N. itascae* n. sp. is underlined. The scale bar denotes the number of expected substitutions per site.

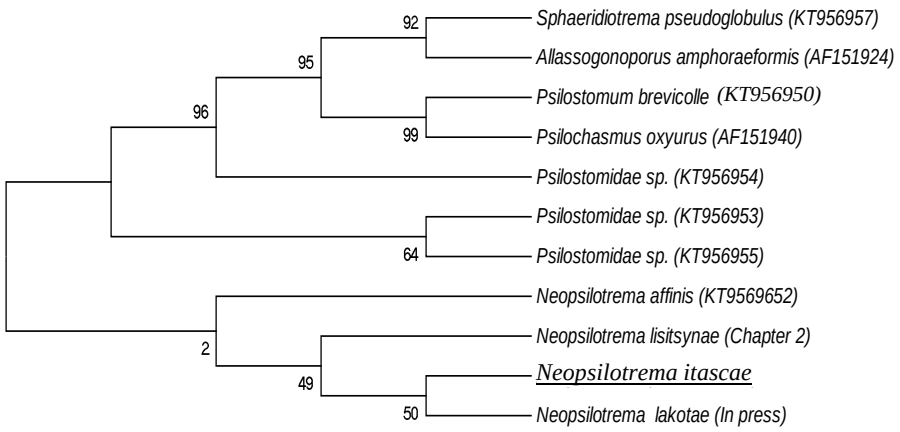

Figure 3.12. Consensus phylogeny of 500 bootstraps using maximum parsimony of Family Psilostomidae members generated 500 bootstraps. Nodule support of branches given out of 100. The *N. itascae* n. sp. is underlined.

Conclusion

Accurate species diagnosis requires a combination of techniques. Morphology was shown to vary highly within some species, while some loci (typically 28S rDNA) were accurate for species diagnosis such as with *N. lisitsynae*. However, the locus chosen may yield inaccurate results occasionally. In the case of *Z. lunata*, 28S rDNA was shown identical to another species of the Family Zygocotylidae, however, morphology clearly distinguishing between species. The requirement for both morphometric and genetic information for accurate species identification was apparent across all three studies. Further work on species identification should utilize both methods for optimal accuracy.

Lake Winnibigoshish yielded several new species of trematodes. The presence of *B. tentaculata* may be associated with the influx of of new trematode species to the area. Further work is needed to examine the parasitic community of Lake Winnibigoshish such as the inclusion of other definitive hosts (i.e. mammals, reptiles, ect.) and other life cycle stages including those within *B. tentaculata*.